



thrustMIT - Project Altair

Team 53 Project Technical Report for SA Cup 2023

Ashwinraj MR ¹, Imaad Shattari ², Kadar Basha Azad ³, Ronan Mark D'Souza ⁴, Darpan Theng ⁵, Utkarsh Anand ⁶,
Tanvi Agrawal ⁷, Sharada Belagavi ⁸, Aastha Bhatnagar ⁹, Arjun Chhabra ¹⁰, Gangarapu Jayadeep, Thakur Pranav
Gopal Singh, Diya Parekh, Raeid Mukadam, Aryaman Gadiya, Anway Das
Manipal Institute of Technology, Manipal, Karnataka (576104), India

This report details the technical specifications of thrustMIT's latest rocket Altair, for the 2023 Spaceport America Cup in the 10k COTS category. Project Altair is designed to reach an apogee of 10,000 feet carrying a non-deployable payload and recover back completely using a reefed parachute. It is powered by a Cesaroni Pro98 M3400-P solid propellant COTS motor. The rocket features a carbon fibre as well as glass fibre composite fuselages along with Aluminium 6061 bulkheads, centering rings, stringers, fins and thrust plate for added structural strength. The avionics is a combination of SRAD and COTS systems for additional redundancy. The payload team set out to demonstrate attitude control by building a 3 DoF parallel manipulator system which will balance itself using a PID based controller under high vibrations and G-Forces. The payload consists of the parallel manipulator which is actuated by three servo motors. Successful implementation of such a control system in the payload will immensely help the team in its future applications of attitude control systems in the rocket such as fin control, thrust vector control etc. A new custom airbrakes mechanism is a unique characteristic of our launch vehicle. This is team's first attempt at implementing active controls into the rocket.

¹Project Manager; Team Leader, Aerodynamics Head

²Deputy Project Manager; Team Manager

³Recovery Lead

⁴Safety Operations Lead; Avionics Head

⁵Launch Operations Lead; Controls Head

⁶Payload Head

⁷Research Head

⁸Propulsions Head

⁹Structures Head

¹⁰Management Head

Nomenclature

<i>ABS</i>	Acrylonitrile butadiene styrene	
<i>C_l</i>	Coefficient of Lift	
<i>CFD</i>	Computational Fluid Dynamics	
<i>CFRP</i>	Carbon Fibre Reinforced Polymer	
<i>CNC</i>	Computer Numerical Control	
<i>CSV</i>	Comma Separated Values	
<i>DoF</i>	Degrees of Freedom	
<i>FC</i>	Flight Computer	
<i>FPS</i>	Frames per Second	
<i>GFRP</i>	Glass Fibre Reinforced Polymer	
<i>GPS</i>	Global Positioning System	
<i>GSM</i>	Grams per Square Meter	
<i>GUI</i>	Graphical User Interface	
<i>LiPo</i>	Lithium-ion Polymer Battery	
<i>MDF</i>	Medium Density Fibreboard	
<i>MP</i>	Mega Pixel	
<i>PCB</i>	Printed Circuit Board	
<i>PDB</i>	Power Distribution Board	
<i>PLA</i>	Polylactic acid	
<i>SD</i>	Secure Digital	
<i>TIG</i>	Tungsten Insert Gas	
<i>WEDM</i>	Wire Electrical Discharge Machining	
<i>WPC</i>	Wood Plastic Composite	
<i>a</i>	Speed of Sound	m s^{-1} (ft s^{-1})
<i>G</i>	Modulus of Rigidity of Fin material	MPa (psi)
<i>AR</i>	Aspect Ratio of the Fins	
<i>t</i>	Thickness of Fin	mm (in)
<i>P_a</i>	Ambient/Atmospheric Pressure	MPa (psi)
<i>λ</i>	Taper Ratio of the Fins	
<i>c</i>	Chord Length of Fin	mm (in)
<i>C_g</i>	Centre of Gravity	m (in)
<i>C_p</i>	Centre of Pressure	m (in)
<i>C_d</i>	Coefficient of Drag	

I. Introduction

thrustMIT is the official student rocketry team of Manipal Institute of Technology, Karnataka. The team will be competing in the 2023 Intercollegiate Rocketry Engineering Competition (IREC) at the Spaceport America Cup (SAC) with Project Altair in the 10,000 ft Commercial Off The Shelf (COTS) Solid propulsion category.

A. Project Background & Scope

thrustMIT was formed in early 2016 to nurture amateur rocketry as a hobby in India by competing in the Spaceport America Cup. This experience will give the team a platform to share its knowledge and get a chance to learn from fellow amateur rocketeers all around the world.

Project Altair is thrustMIT's 5th manufactured rocket and the team's official entry into the 2023 Spaceport America Cup. Having already demonstrated our capability to reach 10,000 ft with our last rocket Rayquaza at the 2022 Spaceport America Cup, the primary mission goal of Altair is to reach the desired apogee demonstrating our new active control systems and complete a non-hazardous descent and recovery. The secondary mission goal is to test the functioning of the scientific payload which aims to demonstrate attitude control by balancing a parallel manipulator mechanism under high vibrations and G-Forces.

On top of everything else, the primary objective of the team is to provide the team members an opportunity to engage in hands-on experience with tackling practical engineering and scientific challenges. This will encourage more students to get involved in the aerospace industry.

To achieve all our goals, the team has researched, designed, manufactured and tested every component of Altair separately making it one of the most complex challenge the team has ever worked on. Despite the financial challenges and a lack of permissions to do flight tests, we have been able to successfully manufacture Altair and get it ready for the competition.

B. Design Goals & Success Criteria

The following table details the overall vehicle requirements, design goals and success criteria for Altair as well as some additional information.

Table 1 Altair's System Requirements

1.0	Vehicle Requirements
1.1	The rocket shall reach an altitude of 3229 m (10 594 ft).
	Final verification will be done at the SAC with the rocket's launch. Preliminary verification will be done through OpenRocket software.
1.2	The rocket shall descend safely from the apogee through parachute & land safely without significant damage.
	Recovery team is primarily responsible to meet this requirement. Detailed recovery related requirements are listed under section. Final verification will be done at SAC with the rocket's launch attempt. Other requirements will be verified through a series of ground tests.
1.3	Rocket shall maintain static stability margin between 1.85 to 3.2 throughout the ascent.
	Verification will be done through flight simulation data.
2.0	Propulsion System Requirements
2.1	The total impulse of the motor shall not exceed 9994.5 N s
	The motor must not exceed a total impulse limit of a M-class motor. As we have used the same rocket motor as last year, this was verified through our last year's rocket launch
3.0	Recovery System Requirements
3.1	The recovery system shall deploy the main parachute in a reefed state when the rocket reaches the apogee.
	Verification will be performed through ground reefing test in winds outside.
3.2	The recovery system triggers the disreefing event when the rocket descends to an altitude of 457 m (1500 ft) above ground level (AGL).
	Verification will be performed through ground reefing test in winds outside.

3.3	The recovery system shall be armed manually through a switch.
Ground testing of arming switch will be performed prior to the launch campaign.	
4.0	Avionics Systems Requirements
4.1	The rocket shall transmit telemetry flight data throughout the flight from ignition to touchdown.
This will be performed by a XBee Pro Telemetry module functionality and Range test will be done on ground.	
4.2	The rocket shall log all system commands and sensor data gathered during flight for post-flight analysis and troubleshooting.
This functionality will be performed by the Teensy 4.1 microcontroller by logging all data into a SD Card. Electrical system integration tests will be performed to ensure that all data is being logged properly into the SD Card.	
4.3	It shall be possible to replace any avionics component with an identical copy without compromising or affecting the avionics systems in any way.
All boards must be trivially replaceable. This ensures that if a component on one board fails in the field during final assembly, it can be replaced with an identical board without issue. All replacement boards will have identical hardware, so no configuration changes will be necessary.	
4.4	All flight electronics shall comply with Appendix B of the IREC DTEG, Safety Critical Wiring Guidelines.
Although the Safety Critical Wiring Guidelines are only explicitly binding on safety critical wiring, it is desirable to ensure all flight wiring is in compliance. This ensures all flight systems are robust and reliable. It also makes pre-flight inspection easier, as all wiring must be held to the same standard. Design considerations and selection of components will be verified for compliance during the electrical design review process. Assembly considerations will be verified for compliance during pre-flight inspection.	
5.0	Aerostructures Requirements
5.1	The rocket fins shall have an aeroelastic flutter threshold velocity atleast 1.5 times higher than the maximum rocket airspeed.
Dimensions of the fin set and fin flutter calculations are available in section II.A.6	
5.2	The airframe shall withstand all bending, compression, and impact loads encountered throughout flight.
Preliminary design validation will use analytical methods of determining loads experienced by the structure. Further validation on manufactured prototypes will be conducted through destructive testing of components.	
5.3	Airframe manufacturing processes shall endeavor to reduce surface roughness in the interest of drag reduction wherever possible.
This will be accomplished through surface finishing techniques such as sanding, polishing, and use of glossy coatings.	
6.0	Payload Requirements
6.1	The payload shall conform to the standard CubeSat form factor of 4U.
Compliance will be ensured throughout all design reviews leading up to manufacturing. Final verification will be accomplished via measurement of dimensions and mass.	
6.2	The payload shall be unnecessary for nominal rocket performance - that is, if the payload is replaced with a dead weight of equivalent mass and form factor, all non-payload mission objectives shall still be met.
The payload will not affect the flight or the trajectory of the rocket in any way.	
7.0	Operational & Safety Requirements
7.1	Rocket “final assembly” (all assembly steps that can happen only immediately prior to launch) shall take no longer than 3 hours to complete.
This requirement is important to ensure that launch day operations are efficient and can be completed in a timely manner. Verification will take place through assembly rehearsals prior to the launch campaign.	
7.2	A safe perimeter shall be established around test and launch sites. Only designated test personnel with Tripoli membership and with proper personal protective equipment (PPE) shall be permitted to enter this perimeter.

II. System Architecture Overview

Altair is a solid propellant rocket standing 2.705 m (106.5 in) tall with an outer diameter of 15 cm (5.91 in) and a pad mass of 30.01 kg (66.16 lb). The rocket body is made up of 3 modular body tubes. Two body tubes have been manufactured from CFRP to keep them lightweight while providing significant structural strength to withstand the various loads acting on the rocket during its flight and one of the body has been manufactured using GFRP to support avionics telemetry. The rocket is powered by a Cesaroni Pro98 M3400-P COTS motor.

Altair is split into 6 major sections as given in the Fig 1:

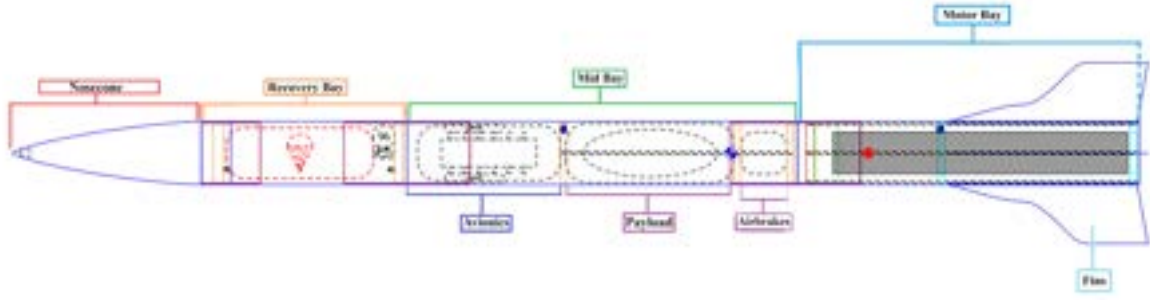


Figure 1 Schematic of Altair as viewed on OpenRocket

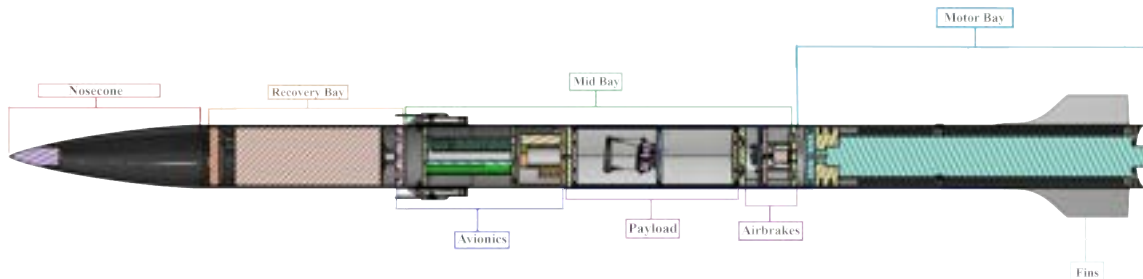


Figure 2 Section view of Altair

A. Aerostructures

1. Nosecone

The primary function of the Nosecone is to reduce the form drag of the rocket by displacing the air as the rocket moves through it. Due to the rocket's maximum speed of 310.9 m s^{-1} (1020 ft s^{-1}) falling within the transonic regime, a Von Kármán Nosecone profile was deemed suitable as it has a low drag coefficient and is well-suited for subsonic and transonic flight regimes. The Nosecone has a fineness ratio of 3:1 and is constructed using CFRP to ensure lightweight and rigidity, capable of withstanding dynamic pressure at the front. To attach the Nosecone to the fuselage, four # 2-56 Nylon shear pins are utilized, which break during parachute ejection.

A 15 cm (5.91 in) coupler is attached to the base of the Nosecone using Epoxy and Resin to integrate the coupler into the Nosecone, aiding in connecting the Nosecone to the Recovery Bay. To serve as an attachment point for the shock cords, a WPC Nosecone bulkhead with a U-bolt bolt fixed to it is connected at the base. To ensure ease of manufacturing, the Nosecone is split into two sections, and the tip of the Nosecone is produced using Aluminium 6061 via a CNC machine, as the small diameter near the tip would be difficult to layup accurately by hand.

To simplify the layup process, a mold for the Nosecone layup was manufactured using MDF by stacking and gluing together two halves with a special wood-working adhesive.

2. Body Tube

The composite body tubes were manufactured in-house using a wooden mandrel to control the inner diameter. The mandrel was covered with a thin layer of plastic, over which a layer of wax was applied for a smooth inner finish of the body tubes. Araldite LY 5052 and Aradur 5052 are the epoxy pair used for hand layups. This pair was chosen for its low viscosity and easy impregnation of reinforcement materials. Its long pot life (2 hours for 100 ml at ambient), and ample processing time allowed the production of large-sized body tubes.

For safety, the members performing the layup wore adequate skin protection. A peel ply layer was applied over the layup to absorb excess resin and prevent foreign particles from adhering during the curing process. After demolding, the body tubes were sanded to produce a smooth circular finish.

Table 2 Altair's Bay Dimensions

Recovery Bay Length	490 mm	(19.3 in)
Mid Bay Length	930 mm	(36.7 in)
Motor Bay Length	815 mm	(32.1 in)
Bay Thickness	2 mm	(0.08 in)

The motor bay and recovery bay were constructed using carbon fiber due to its excellent strength-to-weight ratio, while the mid-bay was made of glass fiber since it contained avionics and payload systems. To achieve this thickness and desired strength, 200 GSM Bidirectional Plain Woven Carbon Fibre and 450 GSM Bidirectional Plain Woven Glass Fibre.

Using Ansys Mechanical, the body tube assembly was simulated. The loading condition was set to 4000N considering the maximum thrust force of the motor and was applied to the thrust plate bolt holes. The bottom edge of the motor bay was constrained using a remote displacement to limit linear movement of the body tube assembly while allowing rotational motion. The top of the recovery bay was also constrained, allowing axial deformation only, and a zero-rotation condition was applied to close out the six degrees of freedom. The Von Mises stress profile of the body tube assembly when subjected to initial thrust loading is depicted in the image below. The maximum stress value of 24.5 MPa (3515.71 psi) was observed on the thrust plate bolt holes. As this value is below the CFRP failure limit, the design was deemed safe for use.



Figure 3 Body Tube

3. Couplers

Altair has two couplers which are designed with an inner diameter of 142 mm (5.59 in) and a thickness of 2 mm (0.08 in) each, and a length of 300 mm (11.81 in) which is twice the body caliber. The coupler joining the mid-bay and recovery bay is fabricated using glass fiber and manufactured using split female molds to ensure accurate control of its outer diameter. The molds for the glass fiber coupler were constructed using Medium Density Fibreboard (MDF). The coupler was manufactured using 450 GSM Bidirectional Plain Woven Glass Fibre with Araldite LY 5052 and Aradur 5052 epoxy pair, similar to the mid-bay body tube.

The other coupler is made of aluminum and is located between the motor bay and mid-bay. This material was chosen to aid in the machining of precise and accurate slots for the airbrakes. The airbrakes are housed inside this coupler. In contrast to the composite coupler, the machining of slots for airbrakes in an aluminum coupler is more feasible.



Figure 4 Coupler

4. Mid-Bay Bulkheads

Within the mid bay of Altair, three bulkheads constructed from Aluminium 6061 have been installed. This selection of material is based on its durability in high-stress scenarios and versatility in relation to machining and welding processes. The bulkheads are affixed to the body tube through four M5 bolts and have been optimized in shape to evenly distribute stress while simultaneously reducing overall weight.

The dimensions of the avionics bulkhead, payload bulkhead, and airbrakes bulkhead are 146 mm (5.75 in), 142 mm (5.59 in), and 142 mm (5.59 in), respectively, with each bulkhead possessing a thickness of 15 mm (0.6 in).

The avionics bulkhead serves to hold the avionics mount securely in place and also maintains the 4U CubeSat and payload bulkhead in their designated positions. The payload bulkhead is specifically engineered to withstand the load of the 4U CubeSat, which houses the payload. Lastly, the airbrake bulkhead is designed to provide secure mounting for the airbrake mechanism.

On the mid bay bulkheads, holes of diameter 3mm (0.12 in) are drilled to allow wires to flow through and reach the airbrakes and recovery bulkhead. In addition, an acrylic sheet has been installed on top of the avionics mount to shield the electronics from probable fire during ejection.

5. Motor Bay

II.A.5.1 Thrust Plate & Damper

During the powered ascent phase, the thrust plate is responsible for bearing the majority of the load generated by the motor. Its primary purpose is to distribute this force to the entire airframe via eight M5 bolts that secure it in place. The thrust plate is also connected to the motor through a centrally located 10 mm (0.39 in) bolt, which aids in distributing the motor load to the rest of the rocket.

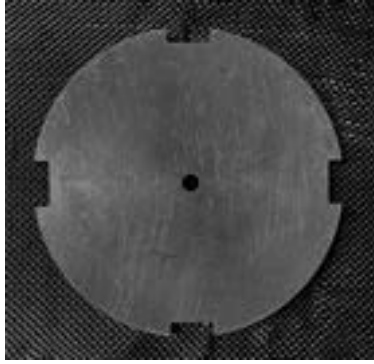


Figure 5 Thrust Plate

To manufacture the thrust plate, we have chosen Aluminium 6061 due to its high bearing yield strength. The thrust plate has an outer diameter of 140 mm (5.51 in) and a thickness of 20 mm (0.79 in). To ensure the load-bearing capacity of the thrust plate, we conducted a simulation that applied twice the maximum thrust generated by the motor, which is 8000N, to the 10 mm (0.39 in) hole in the centre of the plate while constraining the bolt edges to simulate the bolt connections between the thrust plate and the body tube. The simulation results showed that the component was more than capable of handling the load transferred by the motor, as only around 0.03 mm (0.001 in) of deformation was observed. For an image of the thrust plate simulation refer to the Simulation section of the Appendix ??

A damper is inserted between the thrust plate and motor to absorb immediate vibrations and force. WPC due to its high impact strength and durability. Additionally, WPC has good dampening characteristics which makes it an ideal material for this purpose. The thrust plate is supported by four aluminium stringers, which run axially through the motor bay to provide overall stability and rigidity. M5 bolts connect all four stringers to the other components, and they are also intended to house the fin attachment system.



Figure 6 Motor Bay

II.A.5.2 Centering Ring

In order to ensure proper motor placement and prevent radial movement, an aluminum centering ring is utilized. The centering ring has an outer diameter of 146 mm (5.75 in) and an inner diameter identical to that of the motor, which is 98 mm (3.86 in). Four M5 bolts are employed to connect the centering ring to the airframe.

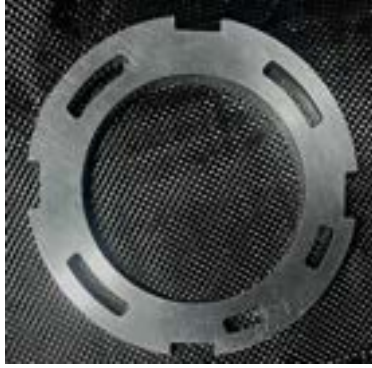


Figure 7 Centering Ring

II.A.5.3 Retainer

The retainer, which is responsible for supporting the motor, is a significant component of the assembly. It has a thickness of 18 mm (0.71 in) and an outer diameter of 146 mm (5.75 in). In order to guarantee its structural integrity, we subjected the retainer to a load equal to twice the wet mass of the motor, which is 40 N (35.96 lbf), while also constraining the bolt holes to replicate bolt connections. During this examination, the maximum deformation observed was a mere 1.2×10^{-4} mm (4.72×10^{-6} in), indicating that the component is highly reliable and safe for use. Furthermore, the fins are attached to the retainer. For an image of the retainer simulation refer to the Simulations section in the Appendix. ??

B. Fins

In rocket design, fins play a crucial role in ensuring flight stability by keeping the centre of pressure below the centre of gravity during ascent, which generates a corrective moment about the centre of gravity. This ensures that the rocket's orientation is corrected by aerodynamic forces in the event of wind gusts. To achieve the required stability and increase aerodynamic efficiency, the team chose a four-fin trapezoidal fin set with the root of the leading edge extended, consisting of two curves. The leading edge alters the airflow over the fins at non-zero angles of attack, providing a better lift to drag ratio than our previously designed fins. The shape profile of the extended part was based on the works done by L. C. Squire [4]. The dimensions of the fins are presented in Table 3 and Figure 9. The fins have a rectangular cross-section with a thickness of 4 mm (0.16 in). The minimum stability caliber of the rocket at the launch rod clearance is 1.85, increasing to 3.2 during ascent.

Table 3 Fin Dimensions

Shape	Trapezoidal With Leading Edge Extension	
Material	Aluminium 6061	
Root Cord	450 mm	(17.72 in)
Tip Cord	150 mm	(5.91 in)
Semi Span	140 mm	(5.51 in)
Thickness	4 mm	(0.16 in)



Figure 8 Fin Profile

A critical phenomenon considered during the design process was fin flutter. Fin flutter is an aeroelastic phenomenon that arises at high speeds, where the physical properties of the fins cause an amplification feedback loop, leading to increased oscillation and eventual failure of the fins. The flutter velocity of the fins is calculated using the following equation:

$$v_f = a * \sqrt{\frac{2 * G * (AR + 2) * t^3}{1.337 * P * (\lambda + 1)(c * AR)^3}} \quad (1)$$

The flutter velocity of the fins was calculated using an in-house MATLAB code developed to visualize the difference between fin flutter velocity and the rocket's speed throughout the entire ascent phase. The calculated flutter velocity was found to be well above the maximum speed of the rocket and below the margin of safe flight speed.

An in-house MATLAB code was developed to visualize the difference between fin flutter velocity and the rocket's speed throughout the entire ascent phase. On performing the calculations, the flutter velocity was found to be 485.51 m s^{-1} ($1592.88 \text{ ft s}^{-1}$), well above the maximum speed of the rocket and below the margin of safe flight speed.

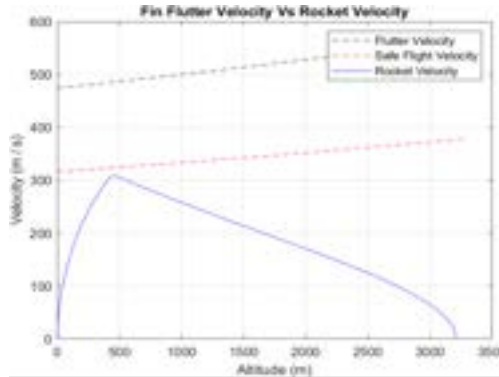


Figure 9 Fin Flutter Velocity vs. Rocket Velocity

The fins were made of Aluminium 6061 and cut to the desired geometry using a WEDM machine, with an 8.3 mm (0.33 in) fin tab to facilitate attachment. The fin was TIG welded into a slot made in the stringer, with a seam weld used to ensure structural integrity under extreme aerodynamic and impact loading conditions, utilizing Aluminium 4043 as the filler material. The stringer was fastened into the centering ring using one M5 bolt and snug-fit into a slot in the retainer. The attachment mechanism was designed to minimize fin flutter and ensure that the fin does not fail under aerodynamic forces experienced during flight and impact loads at ground hit. The fin attachment design allowed for accurate mounting from the outside of the framework after assembly. For the velocity contour of air on the leading edge extended fins at M 0.9 refer to the Simulation section of the Appendix.??

To test the force experienced by the setup during severe impact events and under high forces, an Explicit Dynamics simulation was performed on the fins and their attachment mechanism. A comprehensive examination of the results reveals that the attachment mechanism has suffered only minor damage. As a result, we found that these fins and their attachment method could endure any unexpected hits as well as the aerodynamic forces they encounter in flight. For the explicit dynamics simulations results of the fin refer to the Simulation section of the Appendix.??

1. Rail Buttons

The present rocket design incorporates two 1515 rail buttons with an airfoil-style, manufactured from Ultra High Molecular Weight Polyethylene, a durable plastic known for its high resistance to abrasion and wear. One button is fixed to the avionics bulkhead located in the mid bay, while the other is attached to the motor bay centering ring. The positioning of the rail buttons requires meticulous deliberation to guarantee the rocket is appropriately upheld by the launch rail to attain a straight ascent. The launch buttons must be capable of withstanding the weight of the rocket when placed on the launch pad. To secure the launch buttons to the components, a 1/4"-20 UNC bolt was utilized.

2. Flight Simulations

The utilization of flight simulations presents an expedient and cost-effective methodology for testing the efficacy of designs and systems within a secure and monitored setting. OpenRocket was predominantly utilized for the majority of the flight simulations. The simulation environment was established on the basis of the geographic and meteorological conditions prevalent in Spaceport, New Mexico during summertime.

Specifically, the simulations incorporated an elevation of 1400 m (4.593 18 ft) at 33 deg, with an average wind speed of 2 m s^{-1} (6.56 ft s^{-1}). An initial launch angle of 3 deg was integrated to account for potential deviations during actual launches. Moreover, the launch rail was adjusted to a height of 4.68 m (15.35 ft) instead of 5.18 m (17 ft) as the rocket can only rotate after the aft rail button disengages.

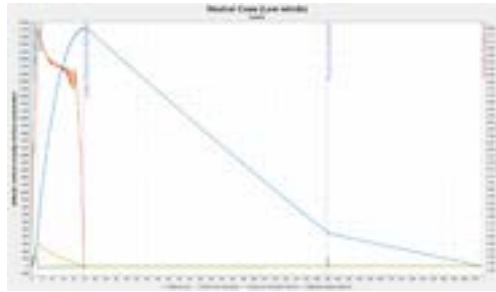


Figure 10 ORK Average windspeed flight simulation results

Under average wind speed conditions, Altair attains an apogee of 3229 m (10 594 ft). However, under worst-case scenarios where wind speed is 4.5 m s^{-1} (14.76 ft s^{-1}), Altair reaches an apogee of 3235 m (10 613.5 ft). Given that the airbrakes possess the capability of reducing the apogee by over 200 m (628 ft), Altair is estimated to reach a height of approximately 3048 m (10 000 ft).

Steady state CFD simulations were done to determine the forces and moments acting on the rocket along with the boundary layer thickness and pressure distribution on the rocket which helped in the placement of the pitot tube.

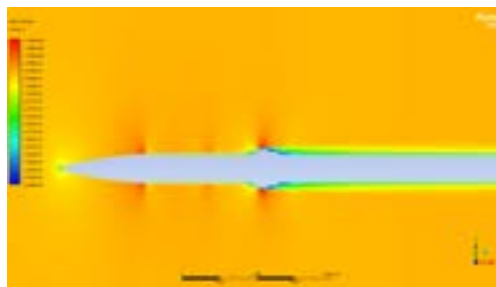


Figure 11 Velocity contour over the rocket at Mach 0.9

The new fins that have been designed have proved superior to last year's. CFD simulations were done to determine the improvement in aerodynamic efficiency of Altair's fins from Rayquaza's last year's rocket, table 4 shows the C_l/C_d of both.

Table 4 Rayquaza vs Altair Fin Efficiency Comparison

Angle of Attack	Rayquaza	Altair
	C_l/C_d	
10	6.689839257	9.785714286
20	19.37082822	21.45153061

C. Recovery

The main objective for this year's rocket launch was to achieve a successful recovery of the rocket. In light of material constraints that prohibited the stitching of an SRAD parachute, the recovery subsystem opted for a Commercial Off-The-Shelf (COTS) parachute. Altair's recovery system incorporates a reefing mechanism, where a single parachute serves as both the drogue parachute in a reefed condition and the main parachute in a dis-reefed condition.

1. Parachute & Shock Cords

In pursuit of successful rocket recovery, the decision was made by the recovery subsystem to employ a COTS parachute, rather than an SRAD parachute, due to material constraints. Altair's recovery system incorporates a reefing mechanism whereby a single parachute, specifically an ultra-compact, 12-gore, 3 m (120 in) annular shaped parachute from Fruitychutes, is utilized as both the drogue and main parachute, reefed to 0.51 m (20 in) in the former case. The reefing diameter was determined via terminal velocity calculations.

Kevlar shock cords measuring 15.8 mm (0.625 in) in diameter are capable of handling loads up to 3000 kg (6600 lb) according to the manufacturer. One shock cord stretches from the recovery bulkhead to the quick link, covering a length of 2.75 m (108.27 in), which is nearly equivalent to the rocket's length. The other shock cord measures 2.5 m (98.43 in). The combined length of both shock cords totals 5.5 m (217 in), which exceeds twice the length of the rocket.



Figure 12 Recovery Setup

2. Reefing

In Altair, a reefing system is utilized due to its advantages in reducing mass, volume, and the number of bays required, as well as simplifying the deployment sequence by employing a single parachute. The reefing system involves the use of piranha line cutters, reefing lines composed of Nylon III, and reefing wires consisting of two sets of 22 AWG insulated copper wires that are covered in nylon sleeves.

Initially, the parachute is in a reefed state, wherein two sets of reefing lines wrap around the skirt through metal hoops sewn on alternate gores, and are tied to zip ties within the piranha line cutters. The cutters are fastened to the skirt and one of the canopy's suspension lines is loaded with 4F black powder charge. The line cutter is linked to the flight computer via reefing wires. Upon sending the main deployment signal from the flight computer, the line cutter is triggered, severing the zip ties and, as a result, detaching the reefing lines. This leads to the dis-reefing of the parachute.

3. Assembly

In the rocket design, the Recovery Bay is positioned immediately below the Nosecone, which is connected to the fuselage by means of four #2-56 Nylon shear pins. A piston-cylinder arrangement is employed at the lower end of the bay for deploying the parachute. Specifically, the cylinder is constructed as an integral part of the 15 mm (0.59 in) thick Aluminum 6061 bulkhead that separates the Recovery and Mid bays, known as the Recovery bulkhead. The piston, which comprises a solid disk with a cylindrical extrusion, is fitted into the cylinder with a clearance fit between them, allowing for easy assembly.

The shock cord linking the recovery bulkhead and the parachute is attached to the parachute through mechanical linkages such as quick and swivel links. The other end of the cord is tied to the eyebolt on the recovery bulkhead. Additionally, the shock cord that secures the nosecone and the parachute is fastened to a U-bolt on the WPC bulkhead in the nosecone via mechanical linkages. To safeguard the parachute from the high-temperature gases emitted by the ejection mechanism, it is folded and packed within a parachute liner (deployment bag).

4. Ejection Mechanism

In order to deploy the recovery mechanism, an electric match consisting of multiple 24 AWG Nichrome bridge wires is passed through a hole drilled in the cylinder section of the 15 mm (0.59 in) thick Aluminum 6061 bulkhead. The flight computer triggers the recovery mechanism when the rocket reaches apogee, causing the electric match to ignite the ejection charge. This builds up pressure in the cylinder, forcing out the piston and the parachute that was placed on top of it. The parachute then pushes onto a 27 mm (1.06 in) WPC bulkhead that is attached to the shoulder of the Nosecone using phenolic resin. This sequence of events generates enough force to break the four #2-56 Nylon shear pins and separate the Nosecone from the rocket body, releasing the parachute.

At a height of 457 m (1500 ft), the flight computer signals the E-match to ignite the charge inside the piranha reefing cutters, which then cut the reefing lines, fully inflating the parachute.



Figure 13 Piston Cylinder

5. Simulations

In order to assess the ability of the recovery bulkhead to withstand the force generated by the ignition of the ejection charge, a test was conducted. The bulkhead was subjected to constraints at the four bolt edges, simulating the bolted connections between the bulkhead and the recovery fuselage. The simulation results showed a deformation of $3\ \mu\text{m}$ (9.84×10^{-6} ft). For an image of the recovery bulkhead total deformation due to force of ejection charge simulation refer to the the Simulations section of the Appendix. ??

The recovery bulkhead was also simulated to check if the bulkhead can withstand the weight of the rocket after the parachute is deployed. Like the previous simulation the bulkhead was constrained at the four bolt edges and force equal to 2.5 times the rocket weight is applied to the eyebolt hole. The maximum deformation observed was $6\ \mu\text{m}$ (4.92×10^{-6} ft). For an image of the recovery bulkhead Recovery Bulkhead Total deformation due to force of rocket weight refer to the the Simulations section of the Appendix. ??

D. Airbrakes

Through continuous research and development efforts since 2019, our team has successfully implemented an air brakes mechanism in our latest project for the Spaceport America Cup 2023. Building on our prior success of securing fourth place in barometer altitude in the SA Cup 2022, the addition of the air brakes mechanism is expected to improve our ability to control the apogee of the rocket and secure a higher position in barometer altitude in the upcoming SA Cup 2023.

The airbrakes are located between the CP and CG of the rocket so that they do not affect the position of CP even upon deployment. The air brakes mechanism has been designed to slow down and control the rocket's coasting ascent by deploying radially and increasing drag. The mechanism is armed by an in-house developed apogee prediction algorithm, which is incorporated into the flight computer onboard. The air brakes are constructed from aluminum and have been engineered to withstand the high forces experienced during the coasting ascent phase of the rocket's flight.

The air brakes mechanism is based on a slider crank mechanism powered by a servo motor and features a spring retraction mechanism to prevent the brakes from opening during the powered phase of the rocket's flight. The control system for the air brakes is based on a simple apogee predictor that utilizes the 4th order Runge Kutta method. The predictor obtains the instantaneous velocity of the rocket from two pitot tubes diametrically mounted on the rocket, and calculates drag through lookup tables obtained from computational fluid dynamic simulations.



Figure 14 Velocity Contour on the Airbrakes at 80m/s

The air brakes consist of eight components, including the brake plate, housing, support plate, battery box, links, shaft, servo motor, and spring. Each brake has an area of 1225.8 mm^2 (1.9 in^2) and has undergone stiffness and strength calculations, as well as static structural simulations for a load of 1.23 kg (2.7 lb) with a factor of safety of 1.5.

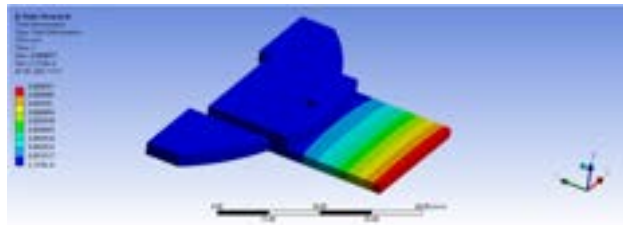


Figure 15 Ansys simulation showing of total deformation for brake plate

1. Assembly

Assembly of the air brakes mechanism involves the sliding of the shaft through the circular plate, bolting the motor onto the shaft using a coupling, and attaching the motor housing onto the circular plate. Brake plates are then placed in the housing, which is attached to the support plate using two M4 bolts. The mechanism is then attached to the rocket's assembly using three M4 bolts bolted from underneath to the bulkhead, with slots provided for alignment with the stringers.

To ensure the safety and stability of the rocket, the air brakes will only open above 1524 m (5000 ft) and if the velocity is less than 289.68 km h^{-1} (180 mi h^{-1}), which is a limit set through aerodynamic constraints and analysis. This limit aims to prevent catastrophic failure and maintain the attitude of the rocket during flight.

E. Payload

STEWIE is a Non-deployable 4U CubeSat payload for Project Altair. The payload weighs 4.2Kg (9.26 lbs) and aims to demonstrate attitude control on a parallel manipulator mechanism under high vibrations developed in the rocket and high G-Forces. The parallel manipulator mechanism is actuated by 3 separate servo motors which are being controlled by a Linear control system developed specially for the payload. Successfully implementing such a payload will immensely help the team in implementing more complex active control systems into our rockets in the future. The payload has been named Stewie as it was inspired by Stewart Platform, a 6-DoF parallel manipulator popularly used as a flight simulator. Stewie's development and application signify a significant advancement in the fields of robotics and control systems within the aerospace industry. Stewie will help provide insights into the practical applications of robotics and control systems within the aerospace industry.



Figure 16 Payload Render

1. Kinematics of the Payload

Stewie is a 3-degree-of-freedom (3DOF) parallel manipulator featuring three legs. Each leg is equipped with a motor situated at the base, serving as the first revolute joint. The motor is connected to link 1, and motion between links 1 and 2 is achieved via a revolute joint utilizing a bolt and nut mechanism. Additionally, a ball joint at the top of each leg connects the leg to the top plate. The degrees of freedom of Stewie were calculated using Grubler's formula.

To accomplish its intended purpose, Stewie's top plate is equipped with an MPU sensor. The sensor will provide information regarding the angles of deviation along the X, Y, and Z axes. This information will be utilized to determine the position of the ball joints with respect to the base frame at any given time. The base frame is defined as the initial frame located at the center of all three motors. The position of the base frame will remain constant throughout the flight, regardless of the position of the motors. Our primary objective is to rotate the motors in such a way that the z-coordinate of all the ball joints is uniform, thereby ensuring that the plate remains parallel to the ground.



Figure 17 Representation of Reference Frames

As previously stated, our primary objective is to determine the appropriate motor angle required to maintain the plate's parallel orientation to the ground. To accomplish this, inverse kinematic calculations were carried out on Stewie,

allowing the control system to learn the positions of the ball joints at various angles. These calculations have yielded the following equations to achieve the desired outcome:

$$\alpha_k = \sin^{-1} (c_k / (a_k^2 + b_k^2))^{1/2} - \text{atan2}(a_k, b_k) \quad (2)$$

Where,

$$a_k = 2|l_{112}|^{(z)} \quad (3)$$

$$b_k = 2|l_1|(\cos\theta_k l_{12}^{(x)} + \sin\theta_k l_{12}^{(y)}) \quad (4)$$

$$c_k = |l_{12}|^2 - (|l_2|^2 - |l_1|^2) \quad (5)$$

The angle α_k will be fed to the control system which will then give us the actual angle of rotation.

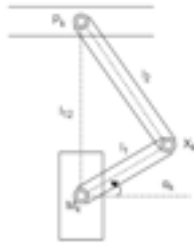


Figure 18 Side View of Leg

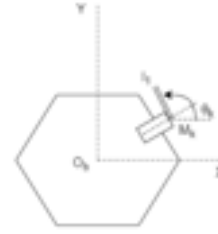


Figure 19 Top view of base frame

2. Electrical Design

The electronics part of the payload consists of two PCBs:

Primary Circuit Board Contains a single Teensy 4.1 microcontroller which is controlling the three servo motors. The control system has been deployed on the microcontroller. Primary Circuit Board is connected through GPIO pins to the Secondary Circuit Board to get orientation values of the payload platform from the Inertial Measurement Unit (IMU).

Secondary Circuit Board Contains a MPU6050 IMU sensor which will provide orientation values of the payload top plate to the primary circuit board. It is attached just below the top plate of the manipulator mechanism.



Figure 20 3D Render of Primary Circuit Board

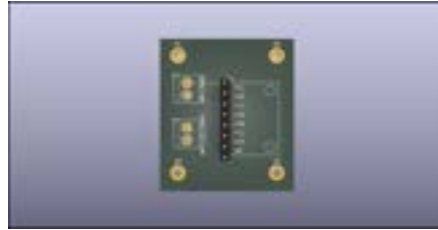


Figure 21 3D Render of Secondary Circuit Board

The system is mounted and powered on the launchpad by pull-pin switches. The microcontroller has an independent power source of 10 000 mAh, 7.4 V LiPo batteries. A redundant 10 000 mAh, 7.4 V LiPo battery has been installed in case the primary power source fails to operate. The circuitry consists of:

- **Teensy 4.1:** It has high-resolution ADC channels and an in-built micro SD card slot, which will be needed to flush large amounts of data. The Teensy 4.1 is a suitable microcontroller often preferred for control system-based applications
- **TowerPro MG90S Servo Motor:** MG90S is a low-cost 13g micro servo motor often chosen for robotics and automation applications. It works on a 5V supply and can sustain a maximum torque of 2.2 kg cm
- **MPU6050:** MPU6050 is a 6 Axis Inertial Measurement Unit that consists of a Gyroscope and an Accelerometer. Due to its low costs and highly accurate data, it is often used in applications where orientation data has to be obtained.

3. Payload Camera

The payload is equipped with 2 RunCam Split-3 Lite cameras at opposite corners of the CubeSat to obtain multiple angles of the payload functioning. This camera was chosen as it has a compact design and a good resolution, making it suitable for use in the payload. The camera has a 2 MP resolution and can record 1080p video at 60 frames per second (FPS). As the camera requires a non-direct power supply, both of the cameras will be powered by two separate LiPo batteries connected to two separate Power Distribution Boards (PDB).

4. Control System

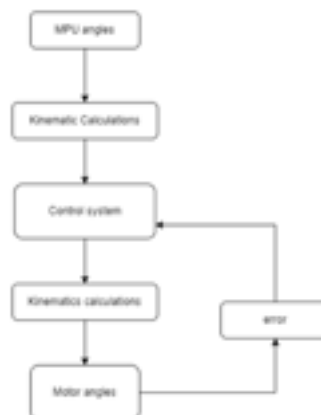


Figure 22 Working of the PID Controller

A Proportional-Integral-Derivative (PID) controller has been designed for controlling the servo motors of the payload to balance the plate with respect to the ground. Fine-tuning of the K_p , K_i , and K_d PID constants was done through prototype testing.

5. Mechanical Design

The 4-U CubeSat is designed with four surrounding plates and three supporting horizontal plates that divide the payload into two compartments. The upper section houses the experimental Stewie and the camera, along with the camera mount attached with fasteners, while the lower section houses the supporting avionics, including the in-house designed Printed Circuit Board, lithium-ion batteries, and power distribution board (PDB) for the camera.

The CubeSat is constructed using Aluminum 6061, with the outer CubeSat plates attached to the supporting plates using M3 countersunk fasteners to maintain the form factor without any extrusions. The CubeSat is attached to the rocket's bulkhead with M4 fasteners, with no hindrance to the payload's independent functionality.



Figure 23 Section View of Payload

The mounts in the CubeSat are 3D printed with ABS over PLA due to its elevated temperature performance and strength. 3D printing was used due to the convenience of building the required and unique design as per requirement.

The supporting plates for the outer plates of the CubeSat are also made of aluminum and bolted together with eight M3 countersunk bolts. The ABS camera mounts are attached to the top plate using M2 fasteners on one of the corners pertaining to the field of view of the camera and better focal length from the top plate. The bottom plate supports the ABS battery mounts bolted with M2 fasteners, and a vertical mount for the PCB mount is held between the middle and bottom plate with M2 fasteners. The boards are arranged in a shelf manner to avoid direct loading on any avionic components.

Refer to Appendix K for mechanical simulations of CubeSat and Stewie.



Figure 24 4U CubeSat

Stewie comprises of three plates, with the middle and bottom being static, while the top is joined through links being dynamic. The middle and bottom plates are made with steel, considering the loading on the top plate, and sufficient factor of safety is considered. The Top plate is 3D printed from ABS plastic. The base plate is joined to the middle supporting plate of the CubeSat with M3 fasteners, and three servo motors are affixed with M2 fasteners to the middle and bottom plate of Stewie. Suitable links are designed to attach to the servo motors, and these are joined to another set

of links which are affixed to the cots ball joints joining the top plate. The pair of links has revolute motion between them constrained up to 180 degrees. The material used for the links is steel too for the load-bearing capacity of steel.

The middle CubeSat plate has slots on all sides, considering the wiring of the camera mounts passing all the way from the top section to the bottom section, connecting to the 7.4 v batteries. This design has proven to be effective in preventing tangling within itself and with the Stewie components moving along.

F. Propulsions

1. Motor Details

Altair utilizes a COTS motor that was selected through an iterative process to meet various launch requirements, including maximum flight velocity and apogee constraints. After careful consideration, the Cesaroni Technology Pro98 9994M3400-P motor was chosen, which is a reusable 98 mm (3.86 in) M-class motor. Table 5 outlines the motor's performance characteristics, and Fig.26 depicts its certification thrust-time curve. The motor's core is composed of four segments and is manufactured with a proprietary Ammonium Perchlorate Composite Propellant. The grains are liner bonded using a manufacturer-recommended adhesive. The thrust-weight ratio at the lift-off is 11.6. Since there was no visible damage, the team decided to reuse the metal casing from the previous year. We performed an X-Ray Non-Destructive Test (NDT) to confirm that there was no significant damage to the casing. The results of which are included in the appendix.

Table 5 Performance Characteristics of Pro98 M3400-P

Total Impulse	9994.5 N s	(2246.85 lb s)
Specific Impulse	228.92 s	
Average Thrust	3421.1 N	(769.09 lb)
Maximum Thrust	3983 N	(895.41 lb)
Burn Time	2.92 s	

The ignition of the motor is conducted by means of the proprietary pyrogen igniter provided along with the motor, known as ProFire. To ensure dependable ignition and mitigate the possibility of a hangfire, two ignitors will be integrated into the motor. For initiating the ignition, the ESRA-provided ignition system will be employed.

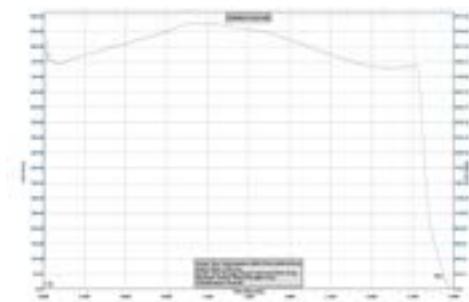


Figure 25 Thrust-Time Curve

G. Avionics

Altair's onboard avionics system consists of the SRAD Primary and Secondary Flight Computers, a COTS Altimeter (RRC3), a COTS GPS (Featherweight GPS), a Flight Camera, and Air Brakes. These components are situated in the midbay, located just below the recovery bay. The midbay is constructed of glass fibre material to promote optimal telemetry link quality between the flight computers and the ground station.

During the assembly of the avionics mount for SA Cup 2022, our team encountered several challenges that were taken into consideration during the design phase. The Avionics Mount serves as a housing unit for the primary flight computer, secondary flight computer, RRC3, Featherweight GPS, and LiPo batteries.

To ensure that the mount is lightweight and robust, it was 3D printed using PLA material. The mount comprises two parts: the battery mount and the FC housing. The battery mount accommodates 5 LiPo batteries, which are zip-tied onto the support. The FC housing is bolted onto the battery mount, and both parts work together to provide a secure and stable housing unit for the avionics components.

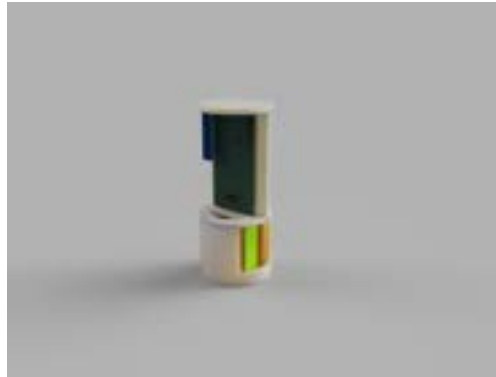


Figure 26 3D Render of Avionics Bay

Two holes are provided on the top of the mount for the recovery and reefing cutter wires, and gaps are made on the FC mount for routing battery wires to the FC. As the body tube is made of GFRP, antennas are taped inside the body tube around the FC, and holes are created on the bay for routing wires from the FC to the camera and pitot.

1. Avionics Mount

The Avionics Mount serves as a housing unit for the THT and SMT flight computers, RRC3, and LiPo batteries, and is 3D printed using PLA due to its lightweight and robust properties. The mount comprises two parts, namely the battery mount and FC housing, with the former accommodating 9 LiPo batteries which are zip-tied onto the support. The battery mount is attached to the avionics bulkhead using M4 bolts, while the FC housing is bolted onto the battery mount.

The flight computer can be inserted into the FC holder and secured using supports. Two holes are provided on the top of the mount for the recovery and reefing cutter wires, and gaps are made on the FC mount for routing battery wires to the FC. As the body tube is made of GFRP, antennas are taped inside the body tube around the FC, and holes are created on the bay for routing wires from the FC to the camera and pitot.

2. Flight Computer[Primary]

The primary SRAD board on Altair serves as the sole flight computer responsible for controlling the rocket's air brakes, ensuring the rocket reaches the desired apogee along with several other functions, including apogee detection and prediction, data-logging, and data-telemetry to the ground station. The Flight Computer is powered by a 7.4v LiPo battery, and the voltage regulators on the computer regulate voltage to 5v and 3.3v for different components. The Teensy 4.1 is the primary compute module on the flight computer. Data-logging is performed on an SD Card mounted on the Teensy 4.1, while data-telemetry is carried out via 2.4 Ghz WiFi modules to the ground station.

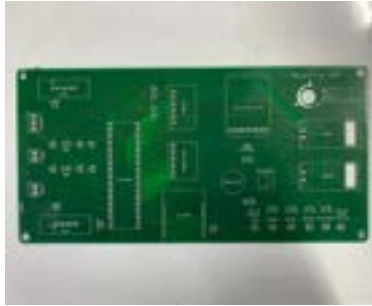


Figure 27 Actual SRAD Primary Flight Computer

3. Flight Computer[Secondary]

The development of a flight computer utilising Surface Mounting Technology (SMT) is a new initiative for our team. With this project, we aim to shift towards SMT-based boards and work with STM-based microcontrollers exclusively. The secondary Flight Computer on Altair serves a critical function in apogee detection and data-logging. The STM32F411 is the primary processing unit on this flight computer. Data-logging is performed on the internal flash of the flight computer, with an external SD Card mounted on the board to provide additional storage capacity. This redundancy is designed to ensure the safety and reliability of the flight data, even in the event of a mishap that results in the loss of the SD Card.



Figure 28 SRAD Secondary Flight Computer

4. COTS Altimeter[RRC3]

The RRC3 from MissileWorks is a highly functional dual-deploy altimeter that uses barometric technology. It has the ability to record multiple flights, up to 15 flights, with a duration of approximately 28 minutes per flight. The device also features an intuitive user interface that allows for easy pre-flight configuration and post-flight analysis through its built-in flight simulator. All of these features are available at an affordable price, making the RRC3 the ideal choice for the project.

5. COTS GPS[Featherweight GPS]

The Featherweight GPS Tracker is a high-performance GPS module with a long-range capability, which uses the LoRa protocol in the 915 MHz band to transmit data up to a distance of 300,000 feet. The extended range, along with its user-friendly interface, makes it a top choice for a commercial off-the-shelf (COTS) GPS module.

8. Ground Station

The ground station is equipped with a 2.4 GHz receiver that receives data from the rocket, which is then processed by its main computation unit, the Teensy 4.1. The processed data is plotted on the SRAD plotter, and also stored on the Teensy 4.1's inbuilt SD card. To keep track of the ground station relative to the rocket, a NEO-6M GPS is also integrated into the ground station.



Figure 31 Ground Station PCB

The plotter is a graphical user interface (GUI) created using Python, designed for visualising live flight data. The data transmitted from the rocket is displayed across multiple plots, enabling a real-time analysis of flight conditions. All the plots feature auto-scaling, with an option for manual scaling as well. The 'start' and 'stop' record buttons facilitate the saving of all values and timestamps to a CSV file. Additionally, the plotter features a 'dummy mode', which plots random values and is activated when no ports are available. Additionally, the plotter includes a real-time 3D rendering of the rocket, providing a visual representation of the rocket's orientation during the flight.

9. Aerocover

The Aerocover has been developed to facilitate the measurement of the rocket's airspeed during flight and to support the RunCam Split 3. The device consists of a hollow housing that is split into two halves, namely, a top and a bottom section. The camera setup and pitot tube are mounted and secured within the housing. The assembly is then attached to the airframe of the rocket using four M3 bolts, which are secured using a nut on the interior of the rocket.

The camera mount is fabricated using ABS+ material through 3D printing technology. In order to withstand the thermal loads experienced during transonic flight and to minimize drag, the surface of the Aerocover has been coated with a layer of varnish. The protective coating renders the surface smooth, which enhances the aerodynamic efficiency of the rocket during its ascent.



Figure 32 Aerocover for Camera and Pitot Mounting

III. Mission Concept of Operations Overview

Altair's primary objective is to attain an altitude of approximately 3048 m (10 000 ft) in line with the International Rocket Engineering Competition (IREC) guidelines, while ensuring a safe and successful recovery. The successful accomplishment of these objectives is crucial for achieving the project's goals of competitiveness and operational safety.

The secondary objective of Altair's mission is to demonstrate the attitude control of a 3-degree-of-freedom (3DOF) parallel manipulator housed in a 4U CubeSat. This objective is to be achieved under extreme conditions characterized by high vibrations, high G-forces, and changing rocket orientation during the flight.

A. Mission Structure

Altair's mission structure consists of eight successive stages: Rocket Preparation, Launch Pad Integration, Arming, Ignition and Lift-off, Powered Ascent, Coasting and Active Air Braking, Apogee and Reefed Parachute Deployment, Disreefing and Secondary Descent, and Landing and Ground Recovery.

Phase 1: Assembly

The assembly process of Altair begins with the installation of the retainer in the motor bay. This retainer is where the stringers are welded to the bottom of the body tube. Afterward, the COTS motor, centering ring, damper, and thrust plate are installed. The thrust plate and damper also secure the coupler to the body tube.

Next, the pre-assembled midbay components, which include the airbrakes, payload, and avionics mount, are inserted into the body tube made of glass fibre. The bulkheads are then attached to the body tube.

The packed parachute, liner, reefing cutters, and shock chords are placed inside the body tube. The recovery bulkhead is fastened to the body tube with the piston cylinder ejection mechanism loaded, and the nosecone is secured on the body tube using shear pins.

Phase 2: Launch Pad Integration

During this phase, Altair is carefully placed on the launch rail and secured in place. The payload electronics are then turned on, and the rail is raised vertically and locked.

Phase 3: Arming

The flight computers are powered on, and all E-matches are checked for continuity. Telemetry and GPS lock are confirmed, and the rocket is made ready for ignition. This phase also involves clearing unnecessary personnel from the launch area and installing the motor igniter.

Phase 4: Ignition ($t = 0.00$ s)

The ignition phase marks the start of Altair's rocket flight. The motor is lit by sending a current through the igniter, and smoke is visible coming out the aft end of the motor.

Phase 5: Lift-off ($t = 0.01$ s)

As the motor produces thrust, the rocket lifts off the rail in just 0.32 seconds, reaching a velocity of 32m/s (105 ft/s).

Phase 6: Powered Ascent ($t = 0.32$ s)

During the powered ascent phase, the rocket accelerates upward under motor power for approximately 3 seconds, reaching an altitude of 510.52 m (1645.41 ft).

Phase 7: Coasting and Active Air-braking ($t = 3$ s)

After the powered ascent phase, the rocket continues to coast until it reaches apogee, which occurs approximately 22 seconds into flight.

During the coasting phase, when the rocket's velocity reduces to 80 m/s (262.4ft/s), the airbrakes are armed to control the altitude and reach the 10,000 ft goal.

Phase 8: Apogee, Parachute Deployment, and Descent ($t=25$ s)

At apogee, the rocket fires its ejection charges, separating from the recovery bay and nosecone into two halves. The parachute inflates, and the rocket falls at a rate of 24 m/s (78.75 ft/s).

Phase 9: Dis-reefing and Secondary Descent ($t=141.3$ s)

The altimeters track the altitude, and upon reaching an altitude of 457 m (1500 ft), the altimeters fire their main charge. This enables the reefing cutter to snip the reefing lines, opening the parachute and leading to a smooth descent velocity of approximately 6.1 m/s (20 ft/s).

Phase 10: Landing and Ground Recovery ($t=213.3$ s)

After the successful completion of the flight, the rocket is located using GPS data received from the Featherweight GPS Tracker and onboard radio Beacon pings. Once found, the rocket's electronics are powered off, and it is taken back to the judges for post-flight evaluation, including data analysis of flight, payload, and airbrake data.

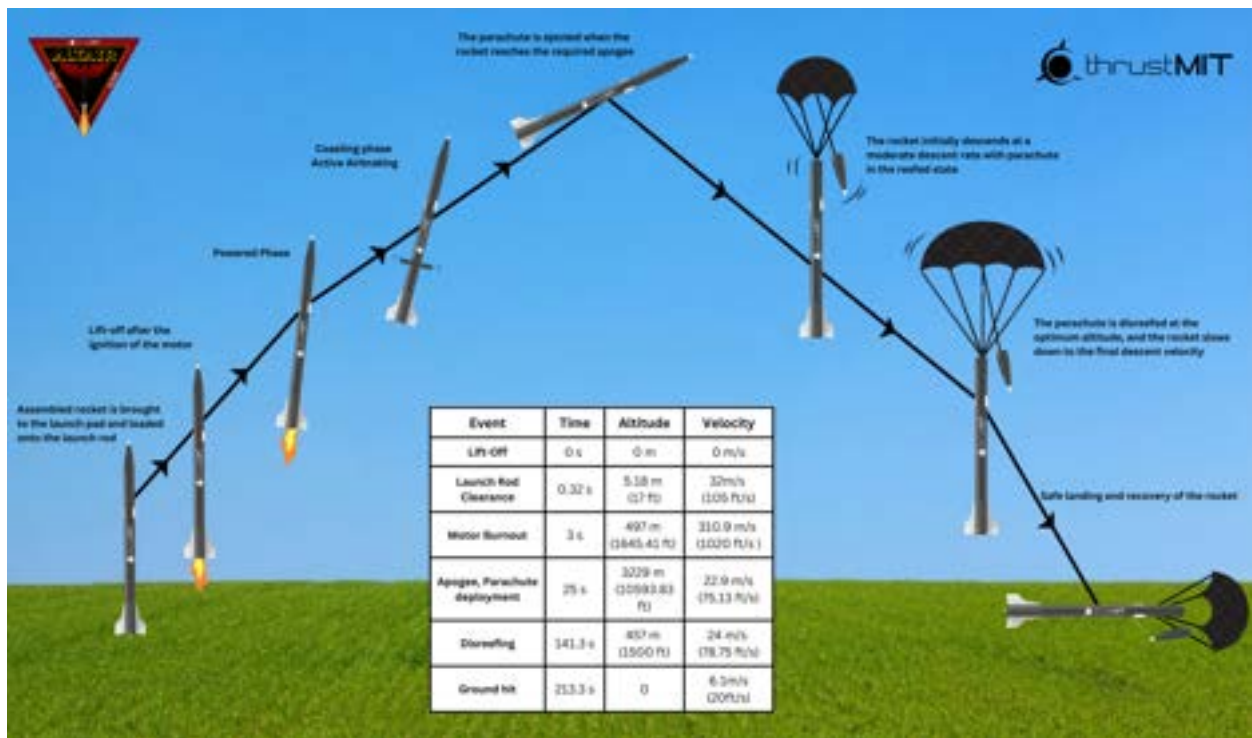


Figure 33 Mission of Concept of Operations

IV. Conclusion & Lessons Learned

Although the team underwent several large changes over the past design cycle, both with respect to project management and technical projects, the strong focus on iteration and learning from previous designs is still prevalent. It has remained the philosophy of the team to innovate and push forward the design of Altair and its supporting equipment.

A. Technical Lessons Learned

1. Leading Edge Extension

Last year, our team focused on integrating innovative fin designs into our rocket and saw a significant improvement in flight performance at the Spaceport America Cup in 2022. This success has motivated us to push our design further and explore new possibilities for even greater efficiency and effectiveness. Our current fin design has great potential, and we are committed to incorporating innovative methods to create an outstanding rocket.

2. Recovery

The Aerodynamics team aimed to improve rocket recovery safety after a previous setback, but faced limitations on flight testing permissions. To increase their chances of success, they dedicated significant time to static ejection tests, refining the recovery process under simulated scenarios. These tests were crucial in allowing the team to analyze rocket behavior and make necessary adjustments for optimal recovery.

3. Layups

During rocket development and assembly, we gained valuable insights regarding CFRP layup shrinkage, component accessibility, and proper part alignment. We realized the importance of providing clearance for metal components and ensuring convenient accessibility for components inside the long body tube. Aligning components with the stringers has proven to be an effective method for proper alignment, critical for safe and reliable operation. These insights have helped us optimize our design and assembly procedures for smooth and safe rocket operation. We will continue to leverage these learnings as we explore new technologies and materials to achieve our goals.

4. Payload

Last year, the payload subsystem aimed to study the effects of vibrations on materials using a piezo sensor. However, due to the rocket's unsafe landing, no data was recorded and the payload suffered minor damages. The team has since focused on rocket development and limited payload experiments to vibrational effects.

To enable future teams to conduct more advanced experiments, the payload team plans to carry out mechanically functional experiments and record data using an onboard SD card. Additionally, they have tested a prototype deployment mechanism for future deployable payloads. This progress could lead to better designs and more advanced scientific experiments in future competitions.

B. Team Management & Operational Lessons Learned

1. The Importance of Documentation in Knowledge Transfer

The pandemic forced our team to reassess its approach to onboarding new members and sharing information. Previously, we relied on in-person communication, with documentation being less of a priority. However, as we were unable to meet in person, we recognized the importance of proper documentation. In response, we implemented new strategies, such as design documents, post-test summaries, and detailed reports, to better analyze and document our systems. Although there is still work to be done, we have made significant progress in our documentation efforts to ensure that we can continue to succeed as a team.

2. Time Management

The team gained valuable experience in managing and leading their subsystem, mentoring new members, and developing essential skills. They dedicated countless hours outside of class to meet project demands and learned the importance of time management, discipline, commitment, and dedication in ensuring success.

Acknowledgements

We would like to thank thrustMIT's faculty advisor Dr. Srinivas G, Assistant Professor - Senior Scale at Manipal Institute of Technology, for his endless support and guidance throughout Altair's design and development process. We would like to thank our college Manipal Institute of Technology, and by extension, our university, Manipal Academy of Higher Education, for graciously providing us with their support and facilities.

The team would like to acknowledge the valuable inputs and recommendations in the design of the rocket by our various mentors and advisors in Manipal Institute of Technology; Dr. Suhas Nayak, Dr. Padmaraj N. H., Mr. Ganesh Nayak, Mr. Nagaraj, Prof. Dilifa Jossley Noronha and Mr. Shrinivas Somayaji. We would also like to acknowledge Dr. Ramya S. Moorthy from Department of Mechatronics for her valuable inputs towards the development of the payload. We would also like to extend our heartfelt gratitude to the Department of Aeronautical and Automobile Engineering, the Department of Mechanical and Industrial Engineering and the Department of Electronics and Communication Engineering for their constant support and assistance.

We would also like to express our gratitude towards our mentor Mr. Bob Schoner, who is serving as our flyer of record and has guided us in optimising the design to ensure a safe and reliable flight.

We are truly grateful for this opportunity to learn and grow, which has been made possible by ESRA, Spaceport, SDL, and all other organisations and individuals involved in conducting this competition and providing us with this wonderful platform.

We want to thank and express our gratitude to all our sponsors and their representatives, without whom this project could not have been completed: PCB Powermarket, Mouser, Altium, Altair, Mavrick Printlab, Babaji Shivram, Simscale, Balaji CNC Technologies, Ansys, Solidworks, Microplacer PCB. Their patronage is deeply appreciated.

Finally, we would like to thank our families and friends whose support has encouraged us at every step.

V. Appendix

A. Appendix: System Weights, Measurements, and Performance Data

A. Rocket Information

Table 6 Rocket Information

Parameter	Value	Source	Optional Comments
Total Length	2705 mm (106.50 in)	CAD	Measured from nose tip to fin end
Airframe Outer Diameter	150 mm (5.91 in)	CAD	
Airframe Inner Diameter	146 mm (5.75 in)	CAD	
Rocket Dry Mass without Motor	22.9 kg (48.28 lb)	ORK	Real life masses were included
Empty Motor Case Mass	3.34 kg (7.37 lb)	Cesaroni official website	
Propellant Mass	4.45 kg (9.81 lb)	Cesaroni official website	
Rocket Wet Mass	30.20 kg (66.58 lb)	ORK	
Payload Mass	4.2 kg (9.23 lb)	CAD	
Number of Stages	1		
Nosecone Length	450 mm (17.72 in)	Measured	Excluding Nosecone Extension
Number of Fins	4	CAD	
Fin Semi-Span	140 mm (5.51 in)	CAD	
Fin Thickness	4 mm (0.61 in)	CAD	
Fin Flutter Velocity	485.51 m s ⁻¹ (1592.88 ft s ⁻¹)	Calculated	
CP at Lift-off	1982 mm (78.03 in)	ORK	
CG at Lift-off	1714 mm (67.48 in)	ORK	
Static Margin at Lift-off	1.85	ORK	

B. Propulsion details

Table 7 Payload details

Parameter	Value	Source
Cluster	No	
Type	Solid	
COTS, SRAD, or Combination?	COTS	
Manufacturer	Cesaroni Technology	
Manufacturer Designation	9994M3400-P	Manufacturer
Total Length	702 mm (27.64 in)	Manufacturer
Casing diameter	98 mm (3.86 in)	Manufacturer
Empty Motor Case Mass	3.34 kg (7.74 lb)	Manufacturer
Propellant Mass	4.45 kg (9.81 lb)	Manufacturer
Motor Wet Mass	8.1 kg (17.87 lb)	Manufacturer
Letter Classification	M	Manufacturer
Total Impulse of All Motors	9994.5 N s (2246.8 lb s)	Manufacturer
Specific Impulse	1982 mm (78.03 in)	Manufacturer
Average Thrust	3241.1 N (769.1 lb)	Manufacturer
Maximum Thrust	3983 N (895.4 lb)	Manufacturer
Motor Burn Time	2.92	Manufacturer

C. Predicted flight data

Table 8 Predicted flight data

Parameter	Value	Source	Optional Comments
Launch Rail	ESRA provided		
Launch Rail Length	4680 mm (184.25 in)	ESRA	Measured from top of the launch rail to the lower rail button
Thrust-to-weight Ratio at Launch Rail	11.6	Calculated	
Launch Rail Departure Velocity	32 m s^{-1} (105 ft s^{-1})	ORK	
Minimum Static Margin During Boost	1.85	ORK	
Maximum Acceleration	126 m s^{-2} (413.39 ft s^{-2})	ORK	
Maximum Velocity	310.9 m s^{-1} ($1020.07 \text{ ft s}^{-1}$)	ORK	
Target Apogee	3048 m (10 000 ft)	-	
Predicted Apogee	3229 m (10 594 ft)	ORK	
Time till Apogee	25	ORK	

D. Recovery Information

Table 9 Recovery Information

Parameter	Value	Optional Comments
COTS Altimeter	MissileWorks RRC3	
Redundant Altimeter	SRAD	
Drogue Deployment Charge (Primary)	3 g (6.6×10^{-3} lb)	4F black powder
Drogue Deployment Charge (Backup)	4 g (8.8×10^{-3} lb)	4F black powder
Main Deployment Charge (Primary)		Reefing cutter
Main Deployment Charge (Backup)		Reefing Cutter
Drogue Deployment Altitude	3229 m (10 594 ft)	Reefed parachute
Drogue Descent Velocity	24 m s^{-1} (78.74 ft s^{-1})	Reefed parachute
Main Deployment Altitude	457.2 m (1500 ft)	Dis-reefed parachute
Main Deployment Descent Velocity	6.1 m s^{-1} (20 ft s^{-1})	Dis-reefed parachute
Ground hit Velocity	6.1 m s^{-1} (20 ft s^{-1})	
Drogue Descent Velocity	213.3s	Measured from motor ignition

B. Project Test Reports

All test videos have been uploaded here.

A. Avionics

Table 10 Avionics Tests

Date of Test	Name of Test	Objective	Inference	Result
13.02.2023	Battery Drain Test	Validating the power requirements of Avionics	When connected to TS835, the battery drained out in 22.5 minutes	FAIL
15.02.2023		Validating the power requirements of Avionics	When connected to SRAD Flight Computer, the battery lasted for 6 hours and had enough capacity left to last for few more hours.	SUCCESS
08.03.2023	Pitot Testing	Validating the MPX5100DP transducers in the Wind Tunnel	Wrong calibration factor leading to wrong values	FAIL
28.03.2023	Pitot Testing	Validating the MPX5100DP transducers in the Wind Tunnel	Successful calibration and validation of the velocity values	SUCCESS
26.03.2023	Vacuum Test RRC3	Validating the performance of RRC3 Altimeter	RRC3 Altimeter was able to detect apogee	SUCCESS
26.03.2023	Vacuum Test SRAD FC	Validating the performance of SRAD Flight Computer	Primary SRAD fired drogue	SUCCESS
04.04.2023	Vacuum Test SMT SRAD FC	Validating the apogee detection test	The flight computer was able to detect apogee	SUCCESS
07.04.2023	Range Test	Validating the range and various types of antennae.	All antennae were validated with our telemetry modules' with a minimum range of 3.5km.	SUCCESS

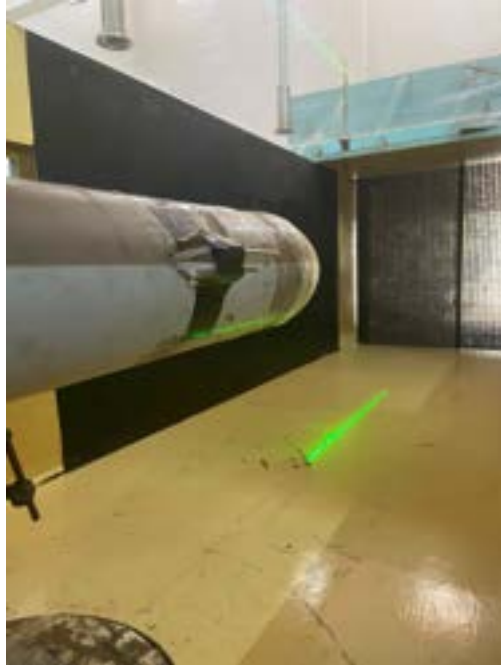


Figure 34 Pitot Testing



Figure 35 Telemetry Test

B. Recovery

Table 11 Recovery Tests

Date of Test	Parachute Folding	Orientation	Inference	Result
Ejection test				
01.11.2022	Conventional	Horizontal	Charge was inefficient, Pressure leak from the bottom of the recovery bay, nosecone was forced into the bay hence was tight	FAIL
01.11.2022			Shear pins did not break, had deep pressurization issues and too much space between the parachute and WPC bulkhead. Duct tape was used. Double spark was observed.	
19.12.2022			Shear pins broke but nosecone did not separate. Parachute caught fire. A lot of pressure leak because of the stringer slots and the clearance between the bulkhead and the body tube.	
05.02.2023	Conventional	Horizontal	Shear pins broke, nosecone separated, and the parachute came out.	SUCCESS
10.02.2023			Shear pins broke but the nosecone could not pull the parachute out since it did not travel much	
14.02.2023			Shear pins broke, nosecone separated, and the parachute came out partially. Inclination angle was increased.	

26.02.2023	Conventional	Horizontal	Improper use of E-match which may have led to the failure of the test (The ematch was not in direct contact of the black powder), Piston was very tight.	FAIL
05.04.2023			Success but set up did not have required support	SUCCESS
06.04.2023	Suspension lines are wrapped differently	Vertical	Shear pins broke, nosecone separated but the parachute didn't come out. Deployment bag and the parachute burned. Pressure leak and improper folding of parachute could be probable reasons. Stuffed Kevlar to prevent the leak.	FAIL
04.05.2023	Conventional		Shear pins broke, nosecone flew, and the parachute came out.	SUCCESS
Reefing test				
19.03.2023		Running with reefed parachute and then dis-reefing the parachute	Loose connection of reefing wires	FAIL
19.03.2023	-		Parachute disreefed successfully and complete inflation of canopy was achieved	SUCCESS
COTS Reefing Cutter test Date				
02.03.2023	-	Placed the reefing cutter with the lines inside on the ground	The weather was very humid, black powder got damp and the wires were shorted.	FAIL
03.03.2023			Worked perfectly; and the same was repeated for reefing tests	Shear pins broke, nosecone flew, and the parachute came out. A lot of pressure leak was observed from the bottom of the recovery bay.



Figure 36 Reefed Parachute



Figure 37 Dis-Reefed Parachute



Figure 38 Reefing Cutter



Figure 39 Reefing Line

C. Payload

Table 12 Payload Tests

Date of Test	Name of Test	Objective	Inference	Result
04.02.2023	Stewie Prototype	Movement in the links according to the input fed by the servo using teensy micro-controller.	When the servo revolves to-and-fro from 0 to 180, the links were moving accordingly but not together. Motor had more amps of current passing through it.	FAIL
13.03.2023	Battery Drain Test	Validating the power requirements of Payload	When connected to TS835, the battery drained out in 47 minutes	FAIL
24.03.2023	Battery Drain Test	Validating the power requirements of Payload	When connected to Payload PCB, the battery lasted for 6 hours and had enough capacity left to last for few more hours.	SUCCESS
04.04.2023	Stewie Prototype	Response to MPU feedback and tallying it with the hand calculations.	The feedback was received, and all the links moved simultaneously together and the values were tallying but the deviation of error of less than 5 percent was seen.	SUCCESS



Figure 40 Payload Prototype Test

C. Appendix: Hazard Analysis

Table 13 Hazard Analysis Matrix

Hazard	Possible Causes	Risk of Mishap and Rationale	Mitigation Approach	Risk of Injury after Mitigation
Burns, respiratory problems due to propellant grain ignition	Inadvertent ignition of propellant in confined spaces	Low, commercially manufactured propellant grain	Safe storage and handling as per manufacturer guidelines in open spaces	Very Low
Skin irritation due to contact with igniter	Improper handling of the igniter resulting in direct contact with ignition charge	Very Low, the igniter is packed in a suitable container	Igniter stored in a cool, dry place and within its packaging until loading into the motor, igniter handled by essential personnel	Very Low
Burns to due inadvertent ignition of ejection charge	Improper handling, ignition sources nearby during handling	Medium	Storing in a cool, dry place and handling with adequate fire-proof safety equipment away from any ignition sources	Low
Skin irritation due to motor adhesive being absorbed by the skin	Exposure to adhesive without safety gear	Medium, improper handling of adhesives during assembly, packaging failure during handling	Wearing proper safety gear (gloves, masks and goggles as per OSHA and manufacturer guidelines), safety briefing before the start of assembly	Low
Eye irritation due to motor adhesive coming in contact with the eyes				
Hand tool Injury	Improper training or human error during the use of tools	Low; Injuries include cuts, scrapes	Members are given proper training and wear proper PPE specific to each tool.	Low
Burns, injury due to ignition of LiPo battery	Improper handling of the battery.	Low	LiPo transported in special LiPo safe bags and stored in cool, dry places.	Very Low
Exposure to Epoxy	Improper PPE worn during lay-up or storage	Low; Eye and skin irritation, Chemical burns	When working with epoxy, members will wear appropriate PPE.	Low

Hazard	Possible Causes	Risk of Mishap and Rationale	Mitigation Approach	Risk of Injury after Mitigation
Injuries due to recovery failure	Failure of altimeter or poor packing of the parachute.	Medium; The rocket parts are in freefall and can injure the spectators or any personnel.	The altimeter will be calibrated properly, and the parachute will be packed properly.	Low
Skin irritation and rashes	Allergic reactions to composite dust	Medium	The dust (if any) should be removed with the vacuum cleaner and disposed of properly. Gloves and other safety equipment should be worn.	Low
	Cuts		Gloves and other safety equipment should be worn while handling composites. Sharp edges on unprocessed parts should be sanded down.	

D. Appendix: Risk Assessment

Table 14 Risk Analysis Matrix

Risk	Possible Causes	Risk of Mishap and Rationale	Mitigation Approach	Risk of Injury after Mitigation
Explosion of solid-propellant rocket motor during launch with blast or flying debris causing injury - CATO	Cracks in propellant grain	Low; certified COTS motor and propellant	Visually inspect grain for visible cracks and imperfections before assembly	Very Low
	Debonding of propellant from wall		Proper cleaning and preparation of the case liner as per manufacturer instructions	
	Gaps between individual propellant segments and between the last segment and the nozzle		Ensure all fits are as per manufacturer specifications	
	Chunk of propellant breaking off and plugging the nozzle		Inspect motor case for damage during final assembly of the motor before launch	
	Motor fails during launch due to manufacturer errors		Motor only used if in proper visual condition on delivery, only essential personnel in the launch crew, crew to vacate to a safe distance behind an adequate barrier before launch	
Deployment charge ignition on the launch rail	The COTS altimeter/relay on the SRAD Flight Computer might misfire.	Medium	The device shall be armed immediately before the vacation of the launch area by essential personal. The SRAD Flight Computer is encoded to fire deployment charges only after lift-off is detected.	Low
Deployment charge ignition before the intended apogee during flight	Inadvertent command sent by SRAD flight computer	Medium	the SRAD flight computer is inhibited from sending the command during boost phase and is programmed to send the command if the pressure values rise for 3 consecutive samples	Low

Risk	Possible Causes	Risk of Mishap and Rationale	Mitigation Approach	Risk of Injury after Mitigation
Motor falls off launch vehicle	Motor is not secured properly.	Very Low; The motor could possibly go into freefall during the flight. If it is still ignited, it may harm personnel in the vicinity or destroy the launch vehicle.	The motor will be installed by a certified mentor. The motor retention system will also be inspected prior to launching the rocket.	Low
Motor ignition during assembly/transport	Misfire of triggering circuit at the receiver end of the ignition system.	Low; COTS Ignition system	The igniter is connected to the motor right before the launch pad is cleared and the firing lines are ensured to be powered down before the connection is made	Very Low
	The propellant is to be stable up to 75 °C (167 °F) and drop tested for impact stability from a height of 12 m (39.37 ft) as per UN test series 3(c) and 4(b) by the manufacturer	Low	The igniter will be loaded into the motor once the rocket is on the launch rail and fully ready for flight will all electronics armed only. Motor shall be stored and assembled as per manufacturer guidelines. Assembly of the motor will only be done by essential personnel in the presence of TRA L3 certified personnel.	Very Low
Motor fails to ignite	Ground support equipment failure; humid weather	Very Low; launch does not occur.	Motor will be stored according to guidelines specified.	Very Low
Rocket deviates from nominal flight path, comes in contact with personnel at high speed	The stability might waver due to poor manufacturing of the fins, inadequate anchoring of the launch rod to the ground, failure of rail buttons during launch	Medium; fins have been made using suitable grade materials	The fins must be checked for any defects/damage before the launch; the rail buttons must be tightly secured and placed into a sturdy launch rod	Low

Risk	Possible Causes	Risk of Mishap and Rationale	Mitigation Approach	Risk of Injury after Mitigation
Recovery system fails to deploy, rocket or payload comes in contact with personnel (ballistic descent trajectory)	Clumsy packing and storing of parachute, charge required was not sufficient; electrical connections may have faltered, detection of apogee by altimeter was not proper	Low; testing of deployment mechanism has been taken place to ensure a smooth recovery	Make sure the parachute has been folded using the proper technique, cautiously weigh the amount of charge being used, check to see if the signals are passed through the connections or not	Low
Melted or damaged parachute	Parachute is not protected from the fire of the ejection mechanism.	Medium; Could prevent parachute from slowing down the rocket which could result in loss of rocket	Ensure that the parachute is sealed from possible fire by use of parachute liner, duct tape and wadding paper	Low
Shock cord breaks	The shock cord is not strong enough to handle the jerk loading and could be burnt due to charge detonation.	Low; The parachute could detach from rocket resulting in failure of proper recovery of the rocket	Ensure that the shock cord can handle the jerk load, use shock cord made from aramid fibres and are wrapped with wadding paper.	Low
Descent rate is too slow	The size of the parachute is larger than required.	Low; The rocket lands far away or outside of landing range.	The proper size of the parachute is calculated to give optimum speed and tested before launch.	Low
Main (disreefed) parachute is deployed at apogee	Accidental firing of main charge by the Altimeters, faulty connections while assembling the rocket	Low	The altimeters are configured to fire the main charge only after they've passed a certain altitude during the descent phase. Wiring is verified before launch	Very Low

Risk	Possible Causes	Risk of Mishap and Rationale	Mitigation Approach	Risk of Injury after Mitigation
Reefing failure causing main parachute not to deploy	Reefing cutter failure, poor electrical connections, sensor failure, battery failure	Medium	LiPo batteries used in the rocket are handled with all necessary precautions and care before and during flight. Wiring connections are tested before flight to fix any loose connections. Sensors are tested on ground multiple times to ensure they work properly during the flight, redundant systems are placed in the rocket to account for sensor, battery or reefing failure	Low
Recovery system partially deploys, the rocket or payload comes in contact with personnel	The packed parachute might have tangled suspension lines or shock cords; faulty shear pins have been attached	Medium; suspension line may tangle during deployment	When packing the parachute, the suspension lines and shock cords must be placed carefully, so they do not tangle up while deploying	Low
Rocket does not ignite when the command is given ("hang fire") but does ignite when the team approaches to troubleshoot	Ignitor partial failure	Low	Utilise two igniters for launch and observe the rocket for a few minutes to either allow non-visible combustion to reach a steady state (thereby resulting in an instantaneous TW $R > 1$) or to "cool off" any combustion remnants	Very Low
Rocket falls from launch rail during prelaunch preparations, causing injury	Improper handling of the rocket	Low	Handling of the only by essential personnel who are capable in performing prelaunch operations	Very Low
Nosecone splits into two halves in-flight	Improper attachment of two halves during layup process	Low	The Nosecone must be inspected for any weak point before assembly; The nose tip and Nosecone bulkhead must be attached securely	Low

Risk	Possible Causes	Risk of Mishap and Rationale	Mitigation Approach	Risk of Injury after Mitigation
Bolt holes in the body tubes and couplers undergo bearing failure in-flight	Insufficient stress concentration clearances given while drilling holes	Low	Adequate clearances must be given while drilling bolt holes in all components; reinforcements must be provided in case a proper clearance can't be provided	Low
Fins shear during flight	Failure of the fin attachment welds or failure of the stringers	Medium	The fins are seam welded using TIG welding to the stringers which are securely fastened to the body tube, centering ring and thrust plate; A specially designed jig is used to ensure positional accuracy of the fins during the welding process.	Low
Fin Flutter	Poor design of fins. Improper attachment of the fins to the stringer.	Low; The rocket would not follow the ideal trajectory and drifts away. On long exposure to this phenomenon, the fins may break.		Low
Aerocover Falls off from rocket	It may not be secured properly on the rocket.	Very Low; Airbrakes may malfunction as the pitot tube flails around. Rocket may not reach desired apogee.	The launch members ensure that the aerocover is mounted and secured properly on the rocket using bolts and adhesives	Very Low
Failure to recover rocket	Recovery team fails to follow and locate the rocket	Low; Unsuccessful recovery of rocket and loss of valuable data.	Proper coordination with the team using radios and keeping in touch with RSO to coordinate movements.	Low
Failure to arm the rocket	Wiring error due to congestion inside the bay, switches fail to arm due to manufacturing fault.	Low	The switches must be tested before mounting them on the rocket. The wires from the switches to the avionics need to be managed and arranged in a non-congested manner to prevent disconnection.	Low

Risk	Possible Causes	Risk of Mishap and Rationale	Mitigation Approach	Risk of Injury after Mitigation
Telemetry Failure	The switches must be tested before mounting them on the rocket. The wires from the switches to the avionics need to be managed and arranged in a non-congested manner to prevent disconnection.	Medium; use of metallic and carbon fiber-like materials in the avionics bay.	This can be prevented through multiple tests with various antennas and material casing. As for the antenna the issue can be solved by matching the polarization of the rocket telemetry antenna and the ground station antenna.	Low

E. Appendix: Assembly, Pre-Flight, Launch and Recovery Checklists

- Pre-Launch Checklist

- ☐ Check and ensure that all avionics switches are in the dis-armed position.
- ☐ Perform a visual check to ensure the integrity of the rocket body and have the flight safety review.
- ☐ Submit vehicle for the launch safety inspection.
- ☐ Fill in and submit the flight card to the Launch Control Officer.
- ☐ At the appointed time, transport the rocket to the launch pad accompanied by required personnel only.
- ☐ Ensure launch pad and surrounding area are clear of all combustible material.
- ☐ Slide the rocket onto the launch rail.
- ☐ Perform a final visual inspection of the rocket to check for any damage during transportation.
- ☐ Raise the rocket and the rail to launch orientation.
- ☐ After obtaining all necessary clearances, enable the Altimeter and Flight Computer's power supplies and payload's power supply.
- ☐ Listen for an audible beep to confirm a successful power up and arming.
- ☐ Power on the camera.
- ☐ Communicate with ground station to verify successful telemetry link.
- ☐ Acquire permission from Range Manager to insert the igniter.
- ☐ Check for continuity and then proceed to insert the igniter into the motor, leaving the leads unconnected.
- ☐ Cross check if the firing line is not "hot".
- ☐ Confirm non-essential personnel have evacuated the launch pad area.
- ☐ Authorised personnel shall connect the igniter to the firing line.

- Motor Bay Assembly
 - ☐ Assemble the Motor.
 - ☐ Attach fin-welded stringers to the retainer and the centering ring and place the motor on the retainer.
 - ☐ Secure the damper and the thrust plate onto the stringers and fasten them to the body tube through the coupler.
- Mid Bay Assembly
 - ☐ Install the batteries to the avionics mount along with the SRAD and COTS flight computers. Ensure that the wiring connections are secure and proper.
 - ☐ Assemble the 4U CubeSat with the payload (Stewie) inside it.
 - ☐ Fasten the servo to the airbrake's housing mount which is fastened to the airbrake's frame.
 - ☐ Assemble the mid-bay stringers to the airbrakes, payload, and avionics mount with the help of their respective bulkheads in that order.
 - ☐ Fasten the mid-bay setup to the body tube.
- Recovery Bay Assembly
 - ☐ Attach reefing lines, reefing cutters, and reefing wires to the parachute which is then folded and kept inside the parachute liner.
 - ☐ Attach shock chords, quick link, and swivel link to the parachute. Tie the other end of the shock chords to the eyebolt on the recovery bulkhead and to a U-Bolt on the nosecone bulkhead respectively.
 - ☐ Fasten the recovery bulkhead to the body tube with the piston cylinder ejection mechanism loaded.
 - ☐ Place the folded parachute inside the body tube after wrapping the shock chords and the reefing wires with wadding paper.
 - ☐ Secure the nosecone on the body tube using shear pins.
- Payload Assembly
 - ☐ Assemble Stewie
 - ☐ Assemble CubeSat with 2 adjacent plates.
 - ☐ Stack batteries and place them on CubeSat.
 - ☐ Fasten cameras, PDB boards, PCB and MPU sensor on their mounts and place the mounts on their assigned place.
 - ☐ Place Stewie on the middle plate and fasten it.
 - ☐ Connect wires and make sure that they don't interfere with the mechanism.
 - ☐ Ensure all parts are in their place and fastened properly and then bolt the remaining plates of the CubeSat.

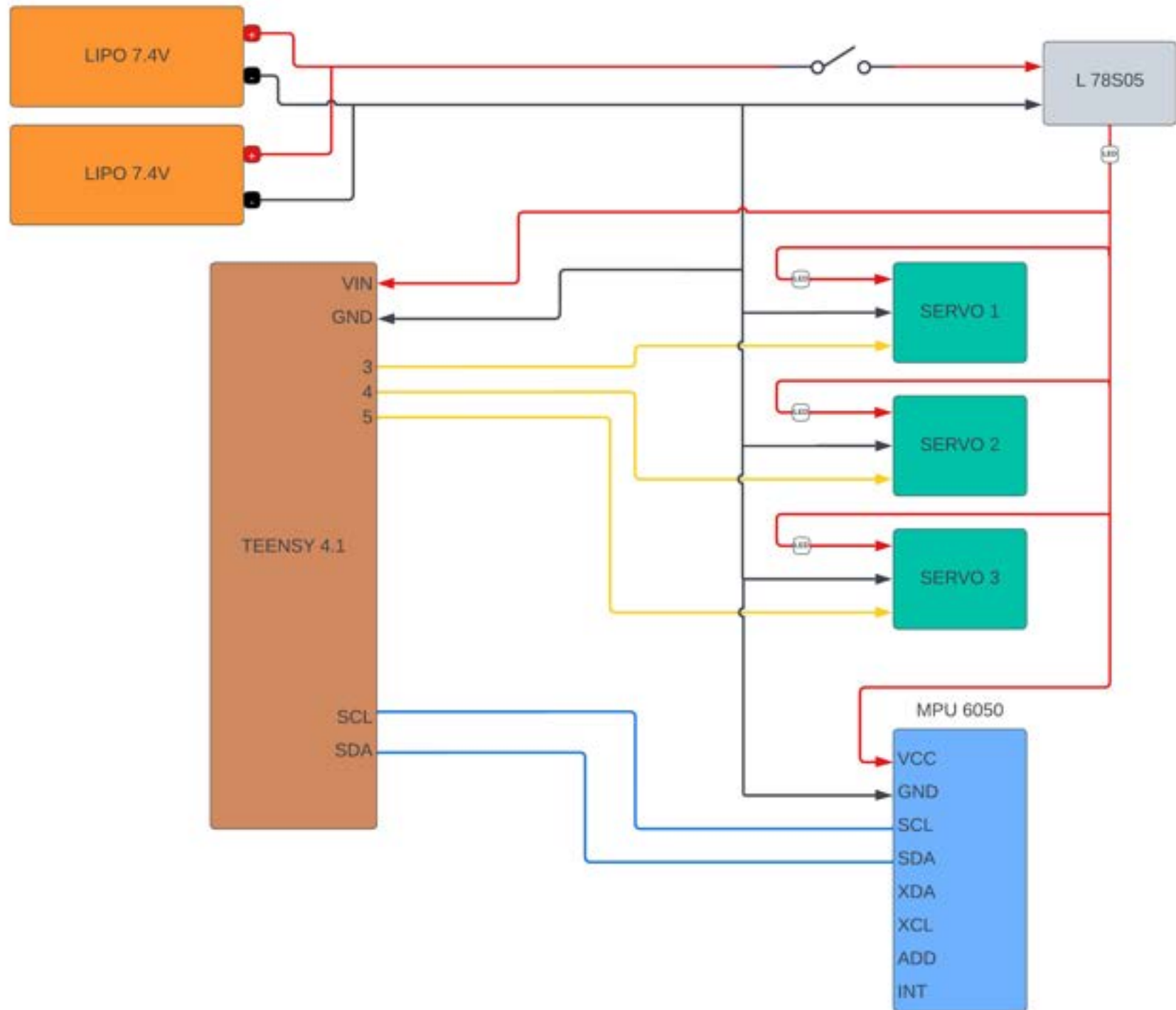
- Recovery Checklist

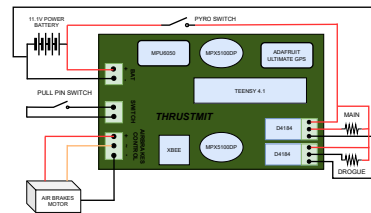
- ☐ Note the approximate location and heading of the rocket during its descent until it lands.
- ☐ Report the location and status of the recovery team to the MCC.
- ☐ If the team could not keep track of the rocket, they should contact the MCC via their recovery backpack radio. They should then provide their Team Identification Number. The MCC will provide the recently updated coordinates received.
- ☐ Upon arrival on the landing site, take photos of the site and launch vehicle.
- ☐ Verify that all energetics are spent.
- ☐ Disconnect all the batteries and recover the data storage devices.
- ☐ Inspect the airframe for damage.
- ☐ Inspect the recovery system for damage or tangling.
- ☐ Secure Payload
- ☐ Secure all parts of the rocket.
- ☐ Disassemble the rocket and place them on the loading bay of the pickup truck.
- ☐ Report back to the MCC and provide them with flight data.
- ☐ Return to the team setup area.
- ☐ Inspect internal components for damage.
- ☐ Remove and clean the motor casing.
- ☐ Pack the parachute setup.

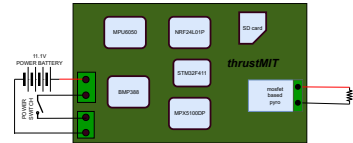
F. Appendix: Wiring Diagrams

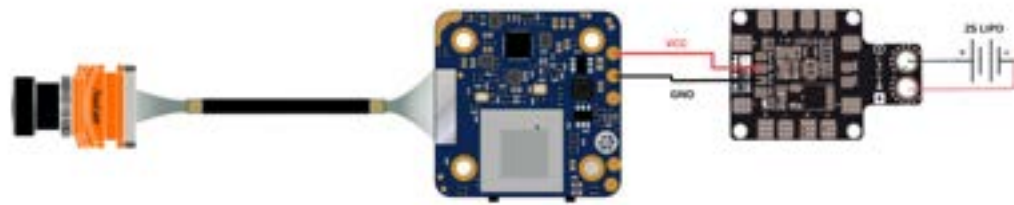
**THIS PAGE INTENTIONALLY LEFT BLANK.
APPENDIX BEGINS ON THE FOLLOWING PAGE.**

PAYLOAD WIRING DIAGRAM











G. Appendix: Team Structure

thrustMIT comprises approximately 30 undergraduate members studying various domains of engineering at Manipal Institute of Technology. Although all the active members are undergraduates, the team also consults the alumni for their constructive inputs. Team Leads have the responsibility of overseeing the overall management of projects and providing guidance to the team. This includes supervising technical, administrative, and operational activities necessary to achieve the main objectives and goals. Subsystem Leads, on the other hand, are accountable for managing specific sections of the rocket and ground support equipment, such as avionics, aerostructures, recovery, propulsion, and payload. They are in charge of ensuring the timelines, integration, and development of each project within their subsystem. Project Leads, selected based on their experience, skill set, and interest, take the lead in technical projects. They are responsible for coordinating and managing all aspects related to their projects, including design, manufacturing, and testing, as well as ensuring the successful integration of their project with other vehicle and ground systems. Team members have the freedom to choose and work on projects that interest them, often collaborating with other sub-teams. The Operations Lead is responsible for overseeing all logistics and procedures related to launch and propulsion testing.

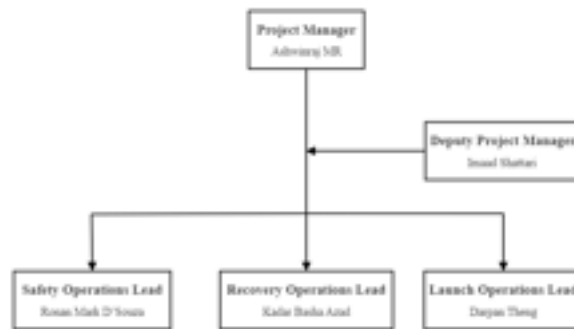


Figure 41 Team Leadership



Figure 42 Team Structure

A. Faculty Advisor
Dr. Srinivas G.

Assistant Professor - Senior Scale, Department of Aeronautical & Automobile Engineering, Manipal Institute of Technology, Manipal Academy of Higher Education

B. Team Mentors
Bob Schoner

TRA L3, Flyer of Record; Assistant Manager - Advanced Engineering Design Lab, Virginia Tech

C. Project Leads
Ashwinraj MR
Imaad Shattari
Ronan Mark D'Souza
Darpan Theng
Aastha Bhatnagar
Sharada Belagavi
Utkarsh Anand
Tanvi Agarwal
Arjun Chhabra

Team Leader, Aerodynamics Head; B.Tech Aeronautical Engineering, Batch of 2024
Team Manager; B.Tech Aeronautical Engineering, Batch of 2024
Avionics Head; B.Tech Data Science & Engineering, Batch of 2024
Controls Head; B.Tech Aeronautical Engineering, Batch of 2024
Structures Head; B.Tech Aeronautical Engineering, Batch of 2024
Propulsions Head; B.Tech Aeronautical Engineering, Batch of 2024
Payload Head; B.Tech Electrical & Electronics Engineering, Batch of 2024
Research Head; B.Tech Mechanical Engineering, Batch of 2024
Management Head; B.Tech Aeronautical Engineering, Batch of 2024

D. Aerodynamics Team
Kadar Basha Azad
Aiyaz Karani
Vedang Bhosale

B.Tech Aeronautical Engineering, Batch of 2024
B.Tech Mechatronics, Batch of 2025
B.Tech Aeronautical Engineering, Batch of 2025

E. Avionics Team**Anway Das****Aman Soni****Anne Monish****Keeratraj Singh****Satwik Agarwal**

B.Tech Electrical & Electronics Engineering, Batch of 2024

B.Tech Electrical & Electronics Engineering, Batch of 2025

B.Tech Computer & Communication Engineering, Batch of 2025

B.Tech Mechanical Engineering, Batch of 2025

B.Tech Computer Science Engineering, Batch of 2025

F. Structures Team**Aryaman Gadiya****Gangarapu Jayadeep****Dhruva Karanth****Parth Jain**

B.Tech Aeronautical Engineering, Batch of 2024

B.Tech Mechanical Engineering, Batch of 2024

B.Tech Aeronautical Engineering, Batch of 2025

B.Tech Aeronautical Engineering, Batch of 2025

G. Propulsions Team**Raeid Mukadam****Vedansh Mittal****Kripal**

B.Tech Mechanical Engineering, Batch of 2024

B.Tech Industrial & Production Engineering, Batch of 2025

B.Tech Aeronautical Engineering, Batch of 2025

H. Payload Team**Diya Parekh****Thakur Pranav Singh****Hrishikesh Singh****Joshvir Singh**

B.Tech Mechatronics, Batch of 2024

B.Tech Mechanical Engineering, Batch of 2024

B.Tech Data Science & Engineering, Batch of 2025

B.Tech Computer Science Engineering, Batch of 2025

I. Management Team**Devika Subash****Vinoy S.****Bharat Dutta****Chalamala Mahesh**

B.Tech Chemical Engineering, Batch of 2025

B.Tech Chemical Engineering, Batch of 2025

B.Tech Mechanical Engineering, Batch of 2025

B.Tech Electronics & Communication Engineering, Batch of 2025

H. Appendix: MATLAB Code for Fin Flutter

```

1  %% CODE FOR CALCULATING FIN FLUTTER VELOCITY %%
2  close all
3  clc
4  clear all
5
6  %% CONSTANTS %%
7  H = [0:100:3300]; % m (HEIGHT [AGL])
8  H1 = [1400:100:4700]; % m (ACTUAL HEIGHT)
9  T0 = 306; % K (TEMPERATURE)
10 P0 = 101325; % Pa (PRESSURE)
11 a0 = 353; % m/s (SPEED OF SOUND)
12 G = 24e+9; % Pa (SHEAR MODULUS OF TORSION)
13
14 %% VARIATION WITH HEIGHT %%
15 T = T0 - 0.0065 .* H1; % K
16 P = P0 .* (1 - 0.0065 .* (H1./T0)) .^ 5.2561; % Pa
17 a = a0 + 0.606 * ((5 / 9) .* (T - 32)); % m/s
18
19 %% FIN DIMENSIONS %%
20 b = 0.14; % m (FIN SEMISPAN)
21 cr = 0.45; % m (ROOT CHORD)
22 ct = 0.15; % m (TIP CHORD)
23 tmax = 0.004; % m (THICKNESS OF FIN)
24 %S = 0.5 * b * (cr + ct); % m^2 (FIN AREA) % Not valid as fin is not a simple
    trapezoidal geometry
25 S = 0.036; % HARD-CODED FIN AREA (WITH LEE)
26 AR = b^2 / S; % (FIN ASPECT RATIO)
27 TR = cr / ct; % (FIN TAPER RATIO)
28
29 %% FORMULA %%
30 Vf = a .* sqrt((G .* 2 .* (AR + 2) .* (tmax ./ cr) .^ 3) ./ (1.337 .* AR .^ 3 .* P .* (
    TR + 1)));
31
32 SVf = (1/1.5) .* Vf; % Safe Flight Velocity
33
34 %% IMPORTING DATA %%
35 A = xlsread('Altair_FFV.xlsx', 'A1:A522'); % Velocity
36 B = xlsread('Altair_FFV.xlsx', 'B1:B522'); % Height
37
38 %% GRAPH %%
39 plot (H,Vf,'-k')
40 hold on
41 plot (H, SVf, '-r')
42 plot (B,A,'-b')
43 legend ('Flutter Velocity', 'Safe Flight Velocity', 'Rocket Velocity');
44 grid on
45 xlabel('Altitude (m)');
46 ylabel('Velocity (m / s)');
47 title('Fin Flutter Velocity Vs Rocket Velocity');

```

I. Non-Destructive Test(NDT) Results of Motor Casing



Figure 43 Section 1A



Figure 44 Section 1B



Figure 45 Section 2A



Figure 46 Section 2B

J. Appendix: Payload

A. Degrees of Freedom

The degrees of freedom of Stewie were calculated using Grubler's formula:

$$F = 6(N - 1 - J) + \sum_{i=1}^k (F_i * J_i) \quad (6)$$

$$F = 6(8 - 1 - 9) + \sum (F_i * J_i) = (1 * 6) + (3 * 3) = 15 \quad (7)$$

DoF= 3

Where,

N= number of links= 8

J= number of joints= 9

F_i = degrees of freedom of a joint

J_i = number of joints with the same degree of freedom

B. Position of Ball Joints

To find the position matrix, forward kinematic calculations were performed. The position matrix of the top plate with respect to the base plate was represented by T_T^B , and the position matrix of the ball joint with respect to the top plate frame was represented by T_P^T . To obtain the position matrix of the ball joint with respect to the base frame, the matrices T_T^B and T_P^T were multiplied. The position matrix of the ball joint with respect to the base frame is represented by T_P^B .

$$T_P^B = T_T^B * T_P^T \quad (8)$$

$$T_T^B = \begin{bmatrix} \cos\theta_Z * \cos\theta_Y & -\sin\theta_Z * \cos\theta_X + \cos\theta_Z * \sin\theta_Y * \sin\theta_X & \sin\theta_Z * \sin\theta_X + \cos\theta_Z * \sin\theta_Y * \cos\theta_X & 0 \\ \sin\theta_Z * \cos\theta_Y & \cos\theta_Z * \cos\theta_X + \sin\theta_Z * \sin\theta_Y * \sin\theta_X & -\cos\theta_Z * \sin\theta_X + \sin\theta_Z * \sin\theta_Y * \cos\theta_X & 0 \\ -\sin\theta_Y & \cos\theta_Y * \sin\theta_X & \cos\theta_Y * \cos\theta_X & Z_T^B \\ 0 & 0 & 0 & 1 \end{bmatrix}$$

$$T_P^T = \begin{bmatrix} 1 & 0 & 0 & x \\ 0 & 1 & 0 & y \\ 0 & 0 & 1 & z \\ 0 & 0 & 0 & 1 \end{bmatrix}$$

$$T_P^B = \begin{bmatrix} \cos\theta_Z * \cos\theta_Y & -\sin\theta_Z * \cos\theta_X + \cos\theta_Z * \sin\theta_Y * \sin\theta_X & \sin\theta_Z * \sin\theta_X + \cos\theta_Z * \sin\theta_Y * \cos\theta_X & X_p \\ \sin\theta_Z * \cos\theta_Y & \cos\theta_Z * \cos\theta_X + \sin\theta_Z * \sin\theta_Y * \sin\theta_X & -\cos\theta_Z * \sin\theta_X + \sin\theta_Z * \sin\theta_Y * \cos\theta_X & Y_p \\ -\sin\theta_Y & \cos\theta_Y * \sin\theta_X & \cos\theta_Y * \cos\theta_X & Z_p \\ 0 & 0 & 0 & 1 \end{bmatrix}$$

Where,

$$X_p = (\cos\theta_Z * \cos\theta_Y) * x + (-\sin\theta_Z * \cos\theta_X + \cos\theta_Z * \sin\theta_Y * \sin\theta_X) * y + (\sin\theta_Z * \sin\theta_X + \cos\theta_Z * \sin\theta_Y * \cos\theta_X) * z$$

$$Y_p = (\sin\theta_Z * \cos\theta_Y) * x + (\cos\theta_Z * \cos\theta_X + \sin\theta_Z * \sin\theta_Y * \sin\theta_X) * y + (-\cos\theta_Z * \sin\theta_X + \sin\theta_Z * \sin\theta_Y * \cos\theta_X) * z$$

$$Z_p = (-\sin\theta_Y) * x + (\cos\theta_Y * \sin\theta_X) * y + (\cos\theta_Y * \cos\theta_X) * z + Z_T^B$$

The new coordinates of the ball joint (output) are represented by X_p , Y_p , and Z_p , which are determined by the angles of deviation (input) along the X, Y, and Z axes of the top plate (θ_X , θ_Y , θ_Z), and the coordinates of the ball joint (x, y, z) when the top plate is in its initial position. The distance between the base frame and the top plate is represented by Z_T^B . (X_p , Y_p , and Z_p) will be input for finding the desired angle of rotation of the motor, α_k .

C. Desired angle of rotation of motor

$$X_K = M_K + R_Z(\theta_K)R_Y(-\alpha_K) \begin{bmatrix} |l_1| \\ 0 \\ 0 \end{bmatrix} = M_1 + |l_1| \begin{bmatrix} \cos \alpha_K \cos \theta_K \\ \cos \alpha_K \sin \theta_K \\ \sin \alpha_K \end{bmatrix} \quad (9)$$

$$|l_1|^2 = (X_K - M_K)^T \cdot (X_K - M_K)$$

$$|l_2|^2 = (P_K - X_K)^T \cdot (P_K - X_K)$$

$$|l_{12}|^2 = (P_K - M_K)^T \cdot (P_K - M_K)$$

$$|l_{12}|^2 - (|l_2|^2 - |l_1|^2) = 2|l_1| \cdot l_{12,z} + 2|l_1| \cdot (\cos \alpha_K \cos \theta_K \cdot l_{12,x} + \sin \theta_K \cos \alpha_K \cdot l_{12,y})$$

Let,

$$a_k = 2|l_{12}|^{(z)} \quad (10)$$

$$b_k = 2|l_1|(\cos \theta_k l_{12}^{(x)} + \sin \theta_k l_{12}^{(y)}) \quad (11)$$

$$c_k = |l_{12}|^2 - (|l_2|^2 - |l_1|^2) \quad (12)$$

We finally get:

$$\alpha_k = \sin^{-1} (c_k / (a_k^2 + b_k^2))^{1/2} - \text{atan2}(a_k, b_k) \quad (13)$$

Where,

O_b is the origin of the base frame

M_K represents the coordinates of 1st revolute joint at the motor M_K with respect to the base frame

X_K represents coordinates of 2nd revolute joint on leg K with respect to the base frame

P_K represents the coordinates of a ball joint with respect to the base frame on leg K

$|l_1|$, $|l_2|$, are the lengths of links 1 and 2 respectively

$|l_{12}|$ is the distance between M_K and P_K

θ_K is the angle made by link 1 of leg K from the X-axis of the base frame when seen from the top view.

α_K is the desired angle of rotation of the motor.

K. Appendix: Simulations

A. Mechanical Simulations

1. Aerostructures

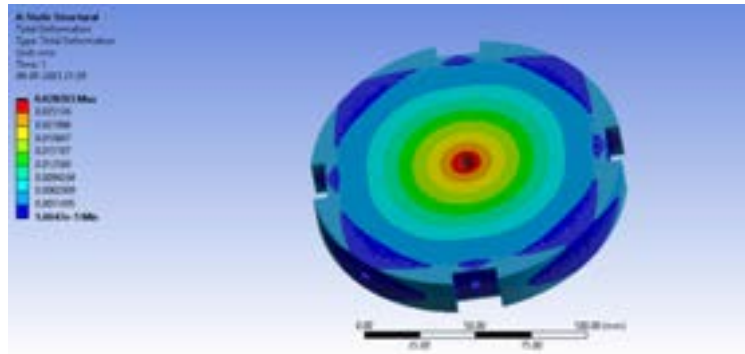


Figure 47 Thrust Plate Simulation

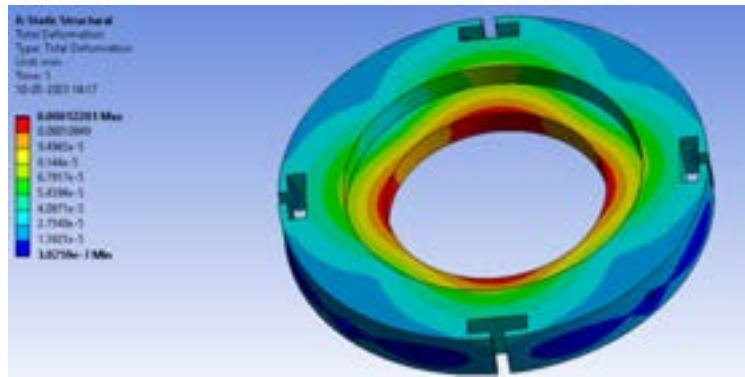


Figure 48 Retainer Simulation

2. Fins

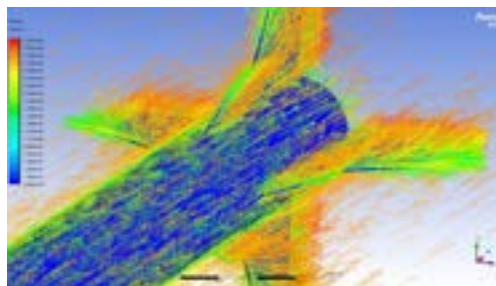


Figure 49 Velocity contour of air on the leading-edge extended fins at M 0.9

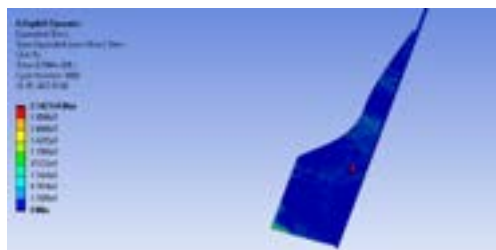


Figure 50 Explicit Dynamics Simulations Results of Fin

B. Bulkhead

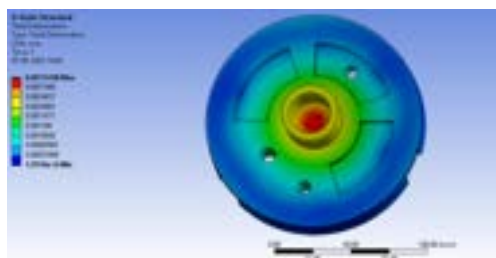


Figure 51 Recovery Bulkhead total deformation due to force of ejection charge

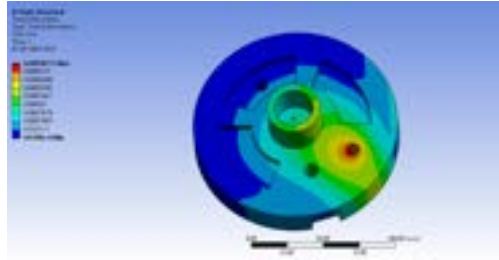


Figure 52 Recovery Bulkhead Total deformation due to force of rocket weight

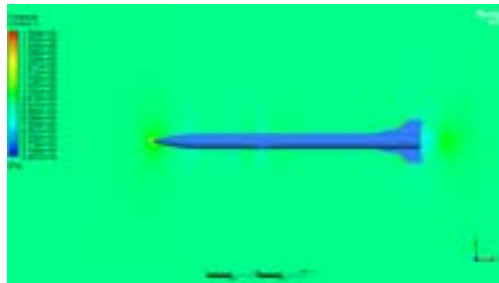


Figure 53 Pressure Contour at Mach 0.9

C. Payload Simulations

1. CubeSat

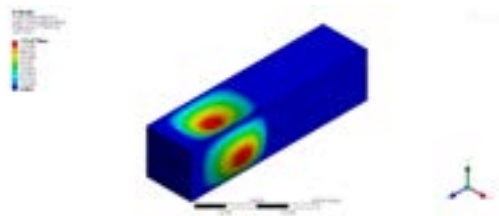


Figure 54 CubeSat Modal Analysis: Total Deformation 1

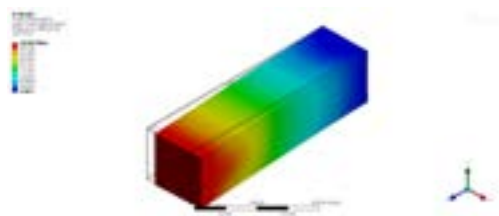


Figure 55 CubeSat Modal Analysis: Total Deformation 2

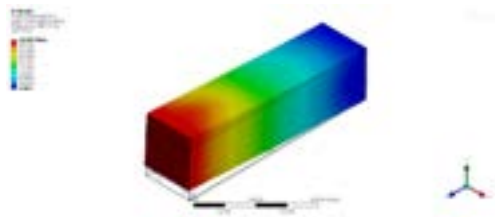


Figure 56 CubeSat Modal Analysis: Total Deformation 3

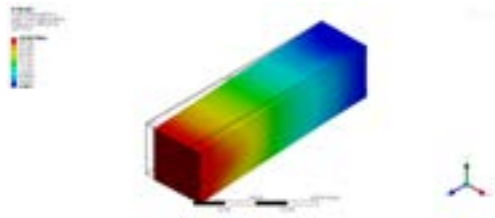


Figure 57 CubeSat Modal Analysis: Total Deformation 4

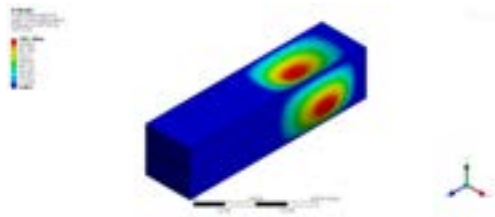


Figure 58 CubeSat Modal Analysis: Total Deformation 5

2. Stewie



Figure 59 Stewie Modal Analysis: Total Deformation 1

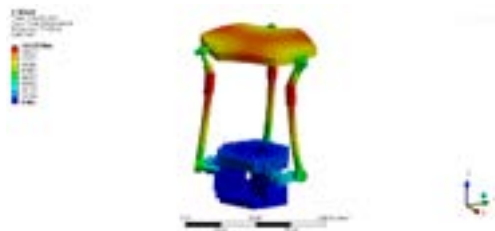


Figure 60 Stewie Modal Analysis: Total Deformation 2



Figure 61 Stewie Modal Analysis: Total Deformation 3



Figure 62 Stewie Modal Analysis: Total Deformation 4



Figure 63 Stewie Modal Analysis: Total Deformation 5

L. Appendix: Apogee Detection

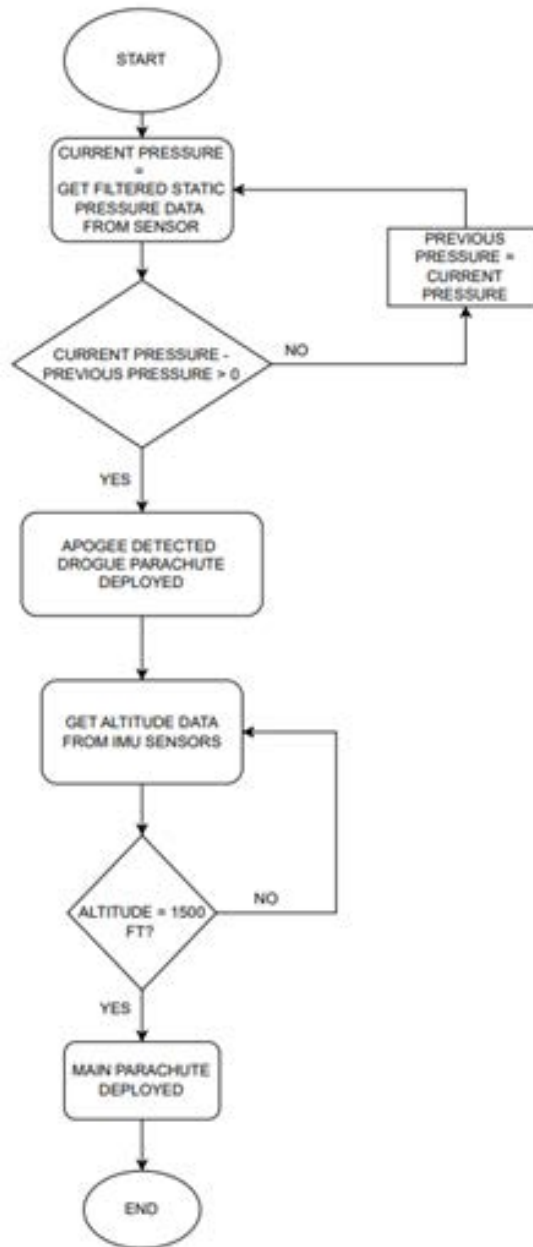
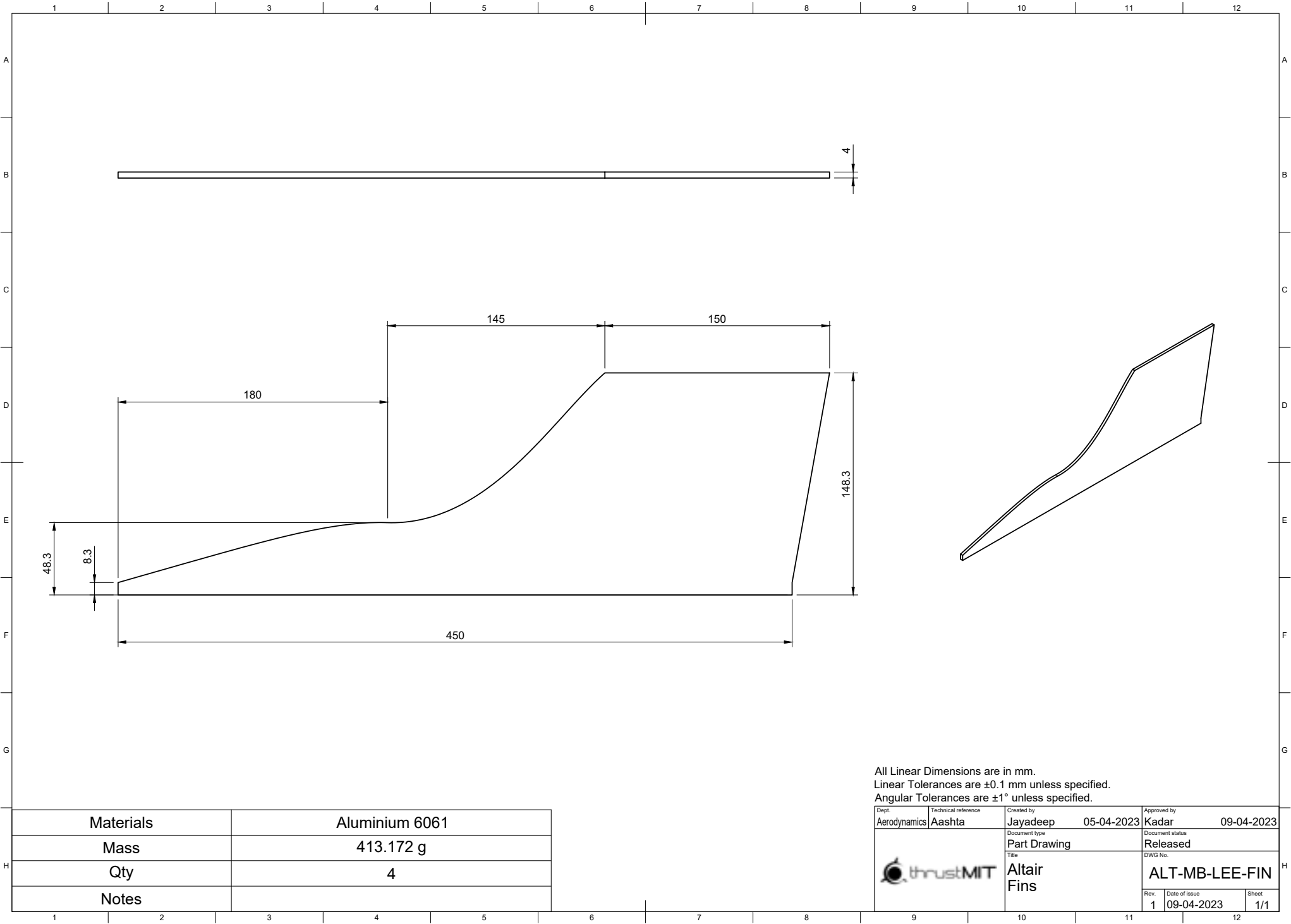


Figure 64 Flow Chart for Apogee detection and parachute deployment events

M. Appendix: Engineering Drawings

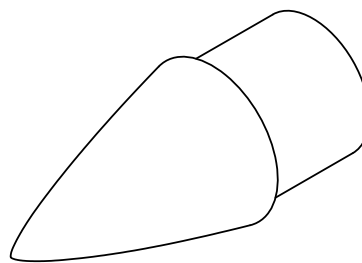
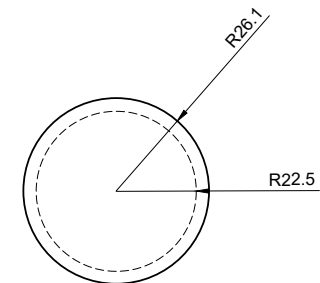
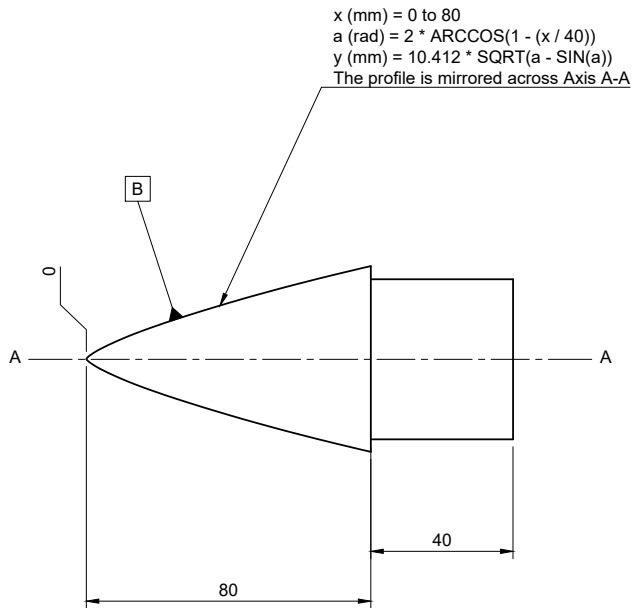
**THIS PAGE INTENTIONALLY LEFT BLANK.
APPENDIX F BEGINS ON THE FOLLOWING PAGE.**



All Linear Dimensions are in mm.
Linear Tolerances are ± 0.1 mm unless specified.
Angular Tolerances are $\pm 1^\circ$ unless specified.

Profile Points Datum B

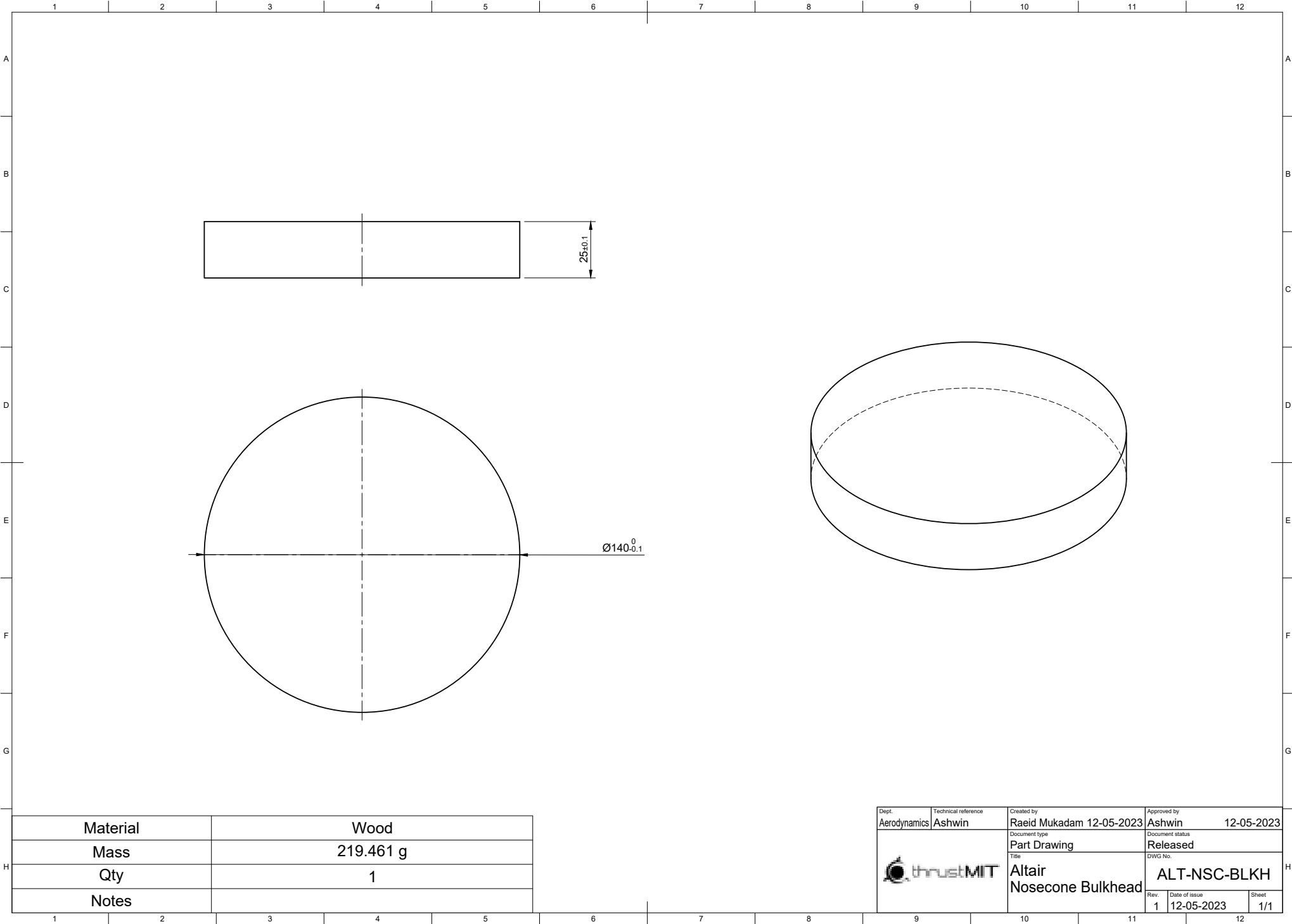
Point No.	X-Coordinate	Y-Coordinate
1	0	0
2	0.2	0.38
3	0.6	0.87
4	1.1	1.36
5	1.6	1.8
6	2.4	2.44
7	3.6	3.3
8	5	4.21
9	7.5	5.68
10	10.3	7.16
11	14	8.95
12	18.5	10.92
13	23.5	12.92
14	28.9	14.89
15	34.9	16.9
16	41.5	18.89
17	48.9	20.89
18	57.4	22.87
19	68	24.84
20	80	26.1




All Linear Dimensions are in mm.
 Linear Tolerances are ± 0.1 mm unless specified.
 Angular Tolerances are $\pm 1^\circ$ unless specified.

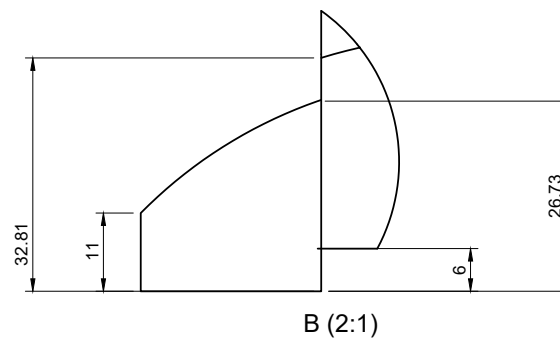
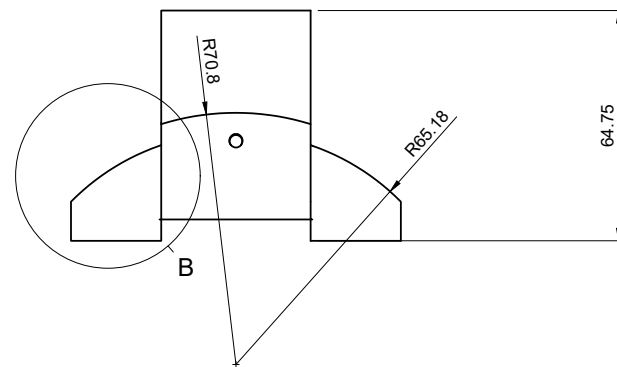
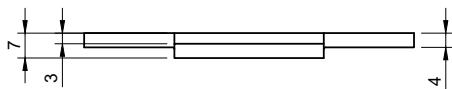
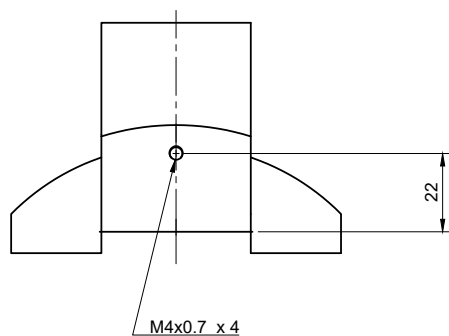
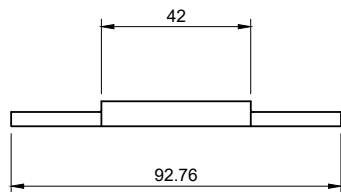
Materials	Aluminium 6061 T6
Mass	360.072 g
Qty	1
Notes	

Dept.	Technical reference	Created by	Approved by
Aerodynamics	Ashwin	Raeid Mukadam 06-04-2023	Jayadeep 09-04-2023
		Document type	Document status
		Part Drawing	Released
		Title	DWG No.
		Altair Nose Tip	ALT-NC-NTIP
Rev.	Date of issue	Sheet	
1	09-04-2023	1/1	



Material	Wood
Mass	219.461 g
Qty	1
Notes	

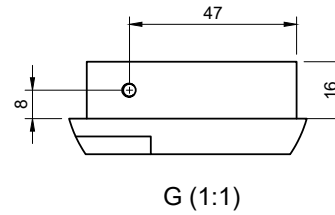
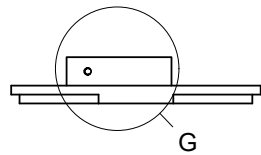
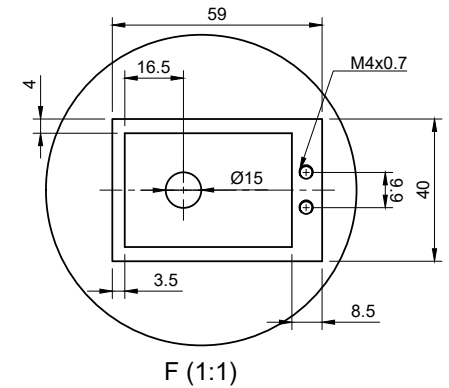
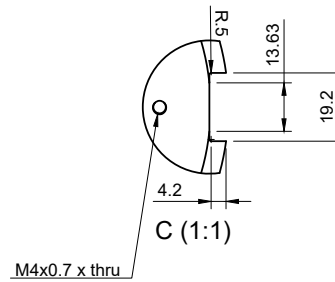
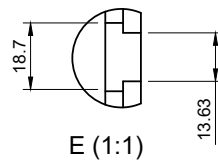
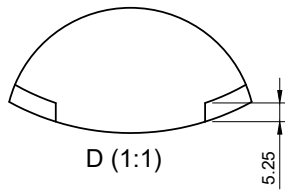
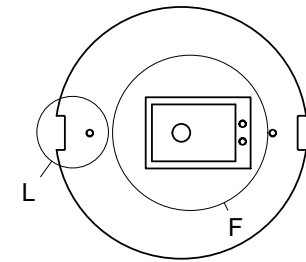
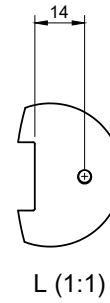
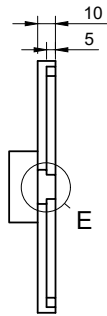
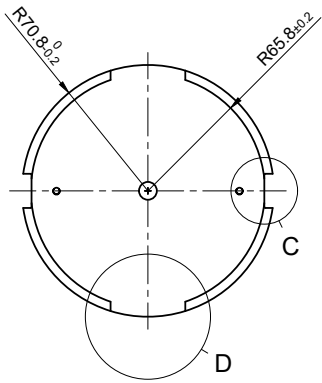
Dept. Aerodynamics	Technical reference Ashwin	Created by Raeid Mukadam 12-05-2023	Approved by Ashwin 12-05-2023
		Document type Part Drawing	Document status Released
		Title Altair Nosecone Bulkhead	DWG No. ALT-NSC-BLKH
		Rev. 1	Date of issue 12-05-2023
		Sheet 1/1	



All Linear Dimensions are in mm.
Linear Tolerances are ± 0.1 mm unless specified.
Angular Tolerances are $\pm 1^\circ$ unless specified.

Material	Aluminium
Mass	46.863 g
Qty	2
Notes	

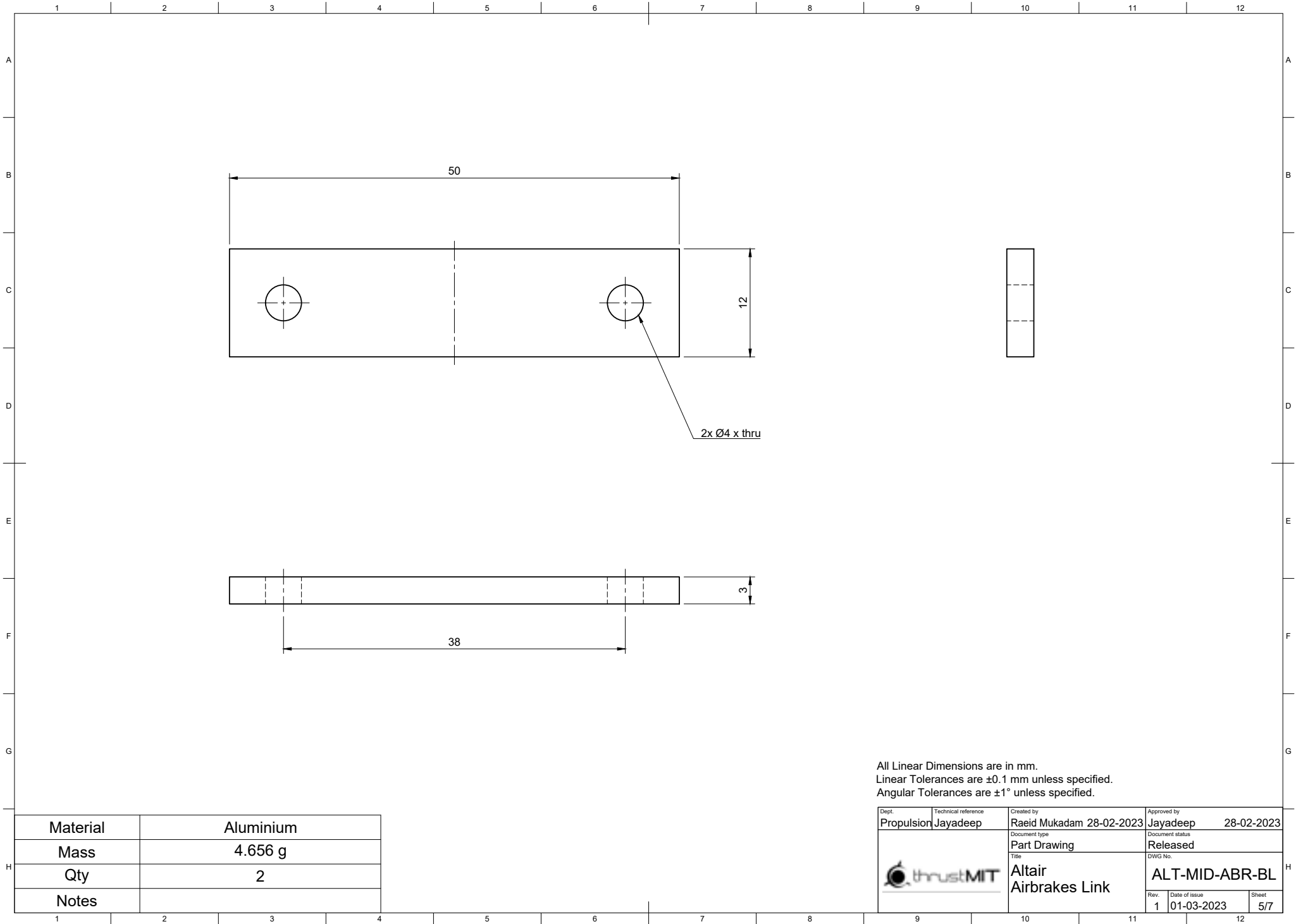
Dept.	Technical reference	Created by	Approved by
Propulsion	N/A	Raeid Mukadam 24-02-2023	Jayadeep 28-02-2023
		Document type	Document status
		Part Drawing	Released
		Title	DWG No.
		Altair Air Brakes	ALT-MID-ABR-ABR
Rev.	Date of issue	Sheet	
1	01-03-2023	1/7	

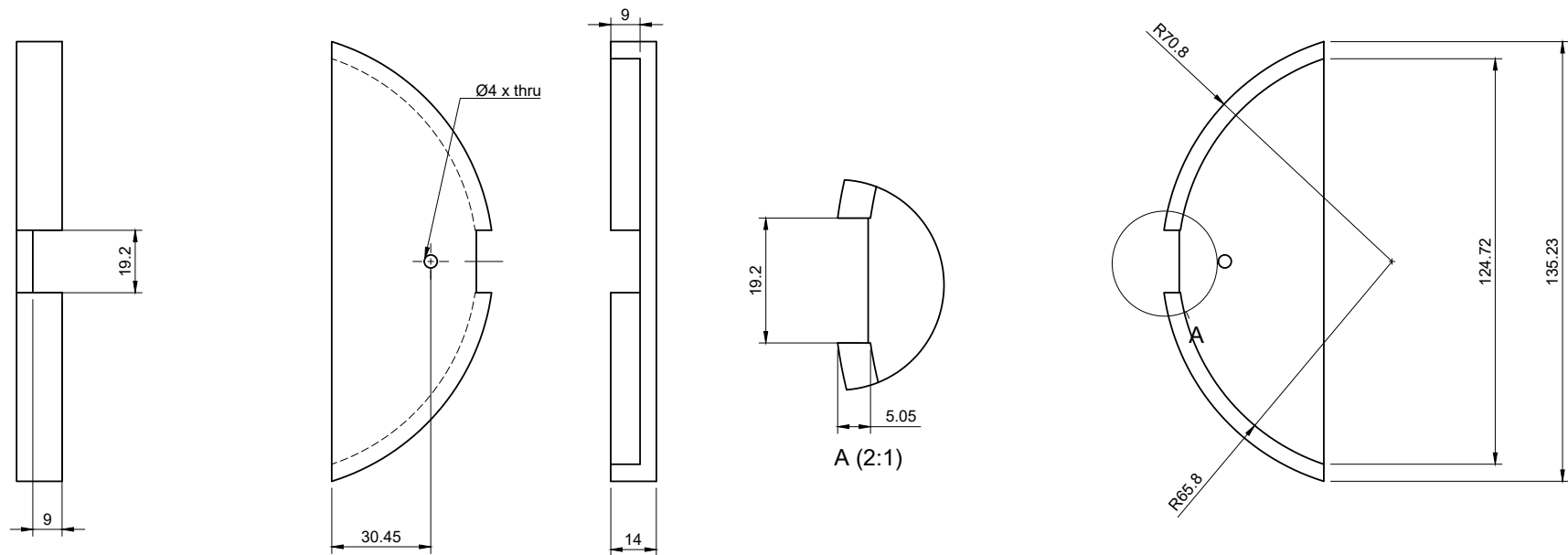


All Linear Dimensions are in mm.
Linear Tolerances are ± 0.1 mm unless specified.
Angular Tolerances are $\pm 1^\circ$ unless specified.

Material	Aluminium
Mass	717.32 g
Qty	1
Notes	


Dept.	Technical reference	Created by	Approved by
Propulsion	Jayadeep	Raeid Mukadam 24-02-2023	Jayadeep 28-02-2023
		Document type	Document status
		Part Drawing	Released
		Title	DWG No.
		Airbrakes Upper Plate	ALT-MID-ABR-UP
Rev.	Date of issue	Sheet	
1	01-03-2023	2/7	

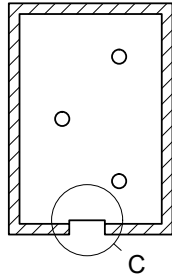




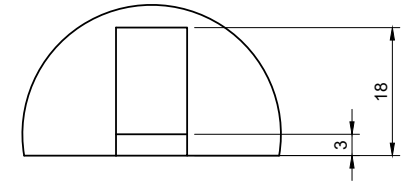
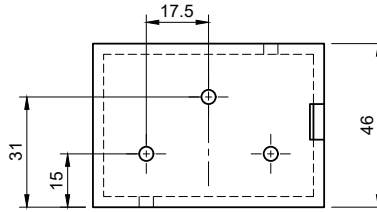
All Linear Dimensions are in mm.
Linear Tolerances are ± 0.1 mm unless specified.
Angular Tolerances are $\pm 1^\circ$ unless specified.

Material	Aluminium
Mass	83.791 g
Qty	2
Notes	

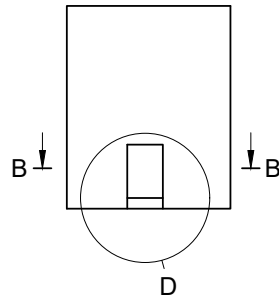
Dept. Propulsion	Technical reference Jayadeep	Created by Raeid Mukadam 27-02-2023	Approved by Jayadeep 28-02-2023
	Document type Part Drawing	Document status Released	
	Title Altair Airbrakes Shadow	DWG No. ALT-MID-ABR-SHDW	
	Rev. 1	Date of issue 01-03-2023	Sheet 3/7



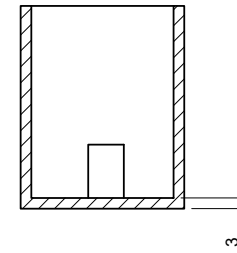
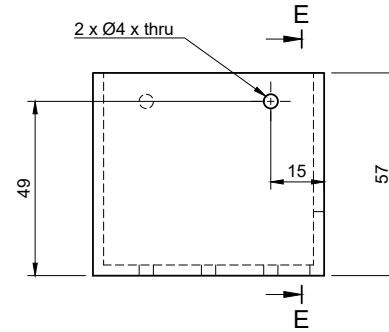
B-B (1:1)



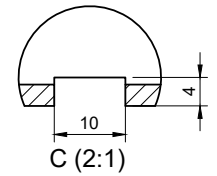
D (2:1)



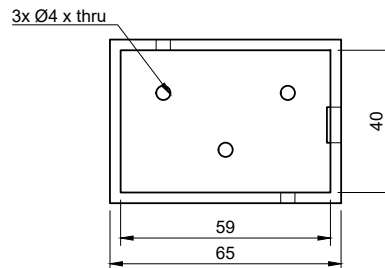
D



E-E (1:1)



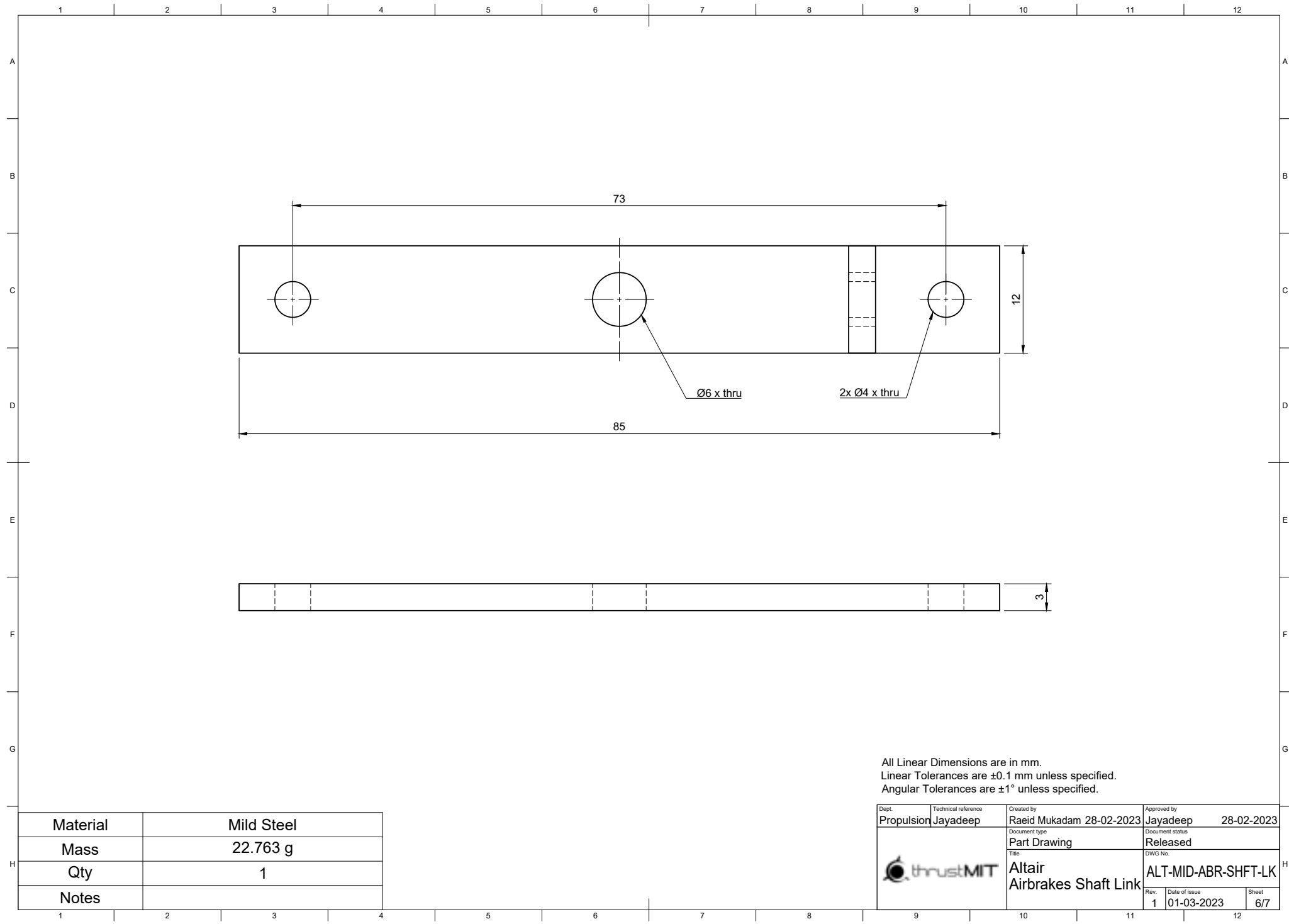
C (2:1)



All Linear Dimensions are in mm.
Linear Tolerances are ± 0.1 mm unless specified.
Angular Tolerances are $\pm 1^\circ$ unless specified.


Material	Aluminium
Mass	114.025 g
Qty	1
Notes	

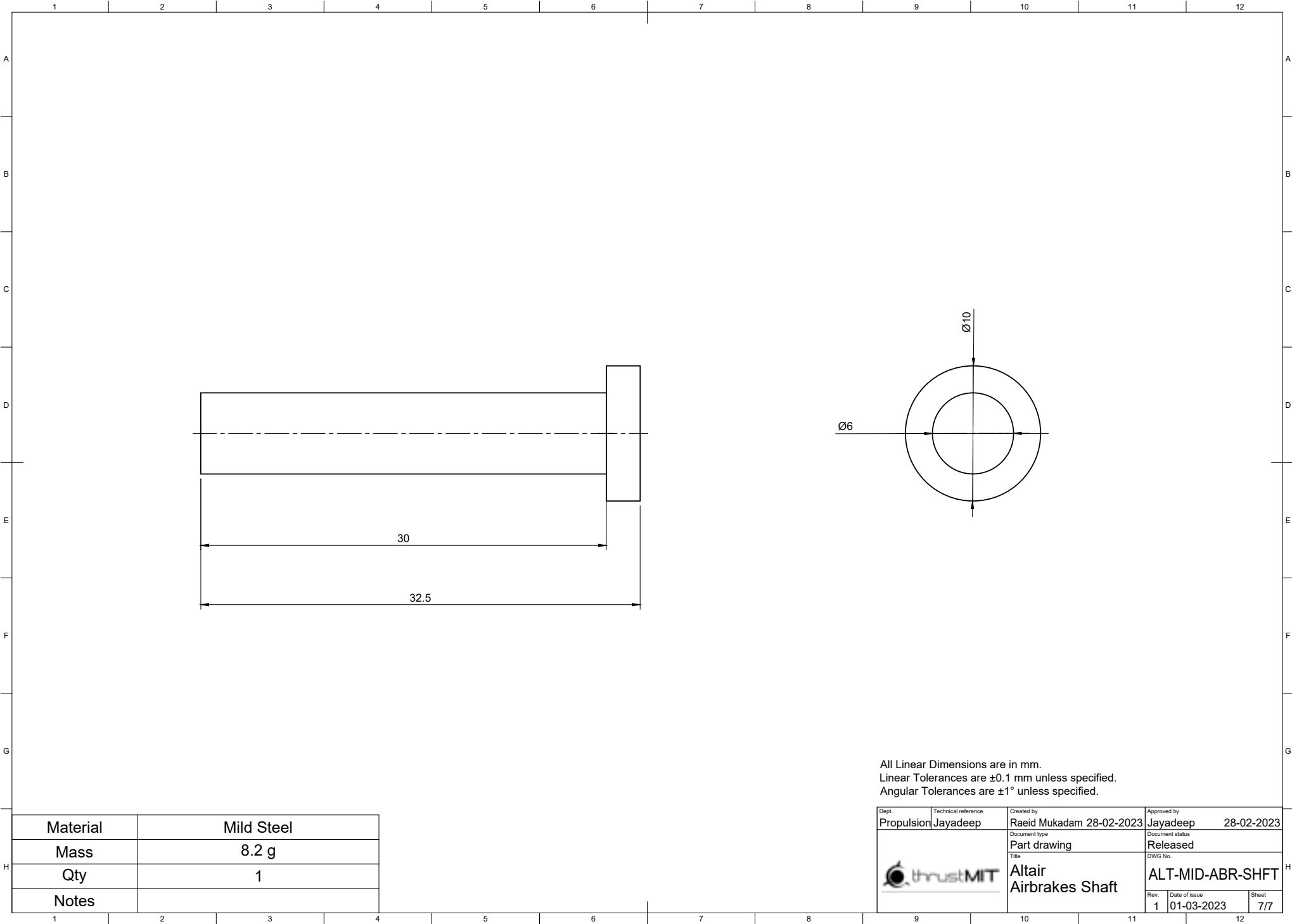
Dept.	Technical reference	Created by	Approved by
Propulsion	Jayadeep	Raeid Mukadam 27-02-2023	Jayadeep 28-02-2023
		Document type	Document status
		Part Drawing	Released
		Title	DWG No.
		Altair Airbrakes Servo House	ALT-MID-ABR-SRH
Rev.	Date of issue	Sheet	
1	01-03-2023	4/7	



All Linear Dimensions are in mm.
Linear Tolerances are ± 0.1 mm unless specified.
Angular Tolerances are $\pm 1^\circ$ unless specified.

Material	Mild Steel
Mass	22.763 g
Qty	1
Notes	

Dept. Propulsion	Technical reference Jayadeep	Created by Raeid Mukadam 28-02-2023	Approved by Jayadeep 28-02-2023
	Document type Part Drawing	Document status Released	
	Title Altair Airbrakes Shaft Link	DWG No. ALT-MID-ABR-SHFT-LK	
	Rev. 1	Date of issue 01-03-2023	Sheet 6/7



1 2 3 4 5 6 7 8 9 10 11 12

A

B

C

D

E

F

G

H

A

B

C

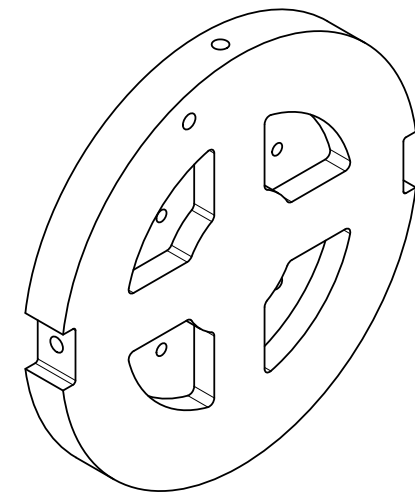
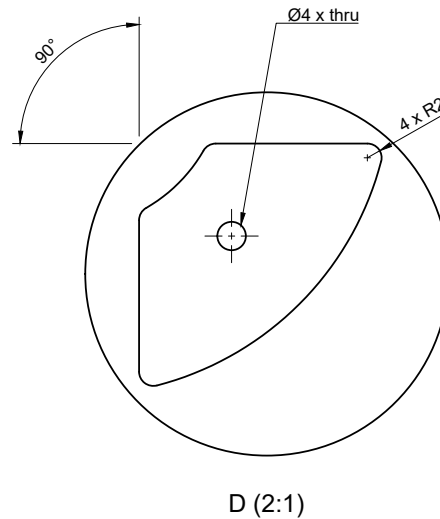
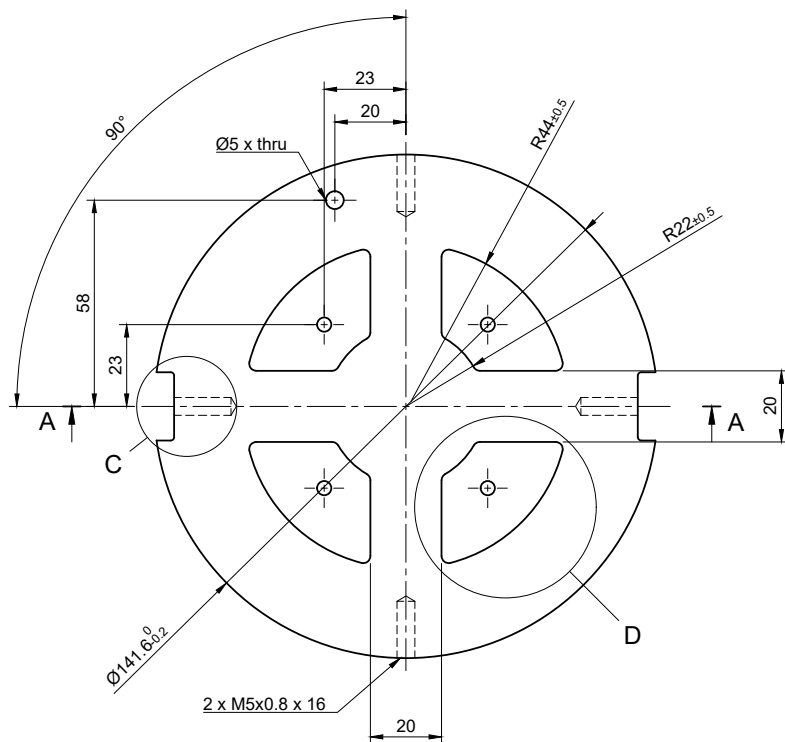
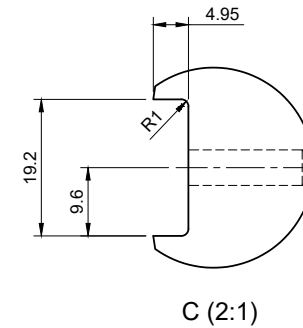
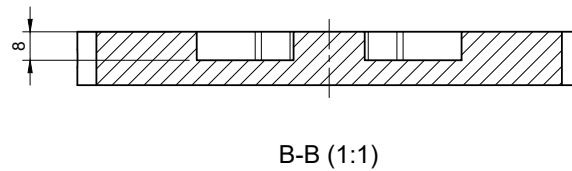
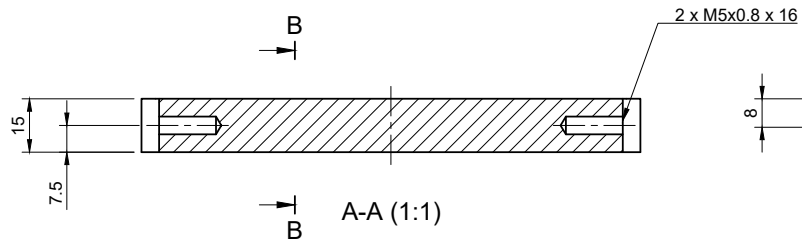
D

E

F

G

H

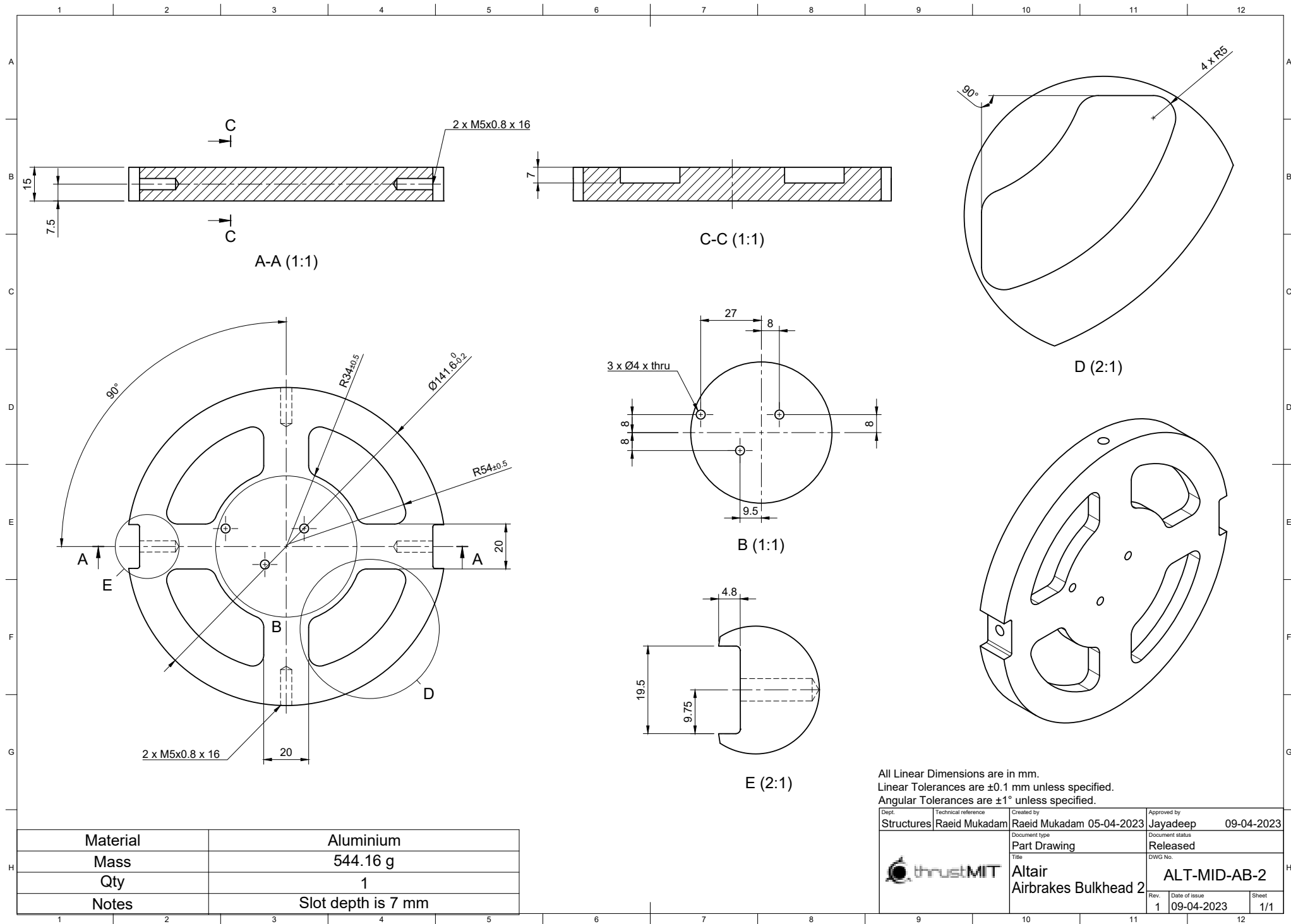


All Linear Dimensions are in mm.
Linear Tolerances are ± 0.1 mm unless specified.
Angular Tolerances are $\pm 1^\circ$ unless specified.

Material	Aluminium
Mass	556.284 g
Qty	1
Notes	

Dept.	Structures	Technical reference	NA	Created by	Raeid Mukadam 04-04-2023	Approved by	Jayadeep 09-04-2023
Document type	Part Drawing	Document status	Disclosed	Title	Altair Airbrakes Bulkhead 1	DWG No.	ALT-MID-AB-1
Rev.	1	Date of issue	09-04-23	Sheet	1/1		





All Linear Dimensions are in mm.
Linear Tolerances are ± 0.1 mm unless specified.
Angular Tolerances are $\pm 1^\circ$ unless specified.

Dept.	Technical reference	Created by	Approved by
Structures	Raëid Mukadam	Raëid Mukadam 05-04-2023	Jayadeep 09-04-2023
Document type		Document status	
Part Drawing		Released	
Title		DWG No.	
Altair Airbrakes Bulkhead 2		ALT-MID-AB-2	
Rev.	Date of issue	Sheet	
1	09-04-2023	1/1	

1 2 3 4 5 6 7 8 9 10 11 12

A

B

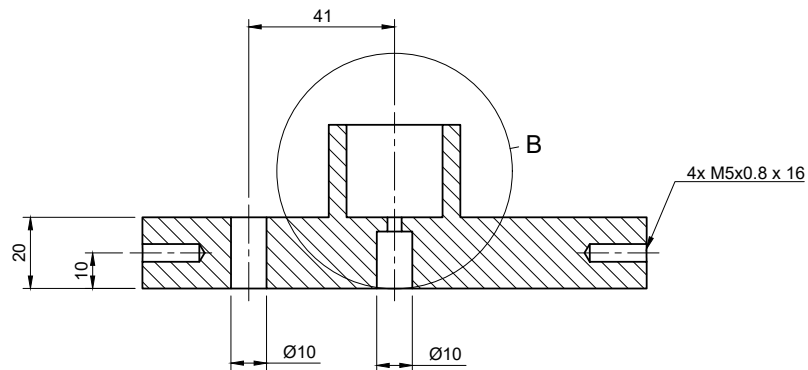
C

D

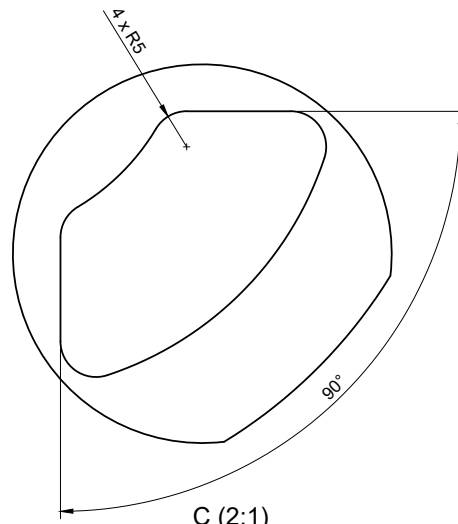
E

F

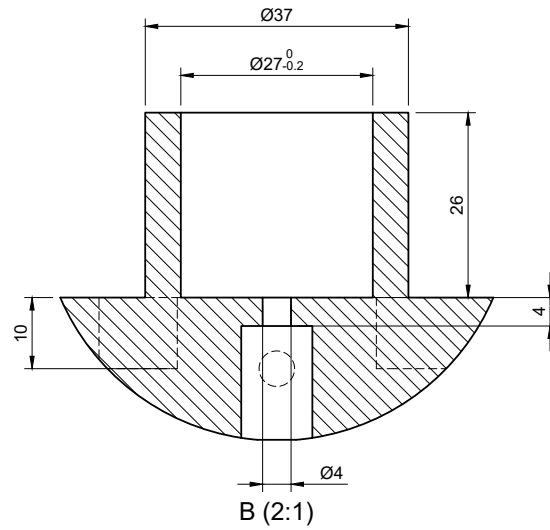
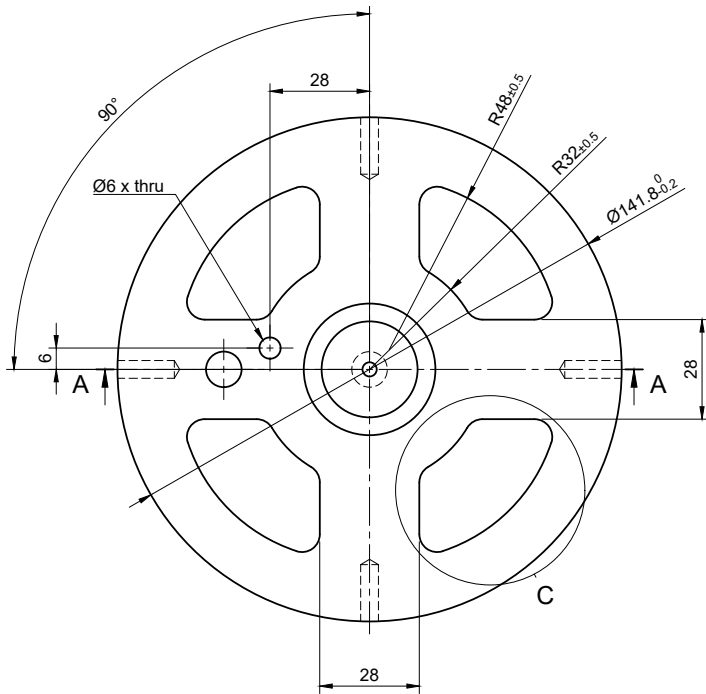
G



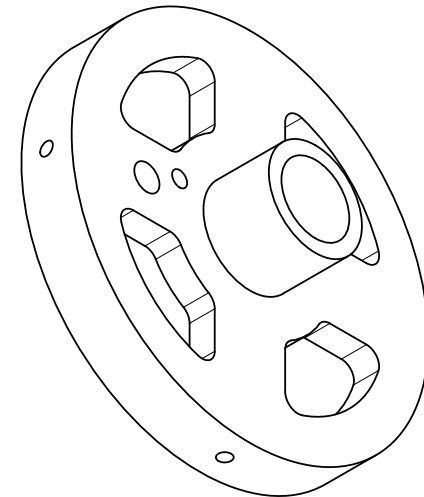
A-A (1:1)



C (2:1)



B (2:1)

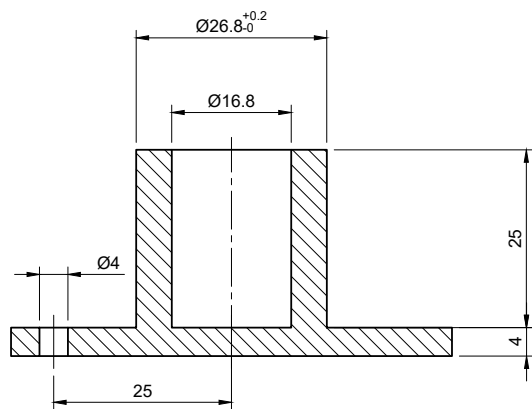


All Linear Dimensions are in mm.
Linear Tolerances are ± 0.1 mm unless specified.
Angular Tolerances are $\pm 1^\circ$ unless specified.

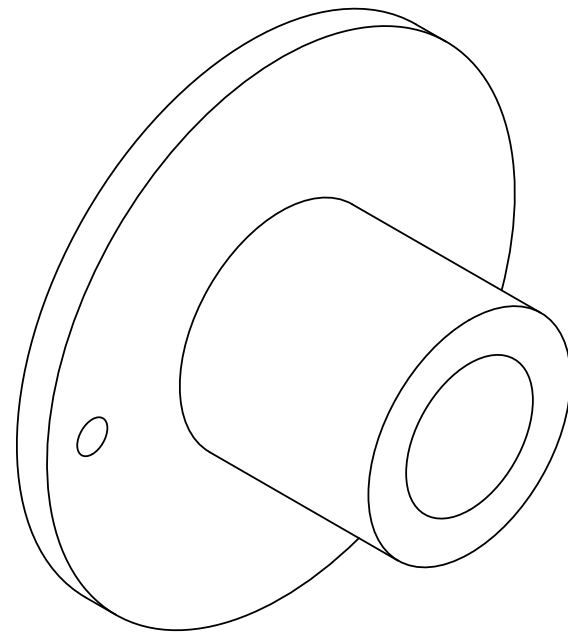
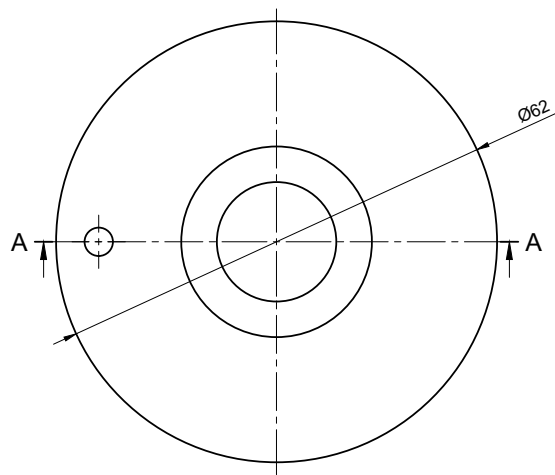
Material	Aluminium
Mass	776.32 g
Qty	1
Notes	Slot depth is 10 mm

Dept.	Structures	Technical reference	Raeid Mukadam	Created by	Raeid Mukadam 04-04-2023	Approved by	Jayadeep 09-04-2023
Document type	Part Drawing	Document status	Released	Document title	Altair Ejection Bulkhead	DWG No.	ALT-RB-EJC-BKHD
Rev.	1	Date of issue	09-04-2023	Sheet	1/1		





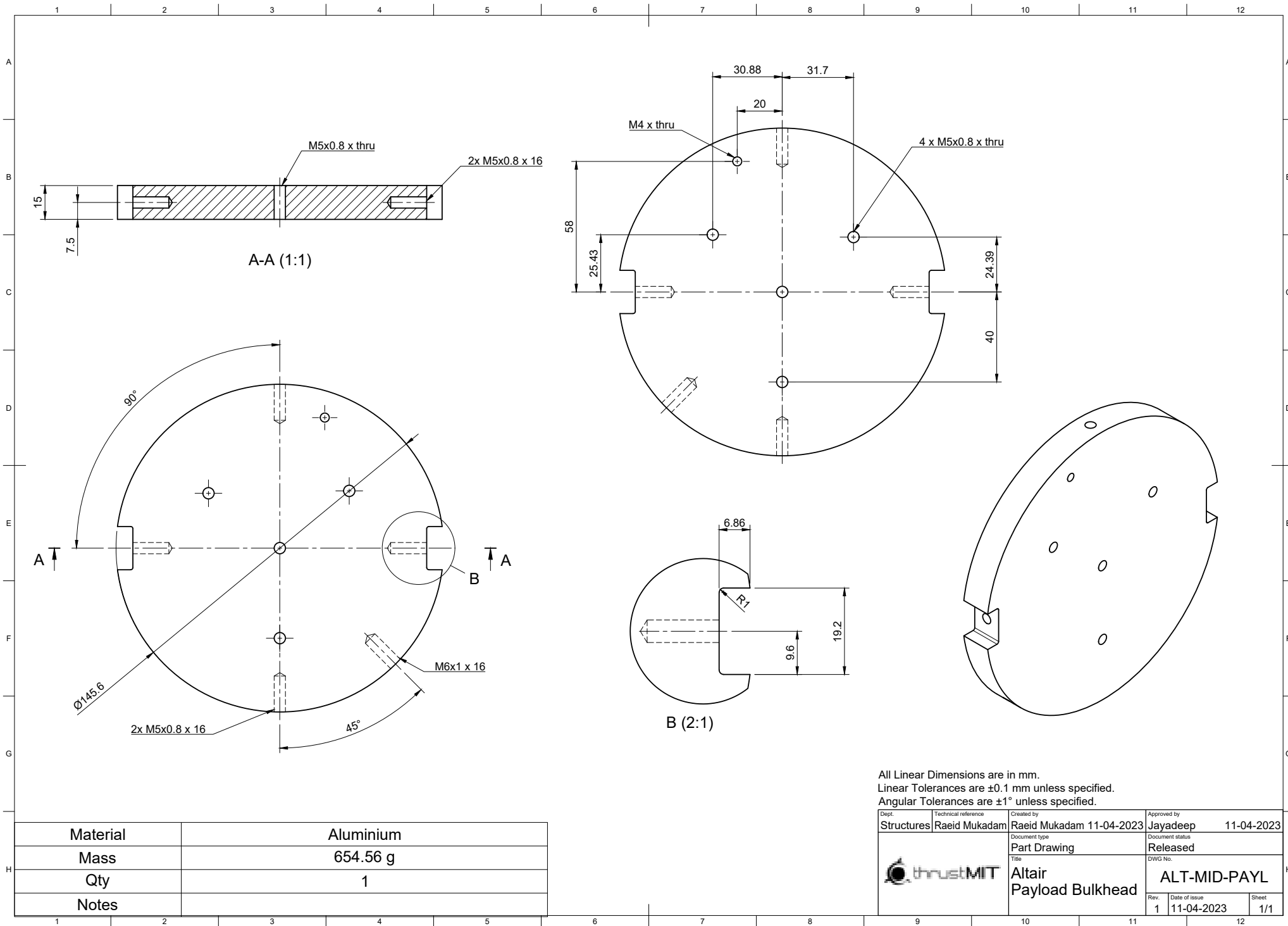
A-A (2:1)



All Linear Dimensions are in mm.
Linear Tolerances are ± 0.1 mm unless specified.
Angular Tolerances are $\pm 1^\circ$ unless specified.

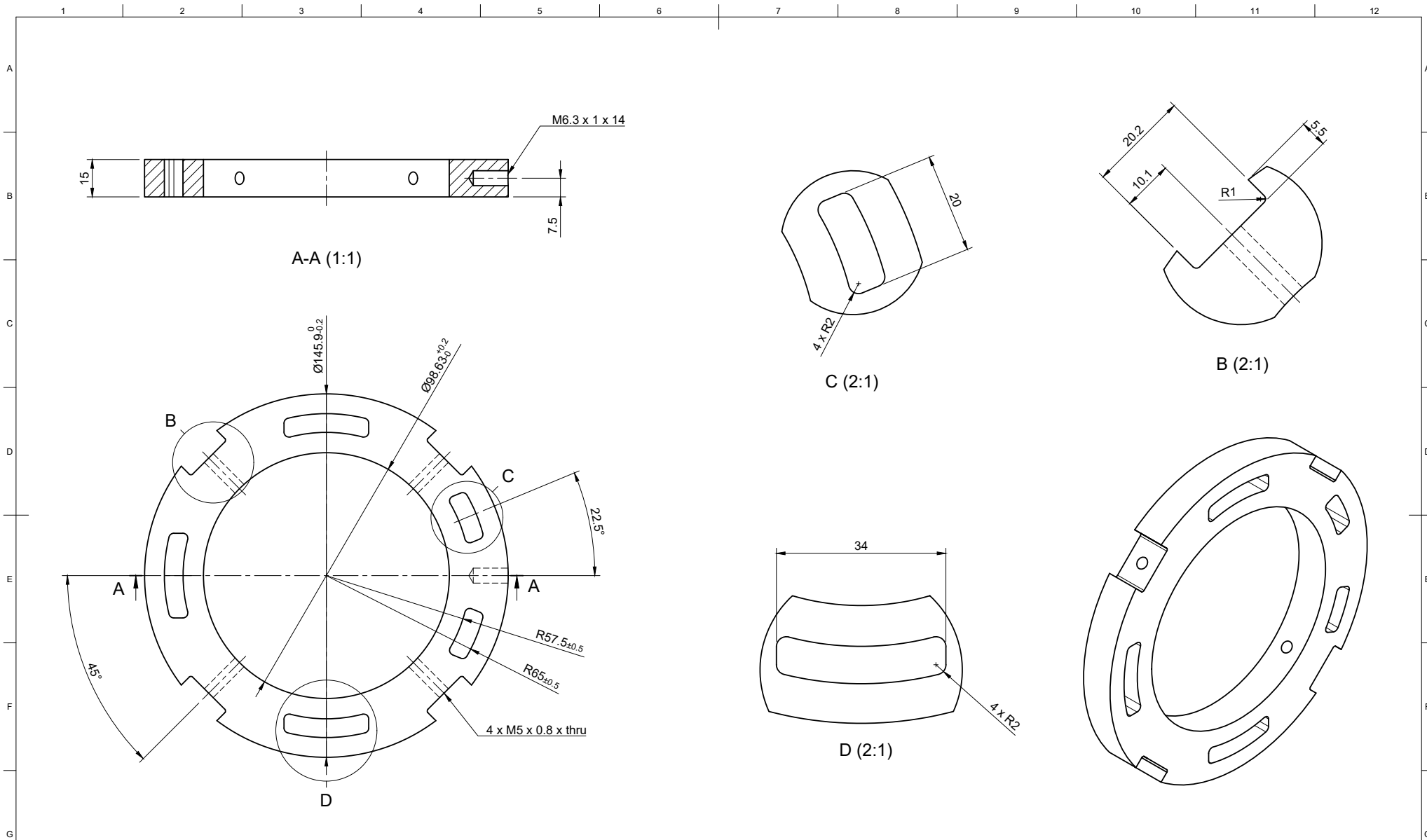
Material	Aluminium
Mass	55.585 g
Qty	1
Notes	

Dept.	Structures	Technical reference	Raeid Mukadam	Created by	Raeid Mukadam 05-04-2023	Approved by	Jayadeep 09-04-2023
Document type	Part Drawing	Document status	Released	Rev.	1	Date of issue	09-04-2023
Title	Altair Ejection Piston	DWG No.	ALT-RB-PISTON	Sheet	1/1		



All Linear Dimensions are in mm.
Linear Tolerances are ± 0.1 mm unless specified.
Angular Tolerances are $\pm 1^\circ$ unless specified.

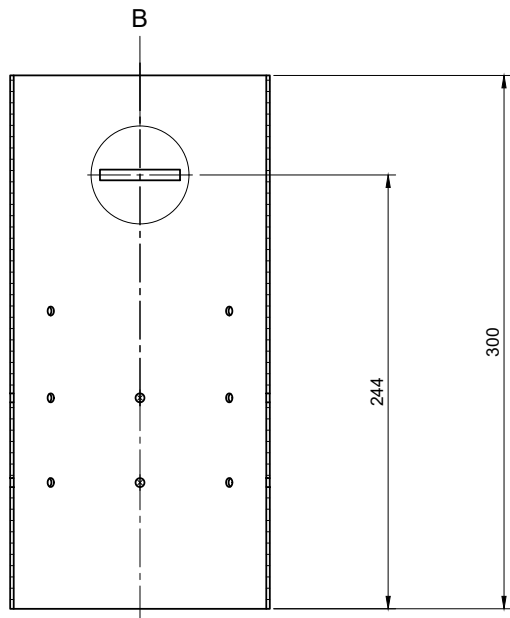
Dept.	Structures	Technical reference	Raëid Mukadam	Created by	Raëid Mukadam 11-04-2023	Approved by	Jayadeep 11-04-2023
Document type	Part Drawing	Document status	Released	Rev.	1	Date of issue	11-04-2023
Title	Altair Payload Bulkhead	DWG No.	ALT-MID-PAYL	Sheet	1/1		



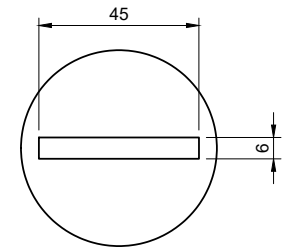
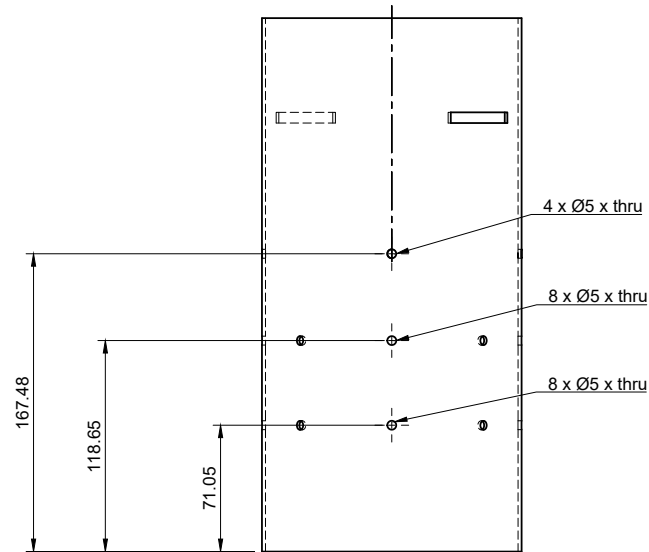
Material	Aluminium
Mass	300.649 g
Qty	1
Notes	Symmetry about A-A exists

All Linear Dimensions are in mm.
 Linear Tolerances are ± 0.1 mm unless specified.
 Angular Tolerances are $\pm 1^\circ$ unless specified.

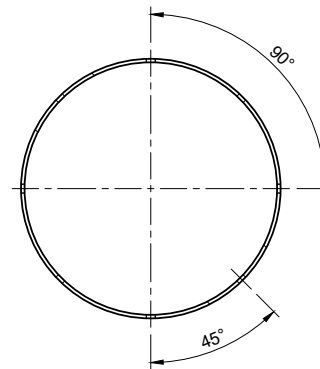
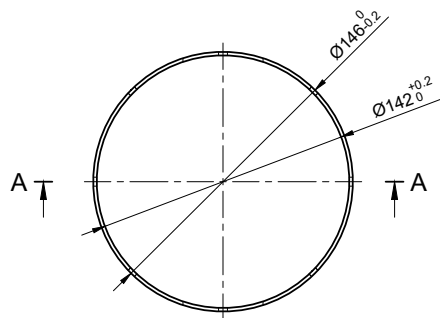
Dept.	Structures	Technical reference	Raeid Mukadam	Created by	Raeid Mukadam 06-04-2023	Approved by	Jayadeep 09-04-2023
Document type	Part Drawing	Document status	Released	Rev.	1	Date of issue	09-04-2023
Title	Altair Centering Rings	DWG No.	ALT-MB-CRING	Sheet	1/1		



A-A (1:2)



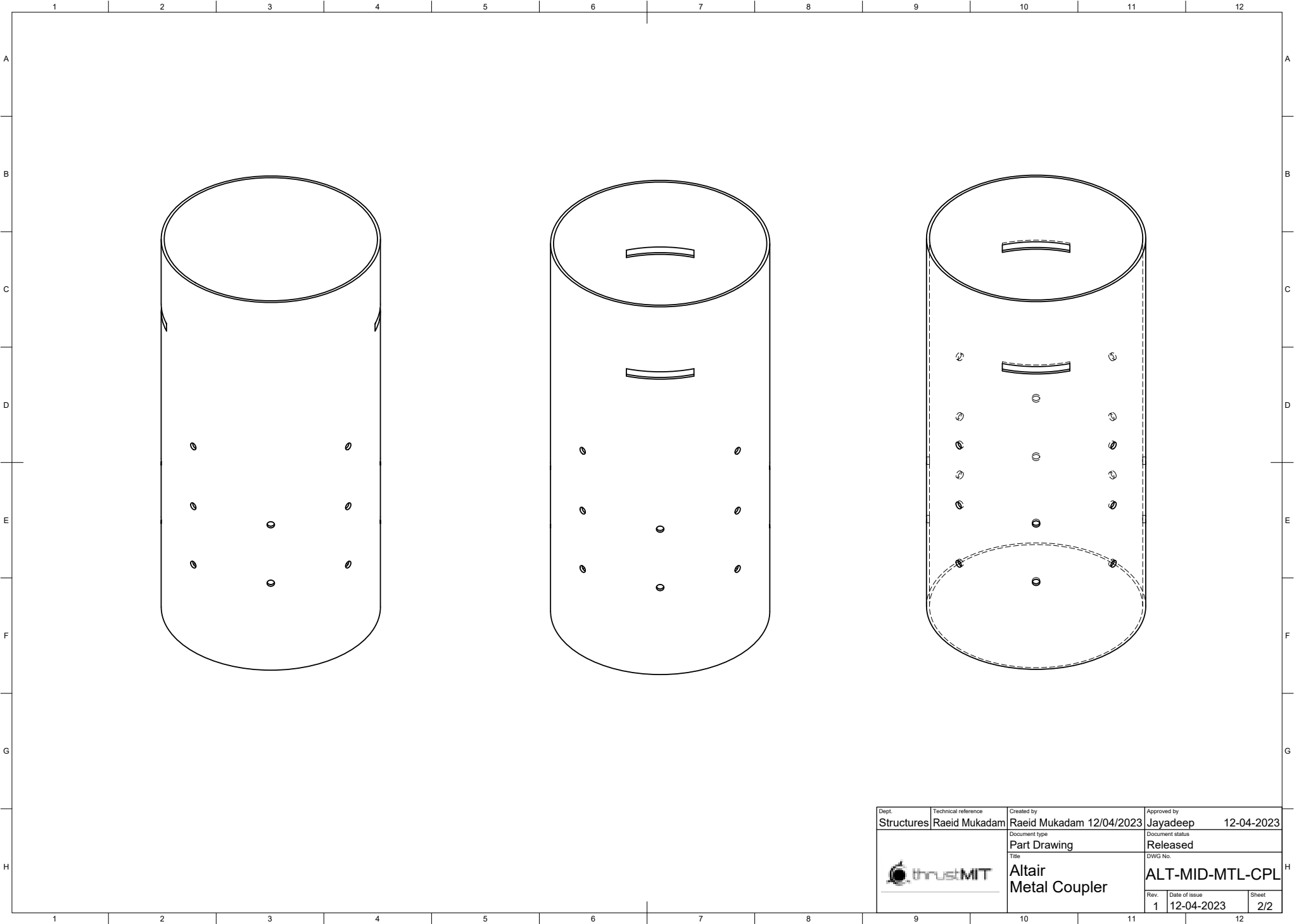
B (1:1)

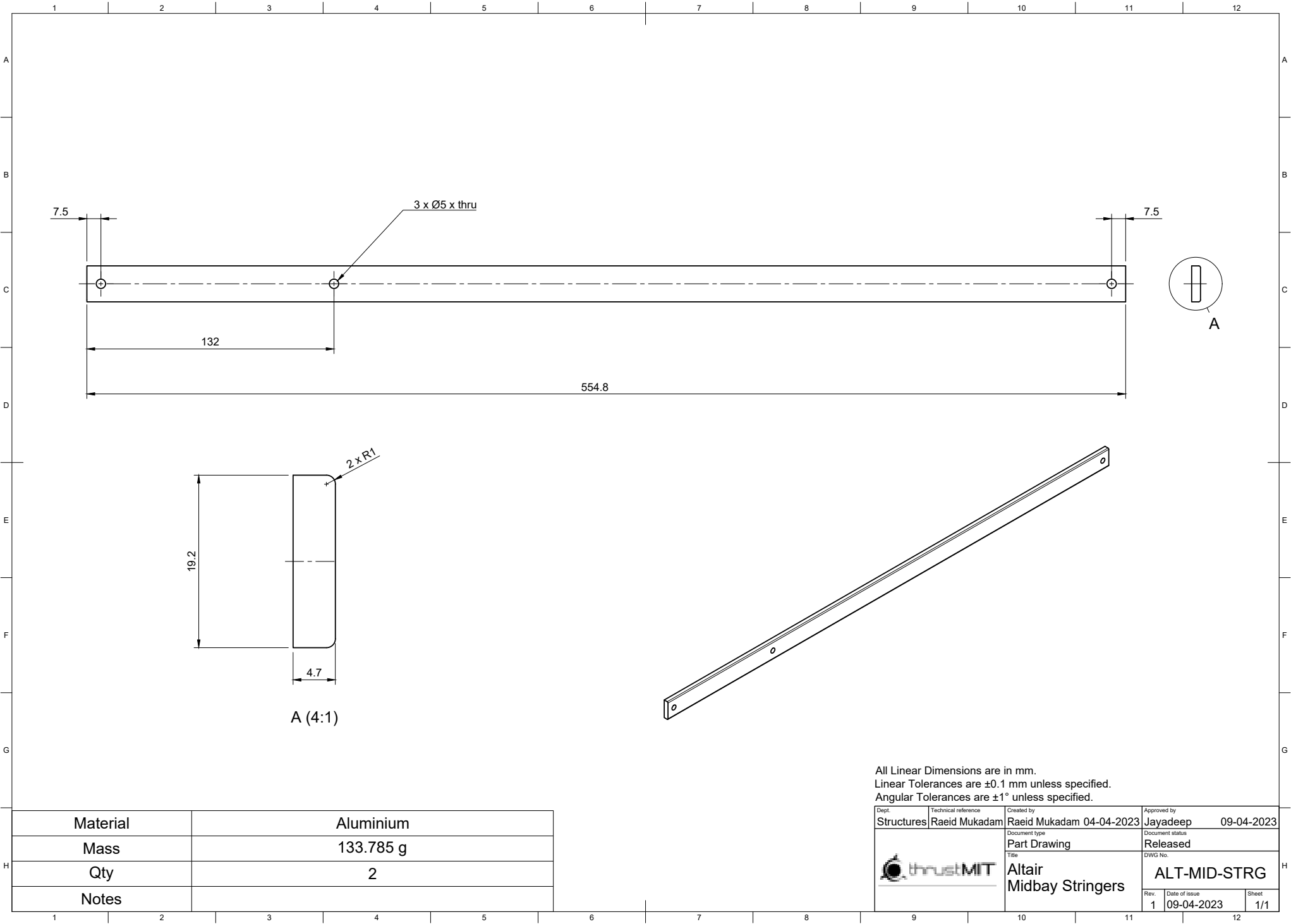


All Linear Dimensions are in mm.
Linear Tolerances are ± 0.1 mm unless specified.
Angular Tolerances are $\pm 1^\circ$ unless specified.

Material	Aluminium
Mass	727.794 g
Qty	1
Notes	There are 2 rectangular slots diametrically opposite each other

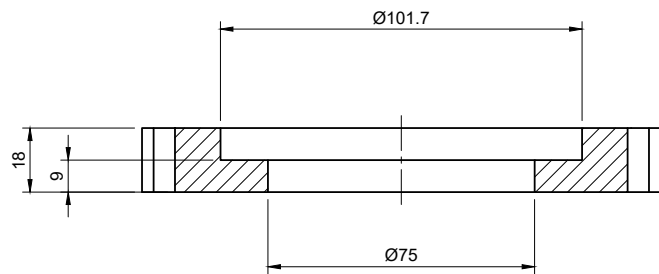
Dept. Structures	Technical reference Raeid Mukadam	Created by Raeid Mukadam 12-04-2023	Approved by Jayadeep 12-04-2023
Document type Part Drawing		Document status Released	
Title Altair Metal Coupler		DWG No. ALT-MID-MTL-CPL	
Rev. 1	Date of issue 12-04-2023	Sheet 1/2	



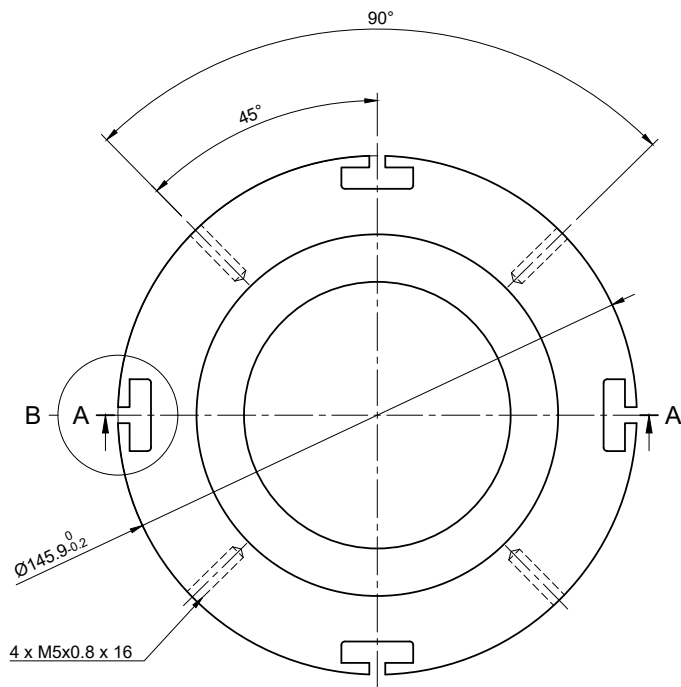


All Linear Dimensions are in mm.
Linear Tolerances are ± 0.1 mm unless specified.
Angular Tolerances are $\pm 1^\circ$ unless specified.

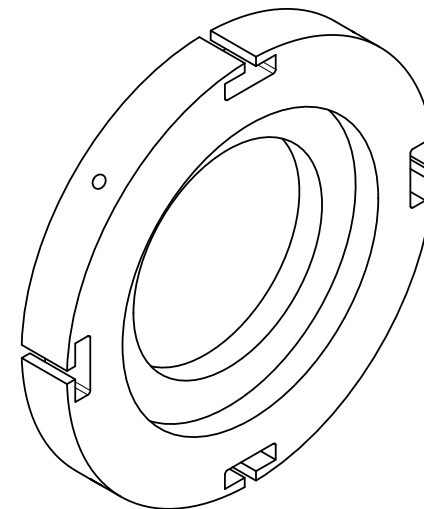
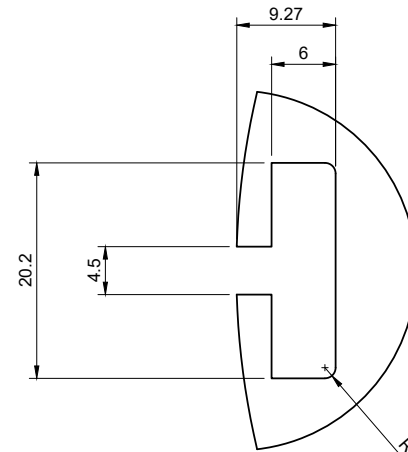
Dept.	Technical reference	Created by	Approved by
Structures	Raeid Mukadam	Raeid Mukadam 04-04-2023	Jayadeep 09-04-2023
Document type		Document status	
Part Drawing		Released	
Title		DWG No.	
Altair Midbay Stringers		ALT-MID-STRG	
Rev.	Date of issue	Sheet	
1	09-04-2023	1/1	



A-A (1:1)



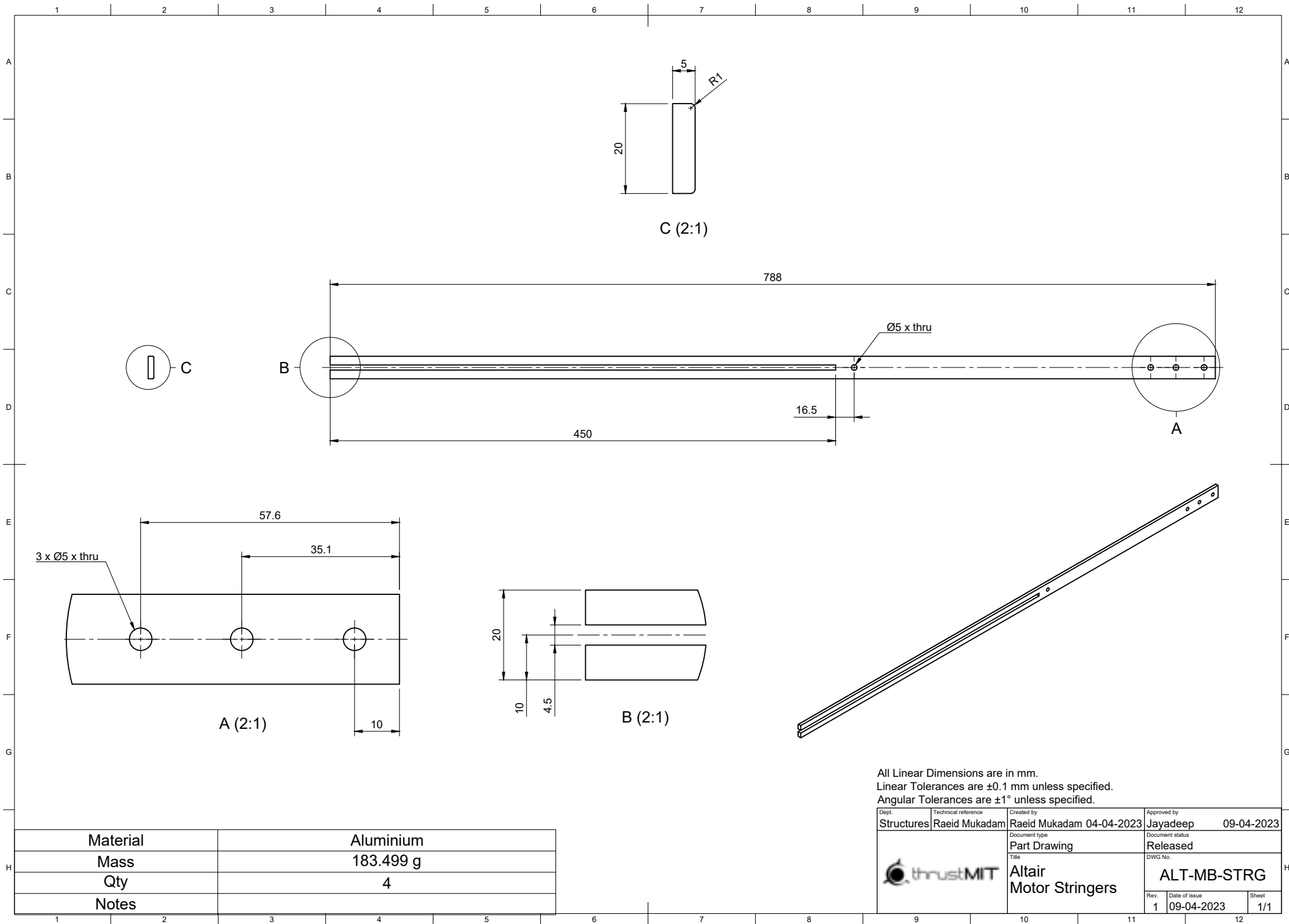
B (3:1)

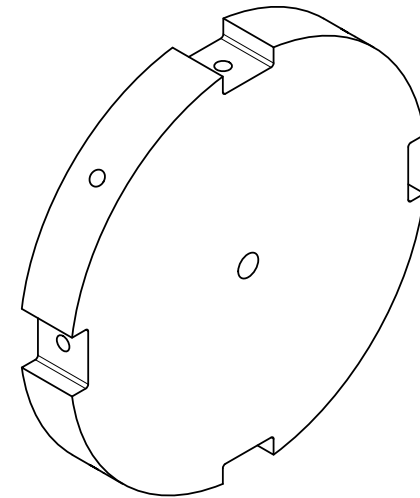
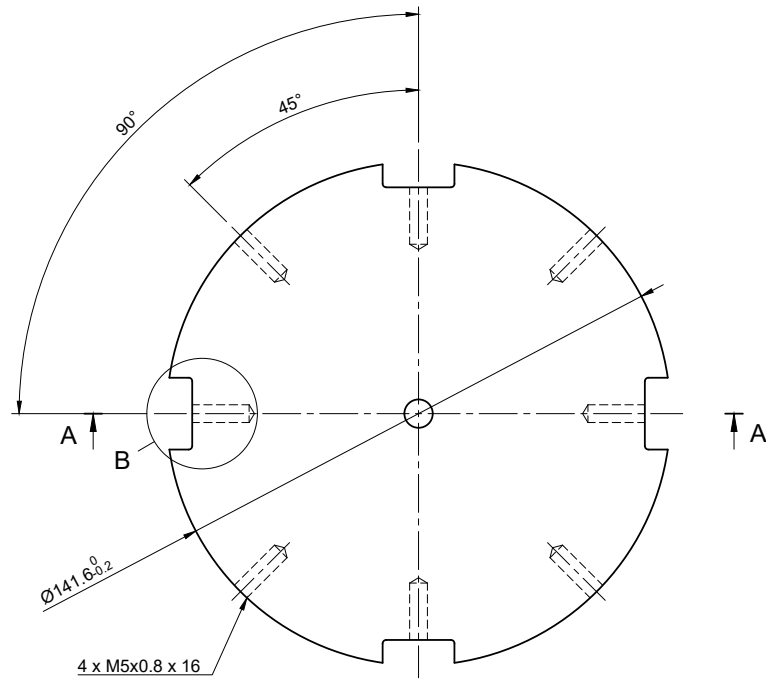
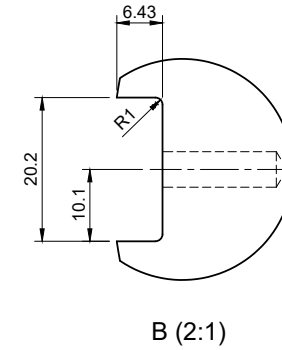
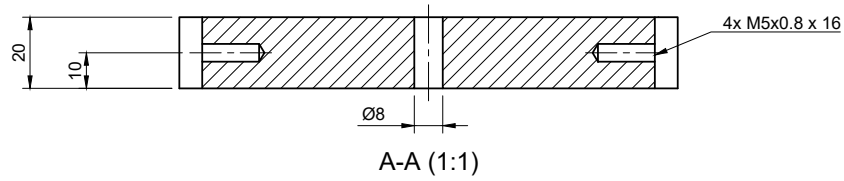


All Linear Dimensions are in mm.
Linear Tolerances are ± 0.1 mm unless specified.
Angular Tolerances are $\pm 1^\circ$ unless specified.

Material	Aluminium
Mass	478.641 g
Qty	1
Notes	

Dept.	Structures	Technical reference	Raeid Mukadam	Created by	Raeid Mukadam	05-04-2023	Approved by	Jayadeep	09-04-2023
Document type	Part Drawing	Document status	Released	Rev.	1	Date of issue	09-04-2023	Sheet	1/1
thrustMIT		Altair Retainer		ALT-MB-RET					

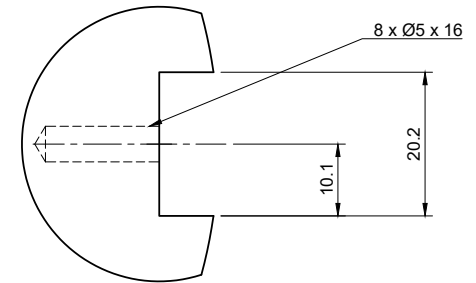
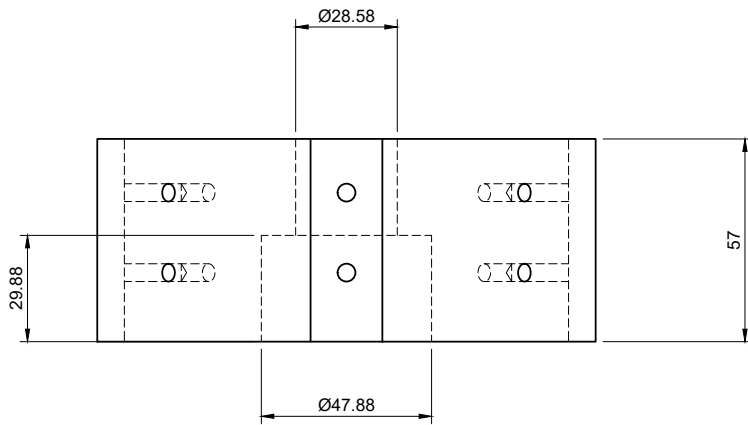




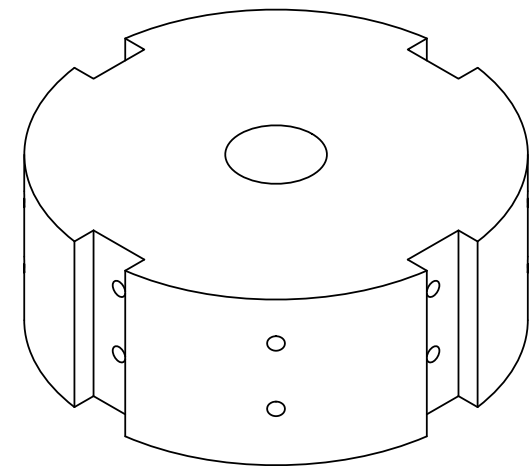
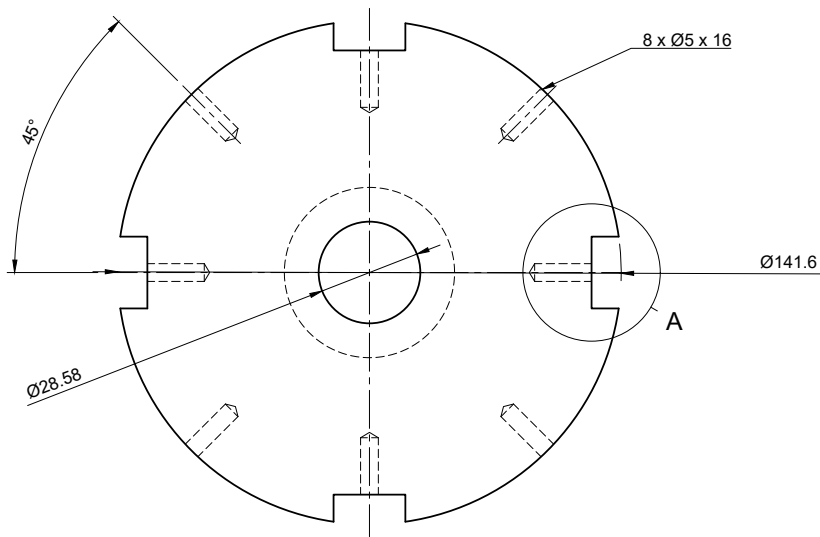
All Linear Dimensions are in mm.
Linear Tolerances are ± 0.1 mm unless specified.
Angular Tolerances are $\pm 1^\circ$ unless specified.

Material	Aluminium
Mass	810.6 g
Qty	1
Notes	

Dept.	Structures	Technical reference	Raeid Mukadam	Created by	Raeid Mukadam 04-04-2023	Approved by	Jayadeep 09-04-2023
Document type	Part Drawing	Document status	Released	DWG No.			
Title	Altair Thrust Plate	Rev.	1	Date of issue	09-04-2023	Sheet	1/1



A (2:1)

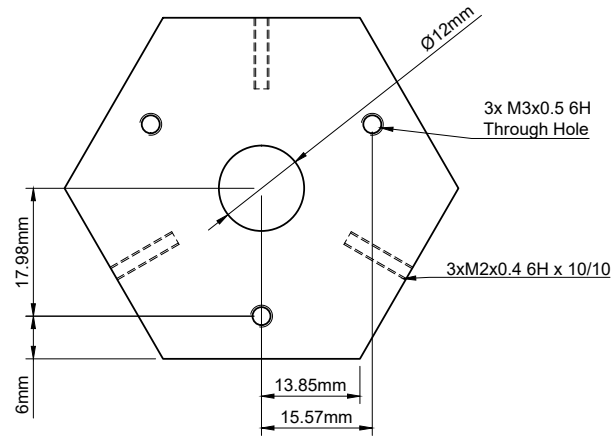


All Linear Dimensions are in mm.
Linear Tolerances are ± 0.1 mm unless specified.
Angular Tolerances are $\pm 1^\circ$ unless specified.

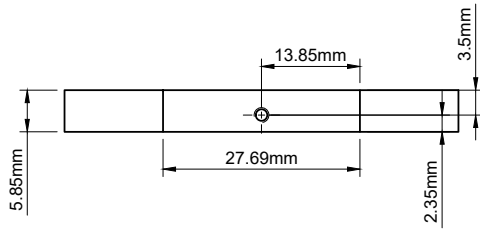
Material	Wood
Mass	627.115 g
Qty	1
Notes	

Dept.	Technical reference	Created by	Approved by
Propulsion	Raeid Mukadam	Raeid Mukadam 12-05-2023	Jayadeep 12-05-2023
Document type		Document status	
Part Drawing		Released	
Title		DWG No.	
Altair Damper		ALT-MB-DMP	
Rev.	Date of issue	Sheet	
1	12-05-2023	1/1	

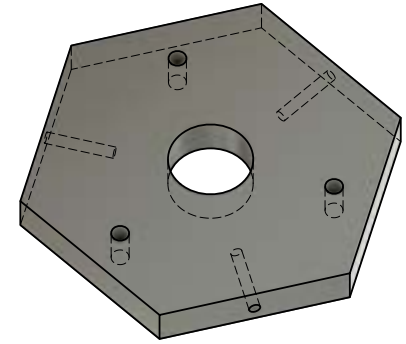
Top view
(2:1)



Front view
(2:1)




Isometric View
(2:1)

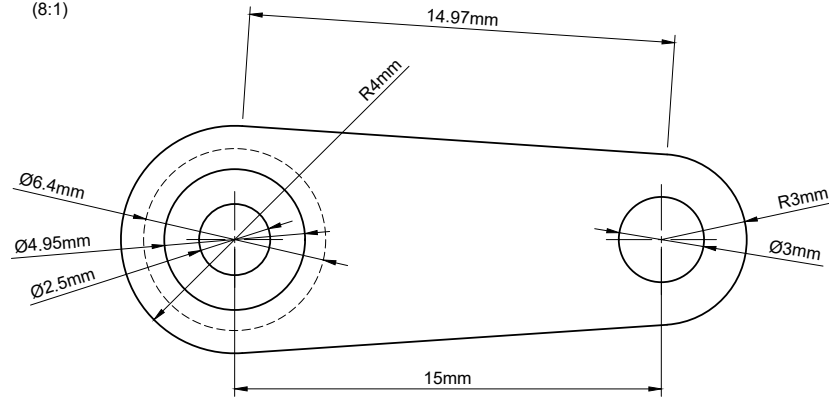


All Linear Dimensions are in mm.
Linear Tolerances are $\pm 0.1\text{ mm}$ unless specified.
Angular Tolerances are $\pm 1^\circ$ unless specified.

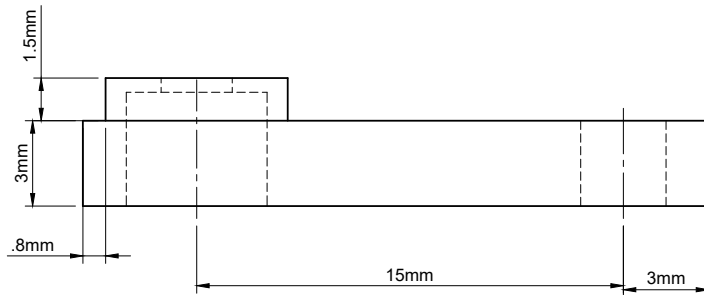
Material	Steel
Mass	85.11 g
Qty	1
Notes	

Dept.	Technical reference	Created by	Approved by	
Payload	Pranav	Pranav	12-04-2023	Ashwin
		Document type	Document status	
		Part Drawing	Released	
		Title	DWG No.	
		Altair Rocket Payload Cubesat Base plate	ALT-PNR-BP	
Rev.	Date of issue	Sheet		
1	12-04-2023	1/1		

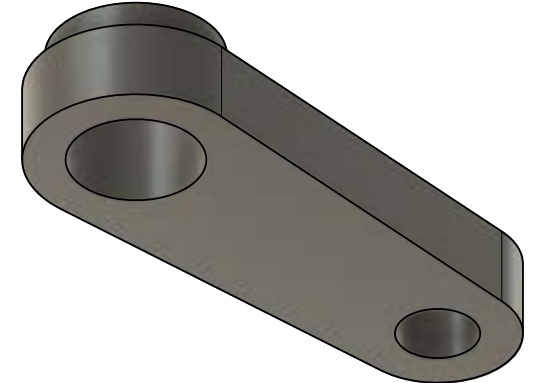
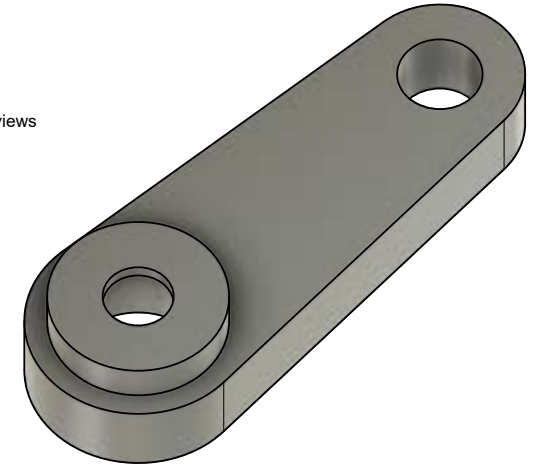
Top view
(8:1)



Front view
(8:1)



Isometric views
(8:1)



All Linear Dimensions are in mm.
Linear Tolerances are $\pm 0.1\text{ mm}$ unless specified.
Angular Tolerances are $\pm 1^\circ$ unless specified.

Quantity	4
Material	Steel
Additional Notes	

Dept. Payload	Technical reference Pranav	Created by Pranav	10-04-2023	Approved by Ashwin	10-04-2023
		Document type Part Drawing	Document status Released		
		Title Altair Rocket Stewie Link Link 1	DWG No. ALT-PNR-STE-LINK		
Rev.	1	Date of issue 10-04-2023	Sheet 1/1		

1 2 3 4 5 6 7 8 9 10 11 12

A

B

C

D

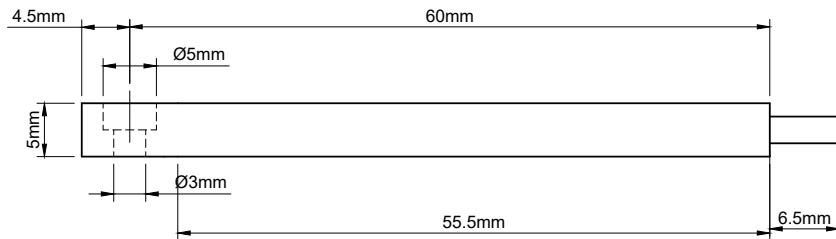
E

F

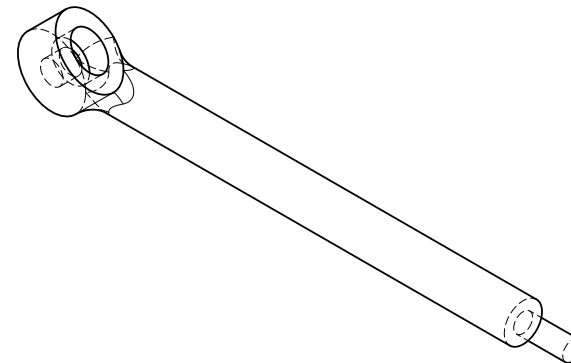
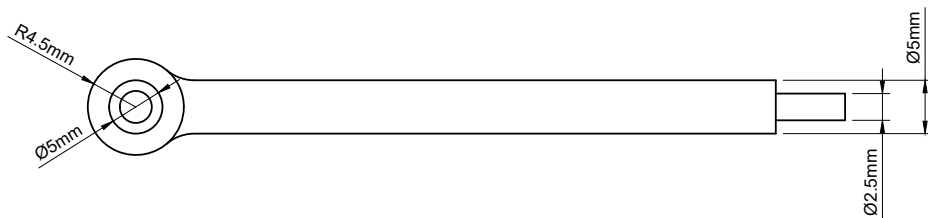
G

H

Front view
(3:1)



Top view
(3:1)




Isometric view
(3:1)



ALL DIMENSIONS ARE IN MM
ALL THE LINEAR TOLERANCES IF NOT SPECIFIED ARE $\pm 0.2\text{mm}$
ALL THE ANGULAR TOLERANCE IF NOT SPECIFIED ARE $\pm 1^\circ$

Sl	Part	Qty	Material	Additional info
1	LINK2 CENTER HOLE	4	Steel	

Dept. Payload	Technical reference Pranav	Created by Pranav	27-04-2023	Approved by Ashwin	27-04-2023
		Document type Part Drawing	Document status Released		
		Title Altair Rocket Cubesat-Stewie LINK 2 center hole	DWG No. PNR-STW-LINK2		
		Rev. 1	Date of issue 27-04-2023	Sheet 1/1	

A

B

C

D

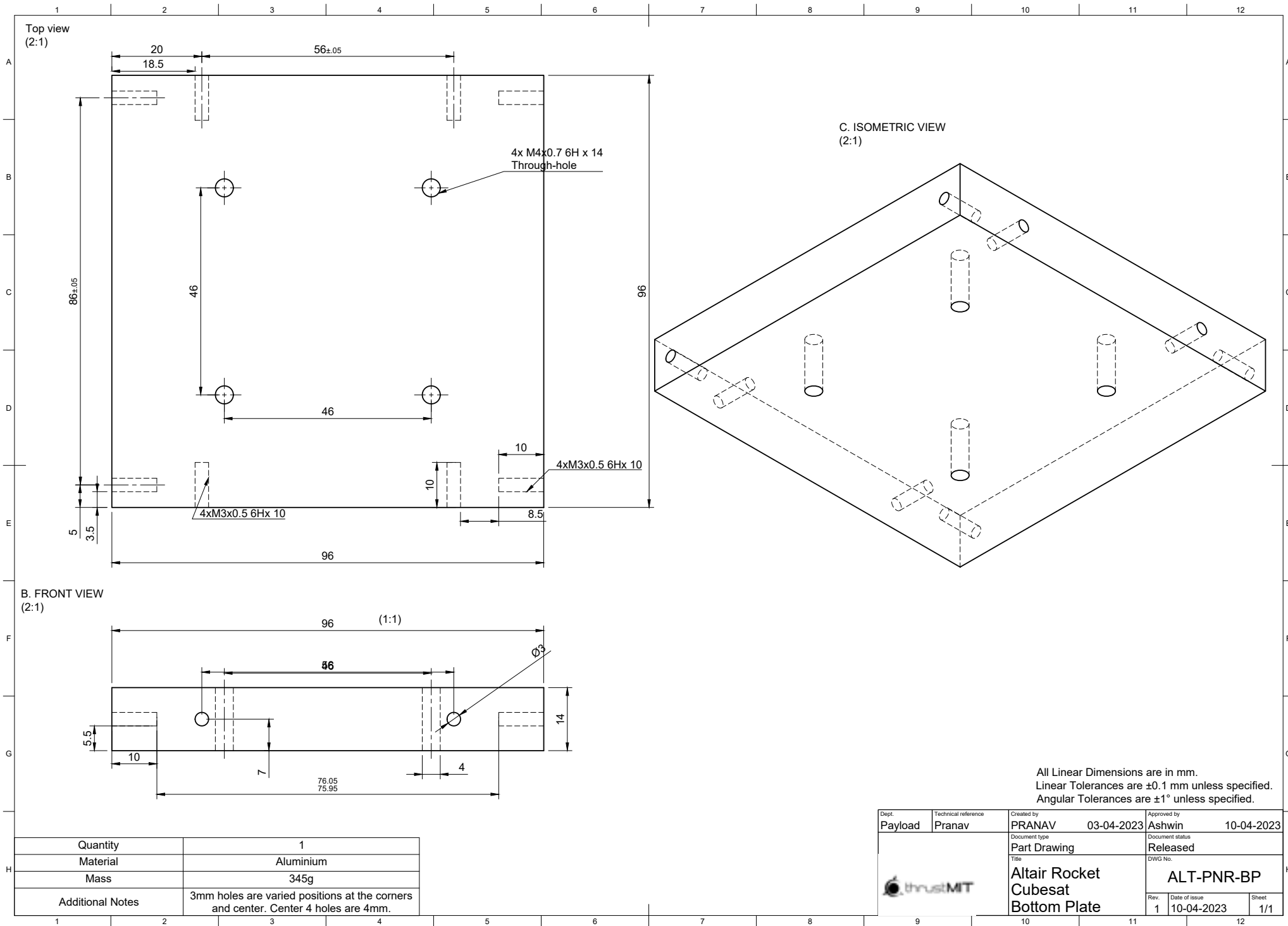
E

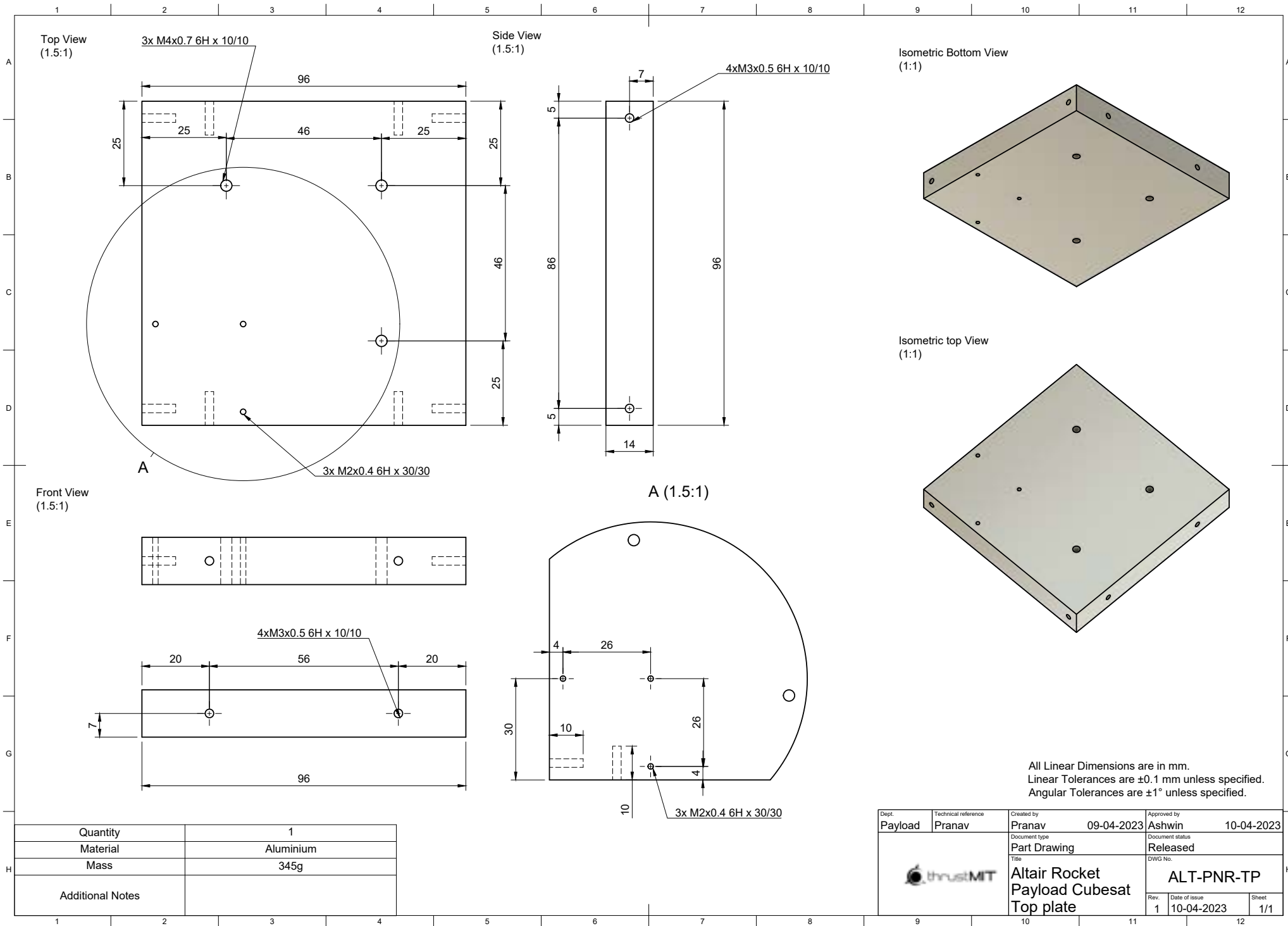
F

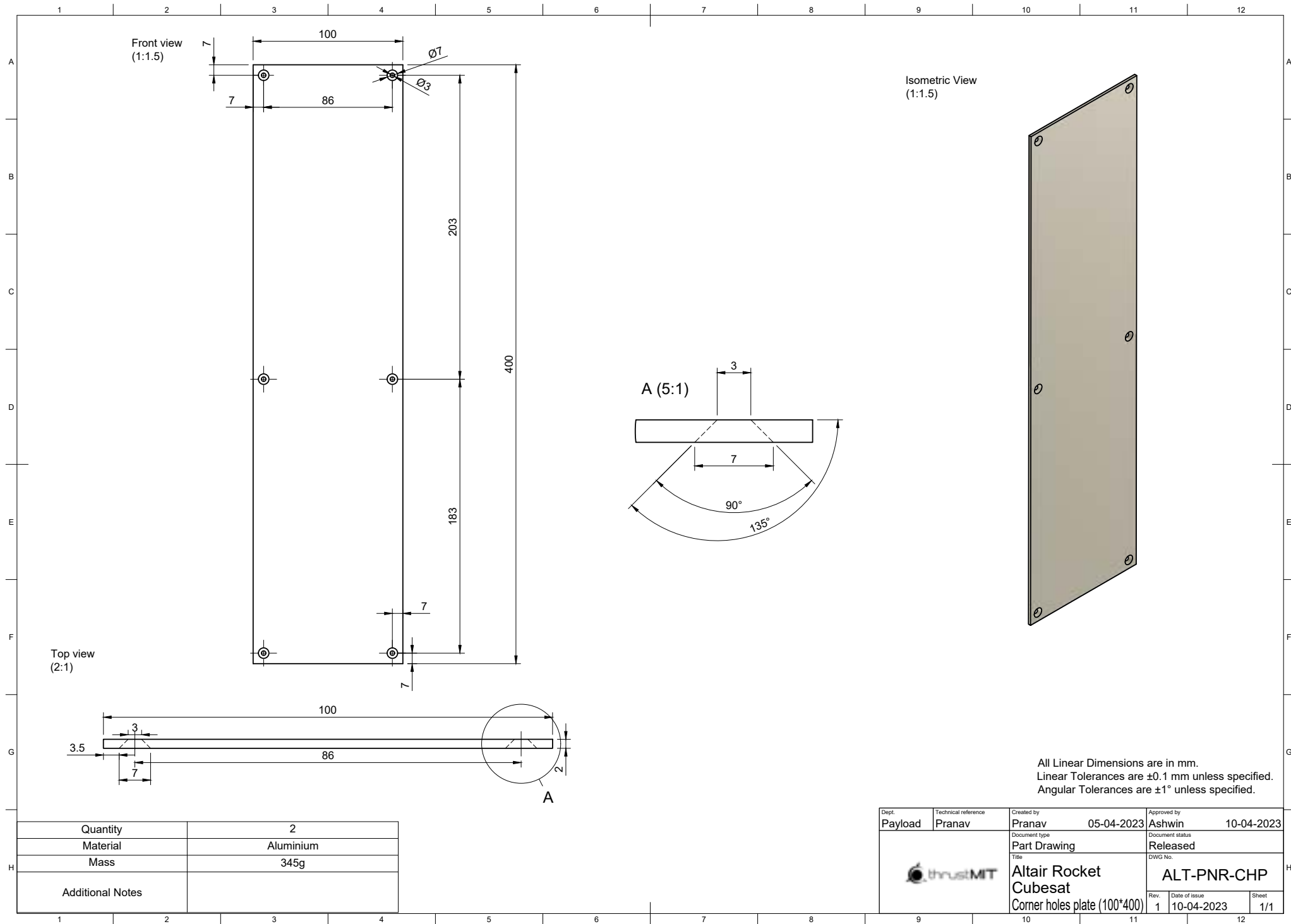
G

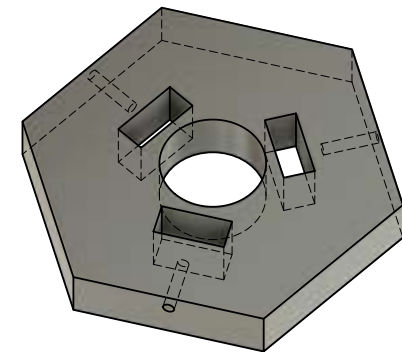
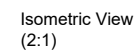
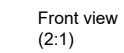
H


1 2 3 4 5 6 7 8 9 10 11 12



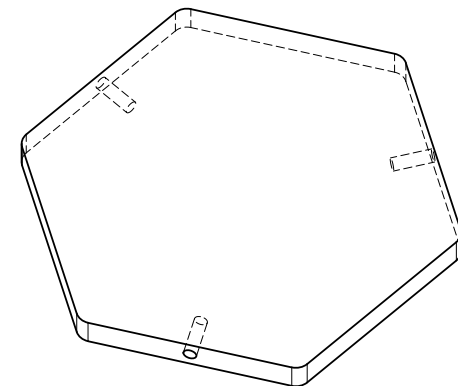
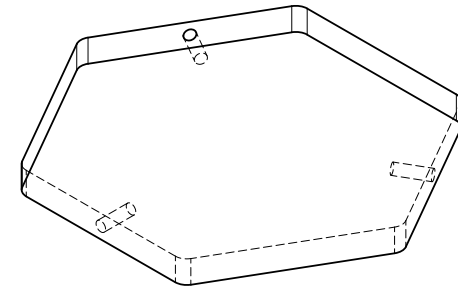
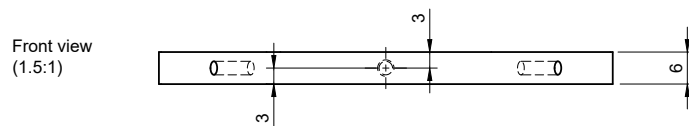
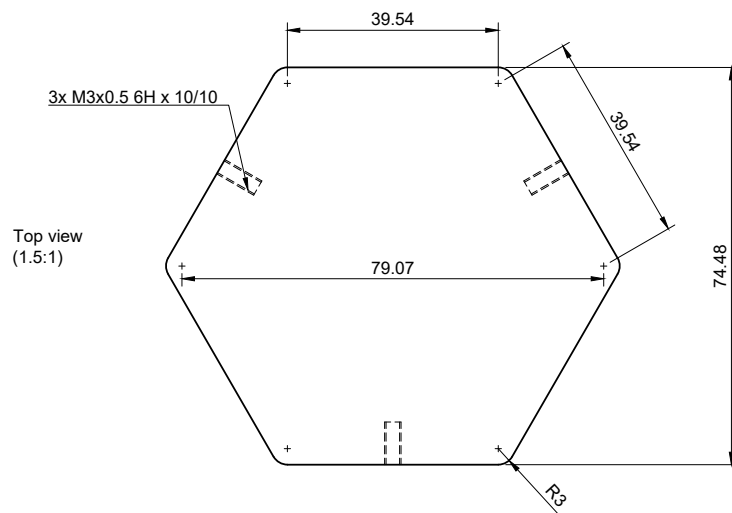







Dept.	Technical reference	Created by	Approved by
Payload	Pranav	Pranav 11-04-2023	Ashwin 12-04-2023
	Document type	Document status	
	Part Drawing	Released	
	Title	DWG No.	
	Altair Rocket Cubesat Payload Plate2	ALT-PNR-STW-P2	
		Rev.	Sheet
		1 12-04-2023	1/1

Quantity	1
Material	Steel
Additional Notes	.



All Linear Dimensions are in mm.
Linear Tolerances are ± 0.1 mm unless specified.
Angular Tolerances are $\pm 1^\circ$ unless specified.

Quantity	1
Material	Steel
Mass	225g
Additional Notes	

Dept. Payload	Technical reference Pranav	Created by Diya Parekh 28-04-2023	Approved by Pranav 28-04-2023
	Document type Part Drawing		Document status Released
	Title Altair Rocket Cubesat Payload top plate		DWG No. PNR-STW-PLATE
	Rev. 1	Date of issue 28-04-2023	Sheet 1/1

References

- [1] Ng, C. C., Ong, S. K., and Nee, A. Y. C., “Design and development of 3–DOF modular micro parallel kinematic manipulator,” *The International Journal of Advanced Manufacturing Technology*, Vol. 31, No. 3–4, 2006, pp. 188–200.
- [2] Knacke, T., *Parachute Recovery Systems Design Manual*, Defense Technical Information Center, 2002.
- [3] Components, A., “How To Calculate Fin Flutter Speed Newsletter 291,” *Apogee Components Newsletter*, , No. 291, 2021. URL <https://www.apogeerockets.com/education/downloads/Newsletter291.pdf>.
- [4] Squire, L., “The Characteristics of Some Slender Cambered Gothic Wings at Mach Numbers from 0.4 to 2.0,” *Journal of the Royal Aeronautical Society*, Vol. 55, No. 518, 1951, pp. 315–324.
- [5] ANSYS Inc., *Fluent Theory Guide*, ANSYS Inc., 2022nd ed., 2022. URL <https://www.ansys.com/products/fluids/ansys-fluent>.
- [6] Nisakanen, S., *OpenRocket technical documentation for OpenRocket version 13.05*, OpenRocket, 2013. URL <http://openrocket.sourceforge.net/techdoc.pdf>.
- [7] Anderson Jr., J. D., *Modern Compressible Flow*, 3rd ed., McGraw-Hill Education, 2010.
- [8] Anderson Jr., J. D., *Fundamentals of Aerodynamics*, 5th ed., McGraw-Hill Education, 2010.
- [9] Anderson Jr., J. D., *Introduction to Flight*, 7th ed., McGraw-Hill Education, 2011.
- [10] Arduino, “Arduino Nano,” 2022. URL <https://docs.arduino.cc/hardware/nano>.
- [11] Bosch, “BMP388 Pressure Sensor,” , -. URL <https://www.bosch-sensortec.com/products/environmental-sensors/pressure-sensors/bmp388/>.
- [12] TDK, “MPU6050 IMU,” , -. URL <https://invensense.tdk.com/products/motion-tracking/6-axis/mpu-6050/>.
- [13] Adafruit, “Adafruit Ultimate GPS Breakout v3,” , -. URL <https://www.adafruit.com/product/746>.
- [14] Digi, “XBee-PRO 900HP,” , -. URL <https://www.digi.com/products/embedded-systems/digi-xbee/rf-modules/sub-1-ghz-rf-modules/xbee-pro-900hp>.
- [15] MissileWorks, “RRC3 "Sport" Altimeter,” , -. URL <https://www.apogeerockets.com/Electronics-Payloads/Altimeters/RRC3-Sport-Altimeter>.
- [16] Featherweight, “Featherweight GPS Tracker,” , -. URL <https://www.featherweightaltimeters.com/featherweight-gps-tracker.html>.
- [17] RunCam, “RunCam Split 3 Lite,” , -. URL https://www.runcam.com/download/split-3-series/RC_Split_3_series_Manual_EN.pdf.
- [18] Newlands, R., Heywood, M., and Lee, A., “Rocket Vehicle Loads and Airframe Design,” Tech. rep., Aspire Space, 2011.
- [19] Hoult, C. P., “Sounding Rocket Structural Design Loads,” Tech. rep., Rocket Science and Technology, 2014.
- [20] ANSYS Inc., *Ansys Composite Pre-Post Guide Release 2022 R1*, 2022.
- [21] ANSYS Inc., *Mechanical User’s Guide Release 2022 R1*, 2022.
- [22] ANSYS Inc., *Explicit Dynamics Analysis Guide Release 2022 R1*, 2022.
- [23] Mallick, P. K., *Fiber-Reinforced Composites: Materials, Manufacturing, and Design*, CRC Press, 2007.
- [24] “BhorForce PC200 Datasheet,” , May 2018. URL <https://bhor.com/wp-content/uploads/2018/05/BhorForce-PC200.pdf>.
- [25] “Huntsman Araldite LY5052/Aradur 5052,” , Nov 2012. URL https://samaro.fr/pdf/FT/Araldite_FT_LY_5052_Aradur_5052_EN.pdf.
- [26] “Multi-Walled Carbon Nanotubes,” , Jul 2020. URL <https://nanocliff.com/product/multi-walled-carbon-nanotubes/>.
- [27] Nayak, S. Y., Shenoy, S., Sultan, M. T. H., Kini, C. R., Seth, A., Prabhu, S., and Safri, S. N. A., “Effect of CNT-Based Resin Modification on the Mechanical Properties of Polymer Composites,” *Frontiers in Materials*, Vol. 7, 2021, p. 609010.
- [28] E756-05, “Standard Test Method for Measuring Vibration-Damping Properties of Materials,” *American Society of Testing and Materials*, 2017.
- [29] Barra, G., Guadagno, L., Vertuccio, L., Simonet, B., Santos, B., Zarrelli, M., Arena, M., and Viscardi, M., “Different methods of dispersing carbon nanotubes in epoxy resin and initial evaluation of the obtained nanocomposite as a matrix of carbon

fiber reinforced laminate in terms of vibroacoustic performance and flammability,” *Materials (Basel)*, Vol. 12, No. 18, 2019, p. 2998.

- [30] Barrett, D. H., “SP-8051 - Solid Rocket Motor Igniters,” Tech. rep., National Aeronautics and Space Administration, 1971.